



# EUROPEAN SOUTHERN OBSERVATORY

Organisation Européenne pour des Recherches Astronomiques dans l'Hémisphère Austral  
Europäische Organisation für astronomische Forschung in der südlichen Hemisphäre

ESO - European Southern Observatory  
Karl-Schwarzschild Str. 2, D-85748 Garching bei München

---

## Very Large Telescope Paranal Science Operations CRIRES User Manual

Doc. No. VLT-MAN-ESO-14500-3486

Issue 85.2, Date 25/12/2009

R. Siebenmorgen, A. Smette, J. Smoker 25/12/2009  
Prepared .....  
Date Signature

A. Smette  
Approved .....  
Date Signature

C. Dumas  
Released .....  
Date Signature

This page was intentionally left blank

### Change Record

Issue/Rev.	Date	Section/Parag. affected	Reason/Initiation/Documents/Remarks
79.1	29/08/06	all	RSI,ASM: First release, issued for P79 Phase1
79.2	08/09/06	all	ASM: Sec. 11, corrected wavelength table
79.3	20/12/06	all	RSI, ASM, comments DMD
79.4	21/12/06	14,15	ASM, minor editorial corrections
80.1	05/03/07	0,1	ASM, corrected layout figure and description
		3	added a web-link
		6	corrected detector gain
			added comments on a non-linearity correction method
			minor updates and corrected typos
		5	updated limiting mag. in noAO
		8	added subsection on entrance window transmission
			updated sensitivities
		10	updated overheads
		11	added 3 recommended DIT values, updated text
		12	updated
80.2	12/03/07	0,8.1,10.3	corrected typos
		7.2,14.2	added paragraph on gas-cell and generic offsets template
80.3	20/03/07	15	corrected J band wavelength ranges
80.4	26/03/07	15	corrected missing entries in Table 4
80.5	07/05/07	1	corrected description
	21/05/07	14.2	new observation template
	05/06/07	7.2	added link to N2O line list; 1st results on RV accuracy
	09/06/07	0,1,7.4	corrected slit length and slit viewer f-o-v
	09/06/07	14.1.1	corrected typo in RA offset
	09/06/07	12	daytime wavecal only for $\lambda < 2400$ nm
	19/06/07	1.4,6.4	contact information, odd-even
	19/06/07	8.4	add important note on intermediate slit
	20/06/07	17,18	new section 17, update §18
	20/06/07	11.1,14.1	added comments on ext. objects, moving targets
	20/06/07	9.3	added comments on std stars
	20/06/07	14.2	added gas cell P2PP parameter description

81.1	31/08/07	8.4	updated	
	31/08/07	8.2	Added Fig. 22: comparison UVES vs CRIRES	
	31/08/07	10.3	Table 3 (overheads) updated	
	31/08/07	15	Slightly changed captions	
	01/09/07	6.4	Added links to method and reference frames	
	01/09/07	9.1	Added link to ETC	
	01/09/07	11.2.1	Added para.: choice of a SVGS in crowded field	
	01/09/07	8.2	Added para. on slit loss due to diff. refraction	
	01/09/07	11.4	Added requirement for fc	
	02/09/07	5, 7.5	Figures added (AO performance, resolving power)	
	02/09/07	11.5	Add a para. on airmass	
	81.2	19/11/07	11.2.4, 14.2, 14.2.5	Added SpectroAstrometry template
		20/11/07	14.1.3	Change default value of SEQ.NGS.USELASTSKY to T
		21/11/07	1.5	New section: NEWS
		21/11/07	10.1	Added: specific comments for SM (telluric OBs)
		22/11/07	14.2.4	Expanded description of generic offsets template
		18/12/07	Table 1	Dark current values corrected
18/12/07		7.2	Changed comment regarding gas-cells	
27/12/07		Tables 4a-5h	Wavelength settings updated	
27/12/07		§7.5, 8.4,9.1, 9.2.1	typos corrected	
27/12/07		§9.2.3, 10.2, 11.1, 11.2.1	typos corrected	
27/12/07		§11.2.4,10.1,13.1, 14.1, 5	typos corrected	
27/12/07		§11.5.3, 5.1	clarified	
27/12/07		§7.3, 5.2	updated	
28/12/07		§5.1.2	AO star bright mag. limit updated	
82.1		20/01/08	§7.2	updated available gas-cells
		20/01/08	§20	added section
		03/03/08	§7.1	updated: new configuration table
	03/03/08	§8.4	updated	
	03/03/08	§11.7	numbering changed	
	03/03/08	§11.6	new sub-section on water vapor	
	03/03/08	§14.1.7	updated	
	03/03/08	§18	updated	
	82.2	19/06/08	§10.2	ETC updated: precipitable water vapor
		19/06/08	Table 3	incl. overhead for derotator motion in spectroastrometry
19/06/08		§9.1, Fig.25	added a fig. with water vapor only transmission	
23/06/08		§7.2	ThAr fibers, CO gas-cell and visitor gas-cells	
23/06/08		§14.1.2 14.3.6	Updated for the use of CO gas-cell	
23/06/08		§1.5	Updated	
23/06/08		§2.1, 11.2.5	Updated for ThAr fiber	
25/06/08		§12	calibration plan updated	
25/06/08		§14.1.7	added note regarding slit width	
25/06/08		§7.1	Added note: vacuum wavelength are used	
25/06/08	§11.4	Added note regarding multiple stars		

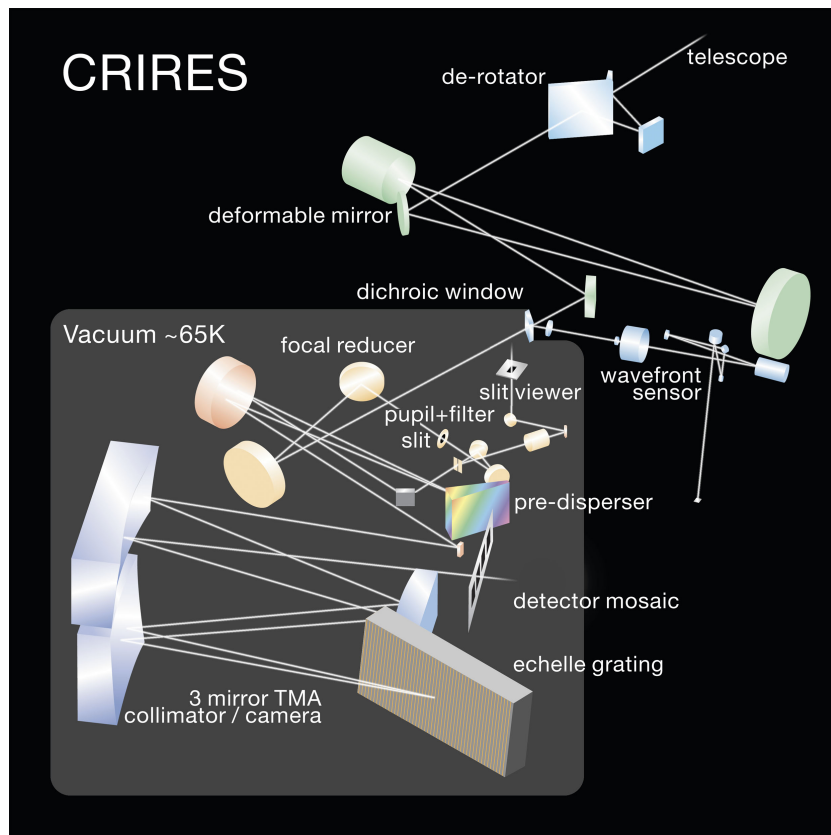
83.1	29/08/08	Tab. 8a	updated with CO gas-cell for order 24
	29/08/08	§1.5	news updated
	29/08/08	§20.1	checklist updated
	29/08/08	§7.2.1	update on identification of ThAr lines
	29/08/08	§7.4	added not regarding slit width
83.2	19/12/08	§7.2.2	radial-velocity measurements: added
	19/12/08	§7.5	spectral resolution: updated
	19/12/08	§6.5	linearity: added
	19/12/08	§14.1.3	WFS last sky measurements: updated
	19/12/08	§8.2	limitations due to differential refraction: removed
84.1	19/12/08	§1.3, 11, 20.2	P2PP links: updated
	04/03/09	§1.5	Section updated
	04/03/09	§14.1	Note added
	04/03/09	§7.1	Slit wider than 0.4" should be avoided.
	04/03/09	§7.2.2	Note added regarding radial velocity measurements
84.2	04/03/09	§11.3	New readout mode
	04/03/09	Tab. 3	Overheads table updated
	04/03/09	§11.1	Differential tracking
	29/05/09	§1.5	Section updated
	30/05/09	§5.1.3	Note added
	30/05/09	§5.1	Max. distance AO star - science target corrected
	30/05/09	§7.2.1	Updated with new ThAr atlas information
	30/05/09	§7.4, Fig 18	F-o-v updated following the May09 intervention
	15/06/09	§14	Added description of differential tracking
			Added description of readout modes
	17/06/09	§6, 11.3	Updated to take into account the new readout mode
	17/06/09	§7.1	Updated to take into account the new configuration table
	17/06/09	Tab 4a -7	Updated to take into account the new configuration table
	17/06/09	§19	Differential tracking section added
	17/06/09	§10.4	Differential chromatic effect section added
18/06/09	Tab 3	Overheads updated	
01/07/09	§7.5	Section updated	
01/07/09	§11.5	Section updated	
85.1	31/08/09	§11.3 and 14.1.8	DIT setting: §reworded
	31/08/09	§14.2	updated
	31/08/09	§19.3	note added
	31/08/09	§7.2.1	gas-cell: note added
	31/08/09	§1.5	updated
85.2	31/08/09	§1.5	news updated
	25/12/09	§6.2	comment on detector glow
	25/12/09	§7.2.2	updated with new RV refs
	25/12/09	§7.5	resolving power reproducibility section ammended
	25/12/09	§8.2	UVES/CRIRES comparison updated
	25/12/09	§11.3 and 14.1.8	DIT setting further updated
	25/12/09	§14.3.2	FF parameters; updated advice for extended targets
	25/12/09	§14.3.3	updated wavelength calibration section
	25/12/09	§14.3.4	updated dark parameters
	25/12/09	§15.1	tables of reference wavelengths updated with new encoder values.
	25/12/09	Figure 18	slit and science detector geometry figure changed
	25/12/09	§19.3	updated differential tracking section

First version of the manual was written by R.Siebenmorgen and A.Smette. L. Tacconi-Garman and M. Hilker provided numerous comments on the various versions of this manual that greatly improved its accuracy and clarity. The content of §7.2.2 (RV measurements) was originally based on discussions with H.-U. Kaeufl, P. Figuera and Andreas Seifarht.

## Abbreviations and Acronyms

AO	Adaptive optics
APD	Avalanche photo-diode
BOB	Broker of observation blocks
CPL	Common Pipeline Library
CRIRES	Cryogenic high-resolution infrared echelle spectrograph
DM	Deformable mirror
DMO	Data management and operations division
ESO	European Southern Observatory
ETC	Exposure time calculator
FC	Finding chart
FoV	Field of view
FWHM	Full width at half maximum
NGS	Natural guide stars
NIR	Near infrared
NIST	National Institute of Standards and Technology
OB	Observation block
P2PP	Phase II proposal preparation
PSF	Point spread function
QC	Quality control
RTC	Real time computer
RTD	Real time display
SDD	Software Development Division
SM	Service mode
SNR	Signal-to-noise ratio
SR	Strehl ratio
TIO	Telescope and instrument operator
TTM	Tip-tilt mount
USD	User support department
VLT	Very large telescope
VM	Visitor mode
WF	Wave front
WFS	Wave front sensor

# Overview



Calibration system	halogen lamp, IR-emitter, ThAr, N <sub>2</sub> O, CO, visitor gas cells
Adaptive optics	60-actuator curvature sensing MACAO system
Slit length	≈ 40 "
Slit width	0.05 " – 3.0 ": recommended 0.2 " – 0.4 "
Echelle grating	40 × 20cm, 31.6 lines/mm, 63.5° blaze angle
Resolving power	100,000 (0.2 "); 50,000 (0.4 " slit)
Wavelength range	0.95μm ≤ λ ≤ 5.2μm
Free spectral range	from λ/70 at 1μm to λ/50 at 5μm
Detector science array	4096 × 512 pixels using 4 Aladdin III detectors
Pixel scale	0.086 "
Slit viewer: filters	J, H, K, 2 H + neutral density
Slit viewer: detector	Aladdin III array
Slit viewer: field-of-view	≈ 35 " × 43 "
Slit viewer: pixel scale	≈ 0.047 "
Pre-disperser	ZnSe prism

This page was intentionally left (almost) blank

# Contents

<b>1</b>	<b>Introduction</b>	<b>1</b>
1.1	Science drivers	1
1.2	Structure and scope of the User Manual	2
1.3	More information on CRIRES	3
1.4	Contact Information	3
1.5	News	4
<b>I</b>	<b>The instrument</b>	<b>8</b>
<b>2</b>	<b>Cold part: the spectrometer</b>	<b>8</b>
2.1	Optics	9
2.2	Mechanics	9
2.3	Detectors	10
<b>3</b>	<b>Warm part: the adaptive optics system</b>	<b>11</b>
3.1	Introduction	11
3.1.1	Atmospheric turbulence	11
3.1.2	Adaptive Optics	12
3.2	Hardware description	13
3.2.1	The corrective optics	13
3.2.2	The Wavefront Sensor	13
3.2.3	Control loop	15
3.2.4	Membrane setting	17
<b>II</b>	<b>Instrument Performance</b>	<b>18</b>
<b>4</b>	<b>Overview</b>	<b>18</b>
<b>5</b>	<b>AO performance</b>	<b>19</b>
5.1	AO guide stars	19
5.1.1	The distance of the AO star	20
5.1.2	The brightness of the AO star	20
5.1.3	The color of the AO star	21
5.2	Limiting magnitude of slit viewer	21
<b>6</b>	<b>Detector characteristics</b>	<b>22</b>
6.1	Dark and gain	23
6.2	Glow	23
6.3	Fringes	23

6.4	Odd-even effect . . . . .	24
6.5	Correcting for detector non-linearity . . . . .	24
<b>7</b>	<b>Characteristics of the spectrograph</b>	<b>26</b>
7.1	Wavelength settings . . . . .	26
7.2	Wavelength calibration . . . . .	26
7.2.1	Standard means: ThAr lamp and N <sub>2</sub> O and CO gas-cells . . . . .	26
7.2.2	Radial velocity measurements . . . . .	28
7.2.3	Visitor gas-cells . . . . .	30
7.3	Flat fields . . . . .	31
7.4	Spectrograph field-of-view, slit width and seeing . . . . .	32
7.5	Spectral resolving power . . . . .	35
<b>8</b>	<b>System efficiency and throughput</b>	<b>36</b>
8.1	Transmission of the entrance window . . . . .	36
8.2	Sensitivity . . . . .	37
8.3	Optical ghosts . . . . .	38
8.4	Stability and reproducibility . . . . .	39
<b>III</b>	<b>Observing with CRIRES at the VLT</b>	<b>40</b>
<b>9</b>	<b>Introduction</b>	<b>40</b>
9.1	Atmospheric transmission . . . . .	40
9.2	Background removal . . . . .	40
9.2.1	Sky emission spectrum . . . . .	40
9.2.2	Nodding . . . . .	40
9.2.3	Jittering . . . . .	40
9.3	Flux calibration and telluric correction . . . . .	43
9.3.1	General procedure . . . . .	43
9.3.2	Telluric correction . . . . .	43
9.3.3	Hot stars as telluric standards . . . . .	43
9.3.4	Late-type stars or G stars as telluric standards . . . . .	44
9.3.5	Catalogs . . . . .	44
9.4	The influence of the Moon . . . . .	44
<b>10</b>	<b>Observing in Visitor and Service Mode</b>	<b>45</b>
10.1	Overview . . . . .	45
10.2	The Exposure Time Calculator . . . . .	45
10.3	Overheads . . . . .	47
10.4	Differential effects . . . . .	47
<b>11</b>	<b>Preparation of Observation Blocks</b>	<b>49</b>

11.1	Information required . . . . .	49
11.2	Observation Blocks and Templates . . . . .	50
11.2.1	Acquisition . . . . .	50
11.2.2	Acquisition sequences with AO . . . . .	51
11.2.3	Acquisition sequences without AO . . . . .	53
11.2.4	Science . . . . .	53
11.2.5	Calibration . . . . .	53
11.3	Detector read-out mode and DIT setting . . . . .	54
11.4	README and finding charts . . . . .	55
11.5	Constraints . . . . .	56
11.5.1	Moon . . . . .	56
11.5.2	Seeing and Strehl ratio for adaptive optics observations . . . . .	56
11.5.3	Seeing for seeing limited observations, no adaptive optics . . . . .	57
11.5.4	Transparency . . . . .	57
11.5.5	Airmass . . . . .	57
11.6	Water vapor . . . . .	57
11.7	Offset conventions and definitions . . . . .	57
<b>IV</b>	<b>Reference material</b>	<b>59</b>
<b>12</b>	<b>CRIRES calibration plan</b>	<b>59</b>
<b>13</b>	<b>Data format and reduction</b>	<b>60</b>
13.1	Format . . . . .	60
13.2	Pipeline . . . . .	60
<b>14</b>	<b>Template parameters</b>	<b>61</b>
14.1	Acquisition templates . . . . .	61
14.1.1	Target and SVGS parameters . . . . .	61
14.1.2	Gas cell . . . . .	63
14.1.3	NGS parameters . . . . .	63
14.1.4	Parameters related to the slit viewer . . . . .	64
14.1.5	Telescope guide star parameters . . . . .	64
14.1.6	Derotator parameters . . . . .	65
14.1.7	Spectrograph parameters . . . . .	65
14.1.8	Science detector parameters . . . . .	66
14.1.9	Notes . . . . .	66
14.2	Observation templates . . . . .	66
14.2.1	Detector . . . . .	67
14.2.2	Gas cell . . . . .	67

14.2.3	CRIRES_spec_obs_AutoNodOnSlit and CRIRES_spec_obs_SpectroAstrometry: nodding and jittering . . . . .	67
14.2.4	CRIRES_spec_obs_GenericOffset only: list of offsets . . . . .	68
14.2.5	CRIRES_spec_obs_SpectroAstrometry only: list of derotator angles, jit- ter reset . . . . .	70
14.3	Calibration templates . . . . .	71
14.3.1	Standard star or telluric observations . . . . .	71
14.3.2	Flat field . . . . .	71
14.3.3	Wavelength calibration . . . . .	72
14.3.4	Darks . . . . .	72
14.3.5	Sky observation . . . . .	73
14.3.6	Template signatures . . . . .	74
<b>15</b>	<b>CRIRES standard wavelength settings</b>	<b>81</b>
15.1	Wavelength ranges . . . . .	81
15.2	Wavenumber ranges . . . . .	93
<b>16</b>	<b>Free wavelength settings</b>	<b>105</b>
<b>17</b>	<b>Reference wavelengths common to different orders</b>	<b>107</b>
<b>18</b>	<b>Calibration source for wavelength calibration</b>	<b>108</b>
<b>19</b>	<b>Differential tracking</b>	<b>111</b>
19.1	Introduction . . . . .	111
19.2	Tracking tables . . . . .	111
19.3	Acquisition and observation . . . . .	113
<b>V</b>	<b>Tips for successful observations</b>	<b>114</b>
<b>20</b>	<b>Checklist</b>	<b>114</b>
20.1	Phase 1 . . . . .	114
20.2	Phase 2 . . . . .	115

# 1 Introduction

The cryogenic high-resolution IR echelle spectrograph – CRIRES – is the infrared ( $0.95\mu\text{m}$  –  $5.2\mu\text{m}$ ) high-resolution spectrograph located at the Nasmyth A focus of UT1 (Antu). It provides long-slit ( $40''$ ) spectroscopy with a spatial sampling of  $0.086''$ . Spatial resolution and signal-to-noise ratio can be maximized by the optional use of a MACAO adaptive optics system equipped with an optical (R band) wavefront sensor.

The main optical elements consist of a prism acting as a pre-disperser and a  $31.6$  lines/mm echelle grating. Total spectral coverage per individual wavelength setting is  $\sim \lambda/70$  thanks to an array of four Aladdin III detectors. Acquisition and guiding are performed by means of a slit viewer equipped with an additional Aladdin III detector and a series of 5 filters (J,H,K and two neutral density H filters).

CRIRES has been designed to exploit the enormously enhanced sensitivity provided by a spectroscopic instrument with a large detector array at an 8m telescope. The quantitative and qualitative improvements of observational capabilities affect all scientific applications aiming at fainter objects with higher spatial (extended sources), spectral and temporal resolutions. Indeed, CRIRES provides:

- High-resolution spectroscopy in the  $1\text{-}5\ \mu\text{m}$  range at the VLT. This instrument employs the largest available grating for a spectral resolving power of up to  $\approx 100,000$  (for 2 pixel Nyquist sampling) with a  $0.2''$  slit;
- Spectral coverage maximized through four  $1024 \times 512$  pixel InSb detector arrays in the focal plane;
- Spectral imaging using a  $40''$  long slit;
- Adaptive Optics to maximize the signal-to-noise ratio (SNR) and spatial resolution.

Functionally, the instrument can be divided into four units:

1. The fore-optics unit provides field de-rotation, cold pupil and field stops, curvature sensing adaptive optics, and slit viewing.
2. The prism pre-disperser isolates one echelle order and minimizes the total amount of background entering the high-resolution unit.
3. The high-resolution unit comprises the collimator, the echelle which is tilt-tuned for wavelength selection, the camera and the science detectors.
4. The calibration unit outside the cryogenic environment contains the light sources for wavelength calibration and detector flat-fielding.

## 1.1 Science drivers

Thanks to CRIRES, new phenomena and objects are now available for spectroscopic studies. Some highlights are:

- *Extra-solar planets:*

- radial velocities
- spectroscopy of CO, CH<sub>4</sub>
- *Solar system:*
  - Giant planets, Titan: H<sub>3</sub><sup>+</sup>, CH<sub>4</sub>, CH<sub>3</sub>, NH<sub>3</sub>, HCN, ...
  - Terrestrial planets: CO, HCL, HDO, H<sub>2</sub>O, ...
  - Mars: imaging spectroscopy of CO depletion at 40km resolution
  - Io: volcanic activity (SO<sub>2</sub>)
  - Pluto, Charon, Triton: CO, CH<sub>4</sub> search
  - Comets: H<sub>2</sub>O abundance, temperatures, velocities
- *Stars:*
  - stellar evolution and nucleosynthesis: CNO abundance
  - stellar mass
  - stellar radii
  - stellar winds and mass loss
  - atmospheric structure and oscillations
  - magnetic field structure
- *Star formation and ISM:*
  - accretion and outflows
  - ISM chemistry and cloud structures: H<sub>3</sub><sup>+</sup>, H<sub>2</sub>O, CH<sub>4</sub>, ...
- *Extragalactic astronomy:*
  - AGN: velocity structure of the broad and narrow line region, [FeII], H<sub>2</sub> lines in low extinction regions, H recombination
  - fine structure lines

## 1.2 Structure and scope of the User Manual

The CRIRES user manual is structured as follows:

- Part **I** provides a technical description of CRIRES and its adaptive optics system (AO).
- Part **II** details the instrument performance.
- Part **III** describes the commonly used observing techniques in the infrared, summarizes the CRIRES observing modes and provides guidelines for Phase 2 preparation.
- Reference material is given in Part **IV**. It includes a description of the calibration plan, the data format, the template reference guide and the defined wavelength settings.
- Finally, Part **V** provides a number of recommendations written to increase the chances that a program is executed successfully.

### 1.3 More information on CRIRES

All CRIRES related manuals are available on the CRIRES instrument web pages together with the most updated information on the instrument:

<http://www.eso.org/instruments/criages/>

Both Service and Visitor mode Observation Blocks (OBs) should be prepared with the latest version of the Phase 2 Proposal Preparation tool (P2PP), available at:

<http://www.eso.org/sci/observing/phase2/P2PP/P2PPTool.html>.

Information for the preparation of Service mode observations with CRIRES are available at:

<http://www.eso.org/sci/observing/phase2/SMGuidelines.html#CRIRES>

Visiting astronomers do not need to submit Observation Blocks in advance of their observations. However, they should prepare them before arriving at the observatory or, at the latest, at the observatory the nights before their observing run. They will find further instructions on the Paranal Science Operations web page and the Paranal Observatory home page:

<http://www.eso.org/paranal/>  
<http://www.eso.org/paranal/sciops/>

Reference frames, static calibration frames, information regarding the CRIRES pipeline and quality control can be found at:

<http://www.eso.org/observing/dfo/quality/>  
[http://www.eso.org/observing/dfo/quality/index\\_criages.html](http://www.eso.org/observing/dfo/quality/index_criages.html)

### 1.4 Contact Information

In case of specific questions related to Service Mode observations and proposal preparation please contact the ESO User Support Department:

[usd-help@eso.org](mailto:usd-help@eso.org)

For Visitor Mode observations please contact the Paranal Science Operations Team. For general information, use

[paranal@eso.org](mailto:paranal@eso.org)

For specific questions regarding the use of CRIRES, use:

[criages@eso.org](mailto:criages@eso.org)

## 1.5 News

### Since the release of User Manual v85.1

- The CRIRES\_spec\_cal\_LampFlats template now accepts new parameters: it allows to set the maximum flux over the frame, as well as the entrance slit width.
- An intervention took place in December 2009 to finalize the installation of metrology fibers. This systems aims at providing repeatability of the wavelength zero point and dispersion to guarantee reproducibility to 1/10 pixel, for the standard settings. Associated overheads have already been included in Table 3. The CRIRES news pages will be updated with the results of the intervention including reproducibility tests. The positioning of the lines on the detector have shifted by  $\sim 30$  pixels in some settings. The tables in Sect. 15.1 have been updated with the new encoder values.

### Since the release of User Manual v84.2

- The entrance slit is now the least reproducible part of the instrument with variations of up to 50% in slit width. Technical tests will take place on September 3 and 4 to check the entrance slit width with the aim of insuring a reproducibility at the 10% level.
- Differential tracking is offered in service mode in P85.

### Since the release of User Manual v84.1

- An intervention took place in May 2009:
  - the science mosaic was moved so that its center is closer to the optical axis of the instrument; an internal baffle was modified; as a consequence, the field-of-view of the science detector is  $\approx 40''$ ; Fig. 18 has been updated;
  - metrology fibers have been installed which will guarantee a better wavelength setting reproducibility for data taken after an intervention foreseen in December 2009. Until then, the only consequence for the user is the presence of additional spectra on ThAr exposures; an example is given in Fig. 15;
  - the intermediate slit mechanism has been replaced by a more reliable one; it improves the wavelength setting reproducibility and decreases the uncertainty on the wavelength range affected by contamination by adjacent orders. As a consequence, the configuration table and standard settings had to be revised (see Tables 4a - 4k and Tables 5a - 5k) allowing a complete coverage without contamination by adjacent orders. Overhead for change of wavelength setting has significantly decreased;
  - the thermal control of the instrument has been further improved;
- The pipeline has been modified such that it is able to process data with different illumination areas: it automatically recognizes which area is illuminated depending on the date the data were taken. In particular, it recognizes data obtained between January 2009 and May 2009, and after May 2009. Cf. <http://www.eso.org/sci/data-processing/software/pipelines/index.html>.
- the ThAr catalogue has been updated with newly identified lines, see §7.2.

**Since the release of User Manual v83.2**

- An intervention took place in January 2009. Its main objective was to install new cryo-coolers. Indeed, the previous ones were causing a lot of vibrations strongly degrading the quality of the VLTI observations: consequently, CRIRES cryo-coolers had to be stopped during VLTI UT runs after which a further  $\sim 3-4$  days were lost for CRIRES operations while the instrument reached its operating temperature. The problems affecting the quality of the encoder reading for the grating, prism and entrance and intermediate slits have been solved considerably improving the repeatability of the functions. Quantitative values on this respect will be made available for the v84.2 of this manual.
- Considerable work has been completed to improve the maintainability of the observation and instrument control software. For the user, its main visible part is the full implementation of the compensation for the differential refraction, as well as the implementation of the differential tracking mode.
- An additional intervention will take place in May 2009. Its main goal is to implement a metrology system to allow to configure the spectrograph in a very accurate and reproducible way.
- A new readout mode has been implemented to window the detector 2 and 3. In turn, it allows to use DITs as short as 0.15s.

**Since the release of User Manual v83.1** The announced major change to the instrument control and observing software was successfully implemented in November 2008, although still incomplete at the time of issuing this manual. The missing parts will be implemented in February and March 2009.

**Since the release of User Manual v82.2 :**

- the CRIRES\_spec\_cal\_Wave template was modified to make use of a variable neutral density filter : this allows optimal illumination of the ThAr lines while avoiding the risk to introduce remanence by the brightest lines..

During P82, a major change to the instrument control and observing software will take place. Implementation of differential refraction correction is one of the advantages visible to the users, allowing to keep the object properly centered while observing at high airmass and with a reference wavelength different from the effective wavelength of the slit viewer filter. §8.2 will be updated once appropriate tests are performed.

In January 2009, an intervention is foreseen. At the time of issuing this Manual, the following actions are planned: (a) replace the cryo-coolers by another model to avoid vibrations affecting the VLTI (currently, the cryo-coolers are switched off during a VLTI-UT run; therefore, CRIRES cannot be used neither during a VLTI-UT run nor a few days after); (b) slightly lower the location of the science detector mosaic which would allow to offer a longer slit length; (c) installation of metrology fibers that would allow to guarantee a better reproducibility of the wavelength settings both in terms of wavelength range and spectral dispersion.

**Since the release of User Manual v82.1 :**

- version 1.7.0 of the CRIRES pipeline is available: <http://www.eso.org/projects/dfs/dfs-shared/web/vlt/vlt-instrument-pipelines.html>;
- a CO gas-cell is available;
- an intervention took place in April 2008; it consisted in
  1. replacing the carriage by a faster translation table;
  2. moving the ThAr lamp mounted on the carriage to a location close to the baffle where it feeds a set of fibers through a neutral density filter. The end of these fibers are fixed on a connector located on the carriage. In this way, a lot of scattered light is eliminated and spectrograph distortion can be estimated for each ThAr spectrum;
  3. installation of an AO fiber for AO calibrations, until then performed using a pin-hole;
  4. an encoder has been installed to control the intermediate slit therefore increasing its reproducibility;
  5. the location of sensors and the values of control loop parameters have been modified to increase the thermal stability of the instrument; a reproducibility of less than 2 pixels has been achieved once the instrument is stable in temperature.
- unfortunately, a detaching Sheldal tape (initially used to decrease possible scattered light) started to vignette the entrance slit, limiting the field first to 12", then 8" after a VLTI run during which the cryo-coolers were switched off to limit the amount of vibrations felt by the VLTI. As a consequence, a new intervention took place in June 2008. The tape has been completely removed. Comparison with the value measured before the intervention indicates that no increase in the amount of scattered light has been observed.
- the CRIRES\_spec\_cal\_Wave template was modified to make sure that the ThAr fibers are properly centered in the slit (temperature effects can slightly modify the MACAO optics located in the light path)..
- the ETC has been modified in various aspects, most notably by allowing the choice of sky and transmission spectra for different amount of precipitable of water vapour in the atmosphere.

**Since the release of User Manual v81.1**

- a first version of the CRIRES pipeline is available: <http://www.eso.org/projects/dfs/dfs-shared/web/vlt/vlt-instrument-pipelines.html>
- a new science template is offered, to apply the spectro-astrometric technique: see §11.2.4
- an intervention took place in December 2007; it consisted in
  1. replacing the slit viewer detector with a new, cosmetically better one; this should decrease the number of bad pixels that affect secondary guiding for faint targets;

2. replacing the entrance slit jaws; the new slit jaws have sharper edges and show a much improved parallelism, leading to a more constant resolution along the slit;
3. the temperature setting of the instrument has been changed slightly (70 K, instead of 65 K) to improve the temperature stability of the instrument; as a consequence, the wavelength configuration table has slightly changed: users wishing to use the standard wavelength settings should refer to the reference wavelengths listed in Tables 4a to 4h or 5a to 5h. Note that these tables now include two new columns referring to the *unvignetted range*, i.e., the spectral range over which the illumination could be reproduced to better than 1%, despite the lack of reproducibility of the intermediate slit (mainly) and other optical elements.

## Part I

# The instrument

## 2 Cold part: the spectrometer

The CRIRES instrument design is presented by [Käufel et al. 2004, SPIE 5492, 1218](#); a summary is presented in the following subsections.

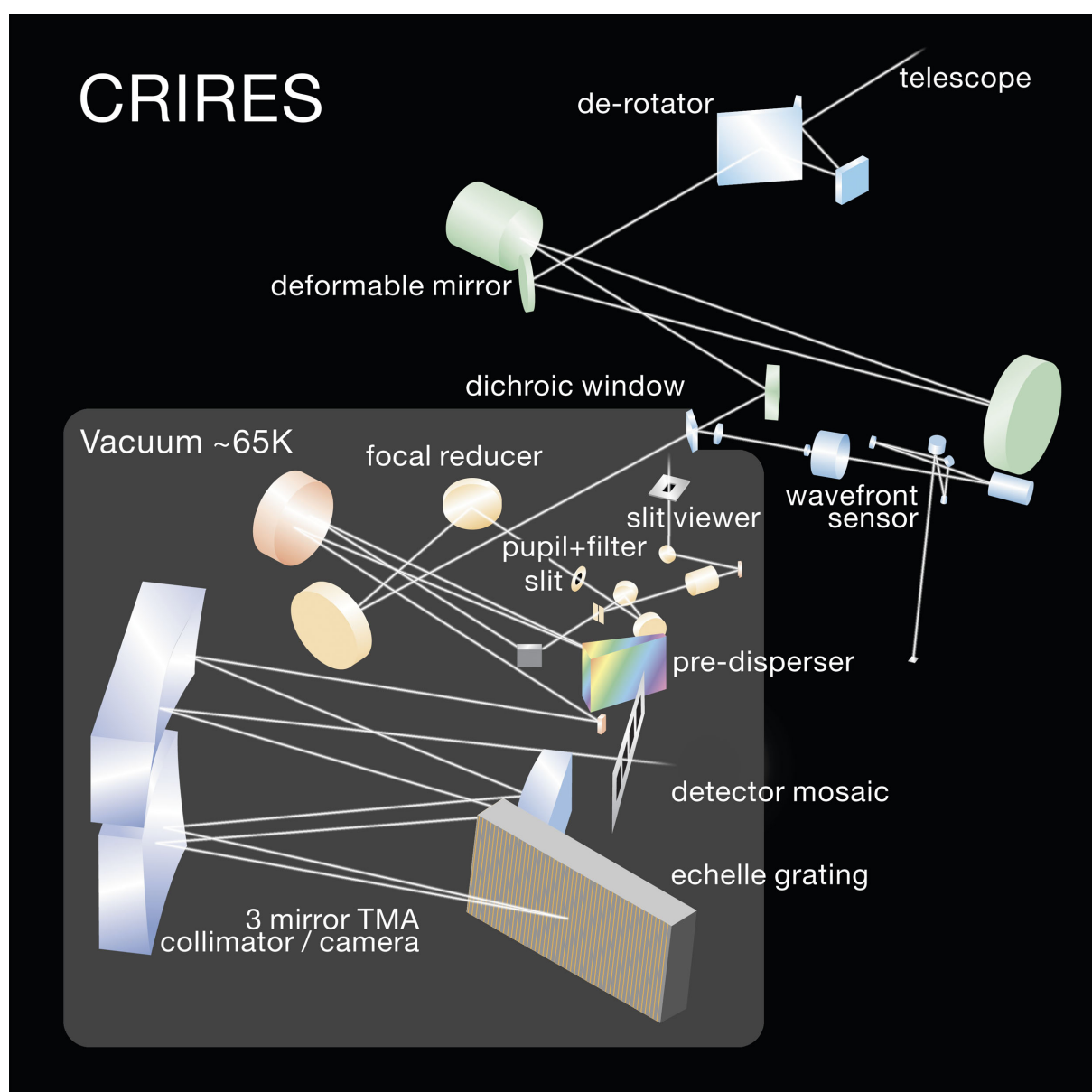


Figure 1: Layout of the CRIRES optical design.

## 2.1 Optics

The optical layout of CRIRES is shown in Fig. 1. Light enters from the direction of the telescope Nasmyth focus, either via the telescope or from the calibration unit after insertion of a calibration mirror in the light-path.

The calibration unit itself consists of an integrating sphere illuminated by a continuum, Halogen lamp for flat-fielding and, together with a gas-cell, for wavelength calibration. An IR-emitter lamp used for technical tests is also located in the integrating sphere. The integrating sphere provides uniform illumination of the entrance slit of the spectrometer and its flux can be adjusted by a moving baffle.

A carriage can then insert one of the following elements in the light path: (i) a gas-cell either for wavelength calibrations when used with the halogen lamp (which creates an absorption spectrum), or for accurate radial-velocity measurements, similar to the way the iodine cell is used in UVES; (ii) a pinhole used for calibration purposes; (iii) an AO fiber for MACAO calibrations; (iii) a set of fibers fed by a Thorium–Argon lamp used for wavelength calibration. This carriage has also a free position, with no optical element.

Light then goes through a 3 mirror de-rotator which can be used to counteract the telescope field rotation for observations with a slit fixed relative to the sky. On the other hand, for point sources, it can also maintain the slit aligned along the parallactic angle to accommodate the differential atmospheric refraction between the R band used by the adaptive optics system and the IR band used for observations and slit viewer guiding.

Next, the adaptive optics (AO) system concentrates the light on the spectrograph’s entrance slit. The AO wavefront sensor uses the visible light reflected by the dichroic (which serves also as entrance window) while the infrared light enters the cryogenic spectrograph. Further details of the AO system can be found in Sect. 3 of this manual. CRIRES can be used without adaptive optics, in which case the AO module just acts as relay optics and the spatial resolution is given by the natural seeing.

The spectrograph itself is housed in a vacuum vessel. Following the input window, a pupil image is formed at the position of a cold stop which limits thermal background. Light then either passes through the slit or is reflected to the slit viewing camera. Light passing through the slit enters the prism spectrometer where it is dispersed and then exits through an intermediate slit sized to limit the wavelength range passing into the high resolution section to a single order. The high resolution spectrograph consists of a  $40 \times 20$  cm, 31.6 lines/mm,  $63.5^\circ$  blaze echelle grating plus a TMA (three mirror anastigmat) which acts first as a collimator and then as a camera to image the spectrum on the four Aladdin detectors effectively forming a  $4096 \times 512$  array.

## 2.2 Mechanics

CRIRES is stationary at the Nasmyth A focus of VLT-UT1 (Antu). The instrument is mounted in a 3 m-diameter, 1 m high vessel. Including its support structure, the total weight of the instrument is 6.2 t, spread between 2 t for the warm part or AO system and 4.2 t for the cold part. The optics inside the cryo-vessel is cooled to  $\sim 70$  K. The detectors are stabilized at  $\sim 25$  K within 0.1 K. A main design feature of CRIRES is its cryogenic mechanisms which are required for scanning the pre-disperser prism and echelle grating.

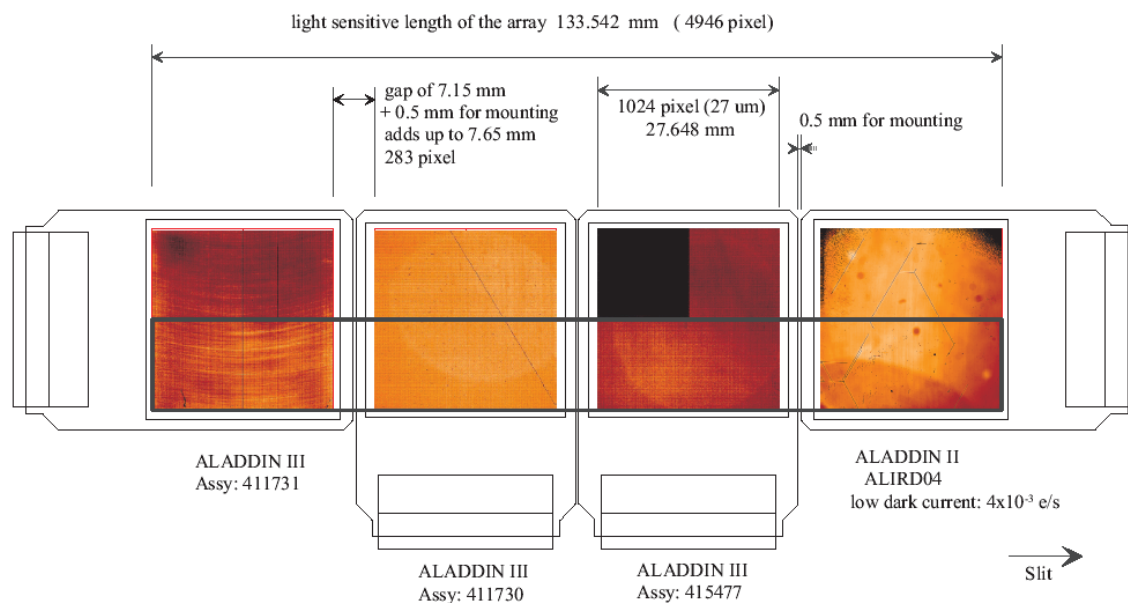


Figure 2: Layout of the mosaic of four Aladdin science detectors, numbered # 1 to # 4 from left to right. The detectors are not science grade arrays and show bad cosmetics. Only the bottom half part of each detector is used as indicated by the thick, black rectangle. The mosaic used for science observations therefore consists of  $4 \times 1024 \times 512$  pixels.

## 2.3 Detectors

The spectrograph focal plane provides a useful optical field of  $135 \times 21$  mm which is well covered by a  $4 \times 1$  mosaic of four Raytheon  $1024 \times 1024$  pixel InSb Aladdin III detectors, with a pixel size of  $27 \mu\text{m}$ . The spacing between 2 successive detectors corresponds to approximately 280 pixels, and is slightly different from one gap to the other. Fig. 2 shows their relative orientation. In particular, it should be noted that only the ‘bottom’ half of the mosaic is used and that the reading-out is executed parallel to the mosaic for detectors 2 and 3 and perpendicular to it for detectors 1 and 4.

A fifth Aladdin III detector is used in the slit viewer. The arrays are read out using standard ESO IRACE controllers having 64 channels ( $4 \times 16$ ) for the science arrays and 32 channels for the slit viewer one.

### 3 Warm part: the adaptive optics system

The adaptive optics system of CRIRES is discussed by [Paufigué et al. \(2004, SPIE 5490, 216\)](#). The multi-application curvature adaptive optics system (MACAO) for CRIRES corrects a turbulent wavefront and provides diffraction limited images at the focal plane. The overall sensitivity is thereby improved by about a factor two for point-sources. To highlight the advantage of combining MACAO and CRIRES a PSF is shown in Fig.3 in AO open loop (uncorrected) and closed loop, where the PSF is reconstructed from wavefront measurements. The non-circular PSF in open loop is due to the very short integration time used.

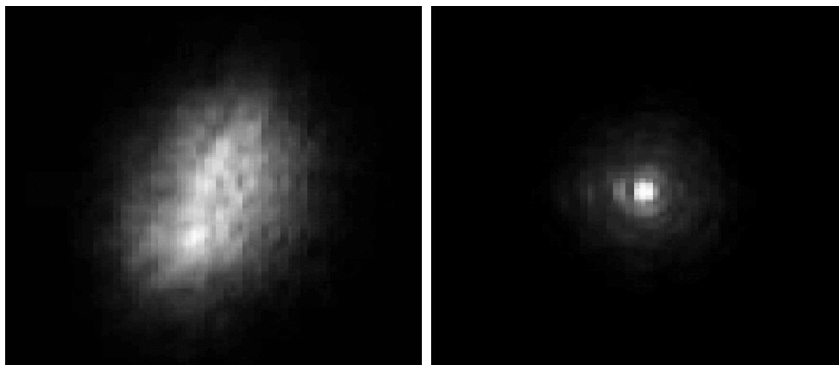


Figure 3: PSF without (left) and with (right) AO correction. Images have been taken in the lab using a turbulence generator.

#### 3.1 Introduction

The following section provides an introduction to the field of adaptive optics and atmospheric turbulence, and essentially is taken from the NACO user manual. For further reading, see for example: “Adaptive optics in astronomy”, Rodier 1999, Cambridge University Press, or “Introduction to adaptive optics”, Tyson 2000, Bellingham/SPIE.

##### 3.1.1 Atmospheric turbulence

The VLT theoretical diffraction limit is  $1.22 \cdot \lambda/D = 0.07$  arcsec at  $\lambda = 2.2\mu\text{m}$ . But the resolution is severely limited by atmospheric turbulence to  $\lambda/r_0 \approx 1$  arcsec, where  $r_0$  is the Fried parameter.  $r_0$  is directly linked to the strength of the turbulence and depends on the wavelength as  $\lambda^{6/5}$ . For average observing conditions,  $r_0$  is typically 60cm at  $2.2\mu\text{m}$ .

Temperature inhomogeneities in the atmosphere induce temporal and spatial fluctuations in the air refractive index and therefore cause fluctuations in the optical path. This leads to random phase delays that corrugate the wavefront (WF). The path differences are, to a good approximation, achromatic. Only the phase of the WF is chromatic. The coherence time of WF distortions is related to the average wind speed  $V$  in the atmosphere and is typically of the order of  $r_0/V = 60$  ms at  $2.2\mu\text{m}$  for  $V = 10$  m/s.

### 3.1.2 Adaptive Optics

A technique to overcome the degrading effects of atmospheric turbulence is real-time compensation of the deformation of the WF by adaptive optics (AO, Figure 4).

The wavefront sensor (WFS) measures WF distortions which are processed by a real-time computer (RTC). The RTC controls a deformable mirror (DM) to compensate the WF distortions. The DM is a continuous thin plate mirror mounted on a set of piezoelectric actuators that push and pull on the back of the mirror.

Because of the significant reduction in the WF distortions by continuous AO correction, it is possible to record near diffraction-limited images with exposure times that are significantly longer than the turbulence coherence time. The residual error from the WF compensation (WF error) directly determines the quality of the formed image. One of the main parameters characterizing this image quality is the Strehl ratio (SR), which corresponds to the amount of light contained in the diffraction-limited core relative to the total flux.

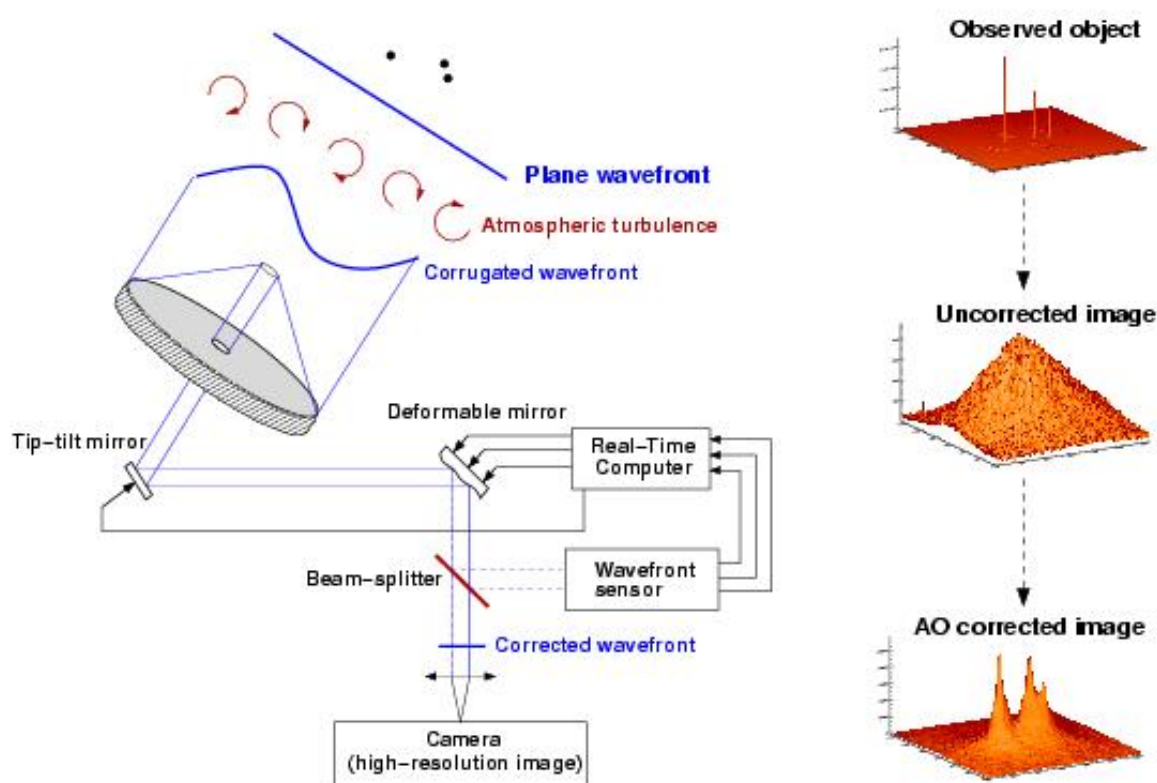


Figure 4: Principle of Adaptive Optics. Note that in practice, and contrary to this schematic design, CRIRES has no dedicated Tip-Tilt mirror, but performs low- and high-order corrections with a single deformable mirror mounted on a tip-tilt stage (see Figures 5 – 6).

An AO system is a servo-loop system working in closed loop. The DM flattens the incoming WF and the WFS measures the residual WF error.

A commonly used WFS is the Shack-Hartmann WFS, used for example in NACO. However, CRIRES, as well as the other ESO MACAO systems, relies on a curvature WFS: it is designed to measure the WF curvature as opposed to the WF slope. This is achieved by comparing the irradiance distributions of two planes placed behind and in front of the focal plane. In practice, a variable curvature mirror (membrane) is placed in the telescope focus. By vibrating, inside

and outside focus blurred pupil images can be imaged on a detector array: in the case of CRIRES, a lenslet array feeds avalanche photo-diodes (APDs). The modulation frequency of the membrane corresponds to the temporal sampling frequency of the WFS. The difference between the inside and outside pupil image measures the local WF curvature.

The performance of an AO system is related to the number of lenslets in the lenslet array, the number of actuators behind the DM, and the rate at which WF errors can be measured, processed and corrected (the server-loop bandwidth).

The performance of an AO system is also linked to the observing conditions. The most important parameters are the seeing, the brightness of the reference source used for WFS and the distance between the reference source and the object of interest.

In case of good conditions and a bright, nearby reference source, the correction is good and the resulting point spread function (PSF) is very close to the diffraction limit. A good correction in the K-band typically corresponds to a SR larger than 30%.

At shorter wavelengths (particularly in the J-band) or in the case of poor conditions or a faint, distant reference source, the correction is only partial - the Strehl ratio may only be a few percent.

## 3.2 Hardware description

The MACAO system for CRIRES is based on a 60-actuator deformable mirror, inserted in a so-called relay optics. These optics and the wavefront sensor optics are mounted on a bread-board located between the Nasmyth focus and the spectrometer. It is about 1.5m wide and a top view of the warm optics overlaid by the optical path is shown in Fig. 5, the assembly of the deformable mirror is displayed in Fig. 6.

### 3.2.1 The corrective optics

The wavefront correction is performed by a 60 electrode bi-morph mirror developed by CILAS, with a pupil diameter of 60 mm. The 60 electrodes are sandwiched between two thin piezoelectric PZT layers with opposite polarization. The outside surface of the PZT layers are grounded and covered with 0.1mm glass layers, the mirror side being silver coated. Applying a voltage to one electrode produces a constant curvature over its surface. The geometry of the electrodes in the 4 central rings (40 electrodes) matches that of the lenslet array sub-apertures, while the 20 remaining electrodes are located outside the pupil and constrain the edge of the pupil to correct 0-curvature aberrations: tip-tilt, astigmatism, etc. The deformable mirror (DM) provides a stroke to compensate atmospheric aberrations up to an optical seeing of 1". In order to relax the use of the outer electrodes of the mirror, the tip-tilt error is slowly offloaded to a tip-tilt mount designed and built by LESIA, which provides a  $\pm 240''$  mechanical stroke, i.e.  $\pm 3.6''$  on the sky, with a 100 Hz -3dB internal closed-loop bandwidth. The assembly of the DM and tip-tilt mount is shown in Fig.6.

### 3.2.2 The Wavefront Sensor

The following functions are sequentially implemented in the wavefront analyzer:

- Extraction of the reference star beam (field selector).

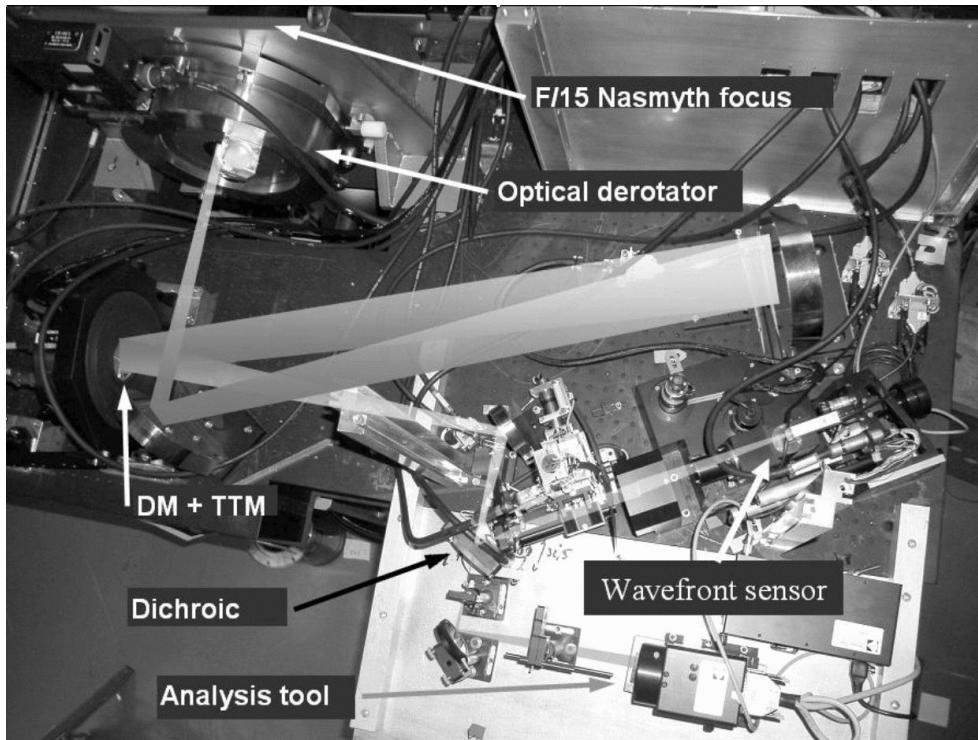


Figure 5: Top view of the warm optics of the MACAO – CRIRES system. From f/15 Nasmyth focus and after the optical derotator, one notices the deformable mirror and tip-tilt mount assembly. Light enters from the dichroic to the cold and warm part of the instrument. For the latter the wavefront sensor and some analysis tools are visible.

- Projection of the reference star image on the membrane mirror (imaging lens).
- Scan of the intra- and extra-pupil regions by modulation of the membrane mirror curvature.
- Creation of a pupil image centered on the lenslet array.
- Reduction of the flux to work within the linear range of the APDs by means of neutral density filters.
- Re-imaging of the 60 sub-pupils on the 60 fiber cores by the lenslet array unit.
- Injection of the collected beams onto the 60 APDs.

The scanning lens of the field selector is mounted on an XYZ table: the XY axes enable the star used for AO correction to be selected in the  $50'' \times 50''$  field-of-view, while the Z stage compensates for the VLT field curvature. The position of the field selector defines the reference for the pointing. The imaging lens creates an image of the AO star on the membrane mirror, which is mounted on an acoustic cavity. A voice coil is mounted to the other end of the cavity, and driven at 2.1kHz by the APD counter module to force an oscillation of the focus mode of the membrane mirror. The incidence angle of the beam on the membrane mirror depends on the position of the guiding star in the field. In order to keep the pupil image (obtained when the membrane mirror is flat) centered on the lenslet array, the membrane mirror is mounted on a 2 axis gimbal mount, which is co-ordinated with the field selector. For each  $(x, y)$  position

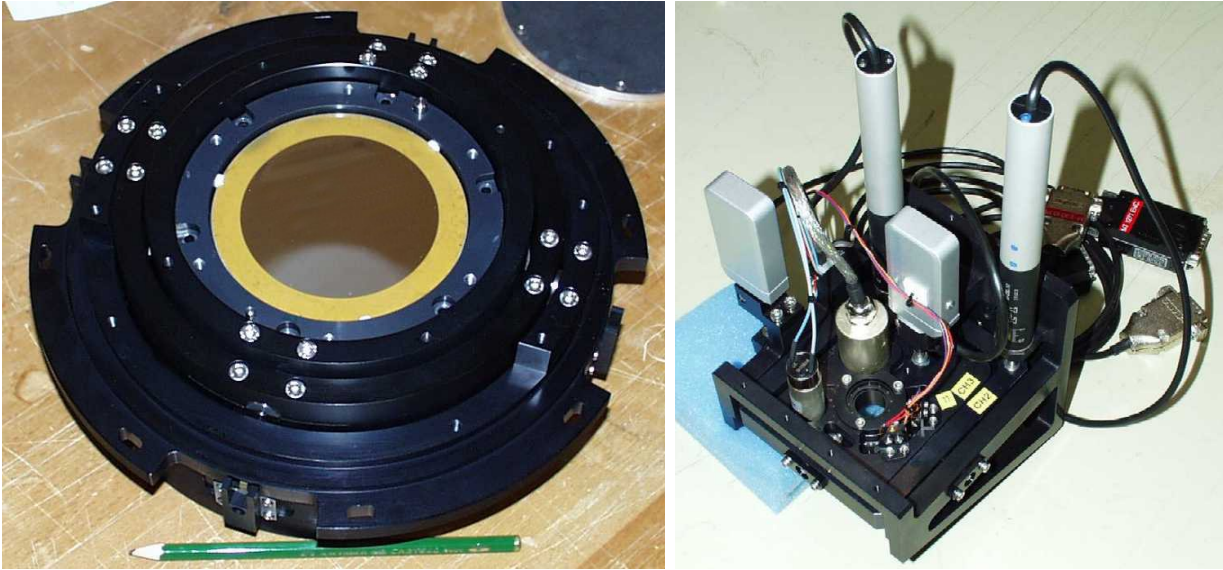


Figure 6: Assembly of the deformable mirror (DM) and tip-tilt mount (TTM) (left) and of the gimbal mount (right).

of the field selector the gimbal mount is moved so that the light is reflected to the same focus. A diaphragm in front of the membrane enables the field to be adjusted to the observing conditions (seeing and guiding reference size). The assembly of the gimbal mount is shown in Fig. 6.

The wavefront sensor box consists of 4 mirrors, which provide parallel beam to image the pupil on the lenslet array. First, the beam is collimated by a spherical mirror. It is then folded by a flat mirror and injected in the beam expander, which adapts its diameter to the lenslet array (14 mm). The optical path of the wavefront sensor box is shown in Fig. 7.

The lenslet array intercepts the beam and divides the flux in 60 sub-aperture. Each sub-pupil is imaged on a fiber, with a  $100\ \mu\text{m}$  core diameter. When the membrane mirror vibrates, the pupil image is projected on both sides of the lenslet array plane. The normalized difference between the intra- and extra-pupil flux collected by each sub-aperture is proportional to the local wavefront curvature, which provides the wavefront error. The fibers drive the signal from the fiber feed module to the APD cabinet, mounted on the instrument. The APD counts are recorded by the APD counter module, synchronously with the membrane signal. The front-end assembly of the fiber bundle is shown in Fig. 8.

### 3.2.3 Control loop

The oscillating membrane produces a signal modulated proportional to the local wavefront curvature. This signal, collected by APDs, is sent to the real time computer (RTC). The RTC computes this modulation, and retrieves the voltages to be applied to the mirror and tip-tilt mount to optimally compensate for the local curvature measured. For this, a precise calibration of the system is required, which includes synchronization of the membrane mirror, determination of the membrane curvature, pupil alignment and interaction matrices.

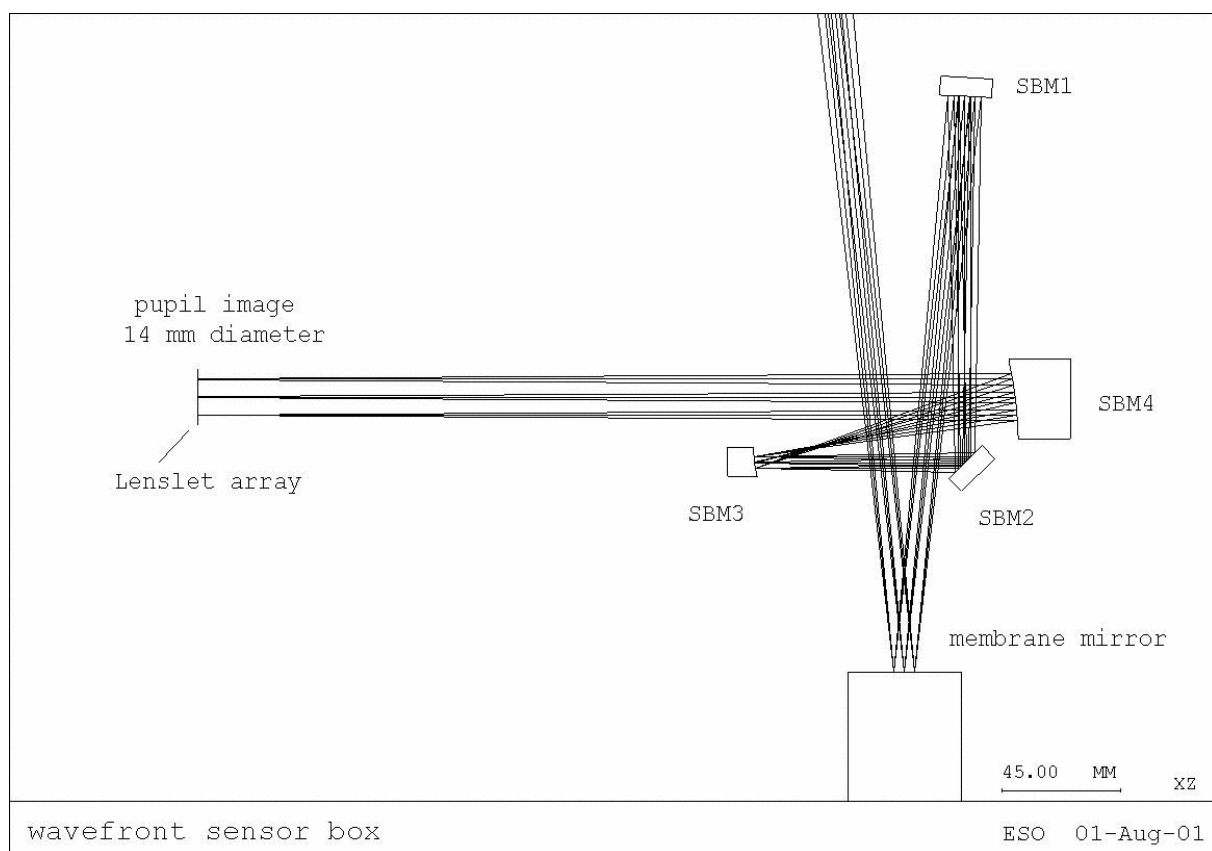


Figure 7: The optical path of the wavefront sensor box.

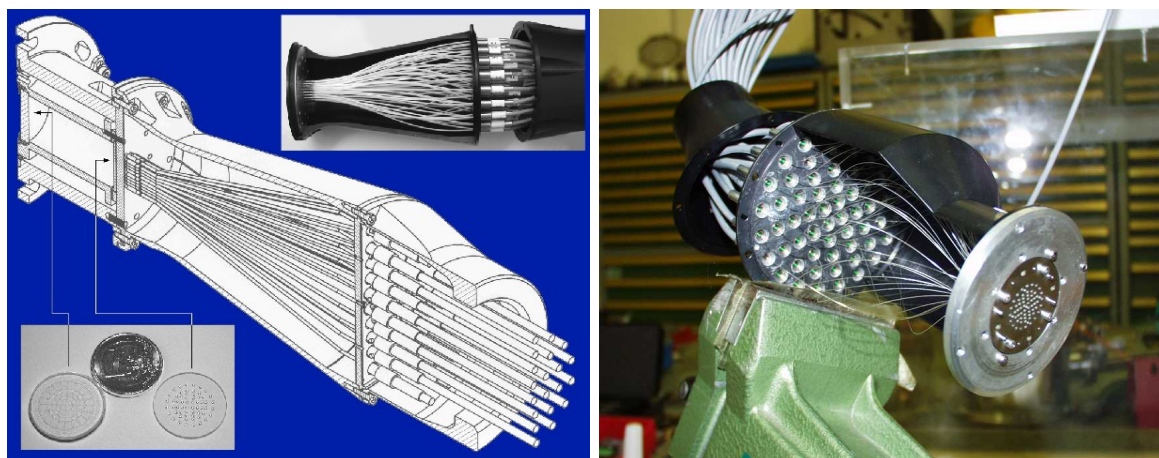


Figure 8: Front-end assembly of the 60 fiber bundle which guide the light to the sensors.

### 3.2.4 Membrane setting

The membrane mirror curvature represents an optical gain for the aberration measurements. A way to increase the performance of the system is therefore to increase the curvature of this mirror. Increasing the curvature, however, requires increasing the field of view of the wavefront sensor optics as well. This and some other non-linear effects can degrade the estimate of the curvature. For the same reason, extended sources will affect the quality of curvature measurement, and lead to a different optimal gain. In some extreme cases, the system can be unable to close the loop (extended 6'' planetary nebula with a faint blue white dwarf in the middle, or a faint star close to the Moon, for example). A trade-off is needed, and an optimal optical gain has to be determined. This optimal gain mainly depends on the seeing, and marginally on the star magnitude and other factors. It is tabulated in the configuration of the software and is transparent to the user.

## Part II

# Instrument Performance

## 4 Overview

The sensitivity of the instrument from K-band up to the L and M bands is limited by the thermal background, whereas it is limited by detector performance in J and H. In the thermal background observations benefit from the high resolving power of CRIRES as telluric features are better removed compared to spectrographs at lower resolution.

Possible sources of fringing (e.g interference filters) were avoided in the spectrograph design. The requirement on the grating reproducibility has been set to  $\sim 0.05$  pixel. Currently, the absolute wavelength reproducibility is achieved by the optical model to  $\approx 3$  pixels.

The detectors are not science grade arrays: they show bad cosmetics and amplifier glow; their response to incident light is non-linear. Information loss caused by bad pixels can be removed by jittering; the amplifier glow in any given exposure can be subtracted out by a dark obtained with the same detector integration time (DIT, see below). However, amplifier glow as well as other systematic effects are best removed by telescope nodding. A method to correct for the non-linearity of the detector has been implemented in the pipeline.

A first light spectrum of the sky is shown in Fig 9. The OH doublet at 1708.6nm is resolved at the resolution of CRIRES. In the dispersion direction the FWHM is 2.8 pixels.



Figure 9: First light spectrum of the sky. The OH doublet at 1708.6nm is resolved at the resolution of CRIRES.

## 5 AO performance

The performance achieved by the MACAO system of CRIRES has been evaluated by laboratory simulations by comparing two cases: (i) in closed loop with guide stars of various magnitudes and (ii) in open loop, thus without AO corrections. The optimization was done over the encircled energy on a  $0.2''$  slit, representative of the available energy for the spectrograph. Lab results are confirmed by on-sky measurements and demonstrate some gain in J (more than to 40% for an optical seeing of  $0.6''$ ) and a strong (factor  $\sim 2$ ) increase of the fraction of the energy available for the spectrograph in the K and M band, respectively (Fig. 10).

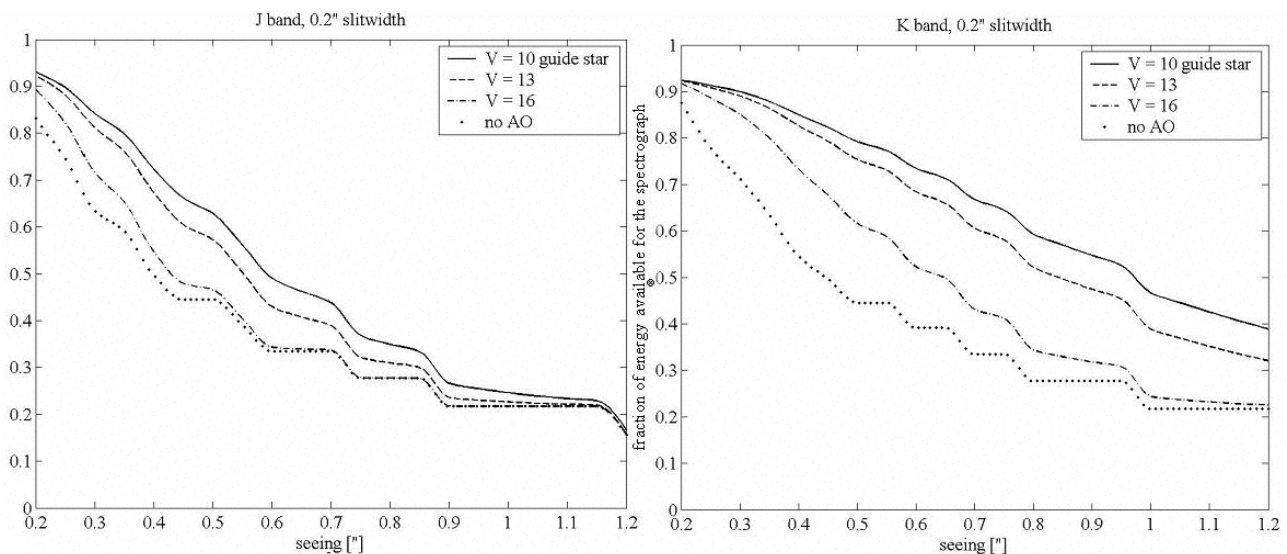


Figure 10: The fraction of energy available for the spectrograph in a  $0.2''$  slit, as a function of optical seeing is shown for the J (left) and K (right) band for AO stars of  $V=10, 12, 16$  mag and without AO correction. For reference please consult the [Exposure Time Calculator, \(ETC\)](#).

Fig. 11 illustrates the increased throughput made possible thanks to the use of the adaptive optics. The graphs shows the spatial profile (summed over a few columns) at  $\lambda = 2170\text{nm}$  of the spectrum of a  $m_{\text{RTC}} = 5.3$ , in open- and closed- loop. The DIMM seeing was  $0.67$  and  $0.72''$ , respectively, and the coherence time was  $3$  ms. In both cases, the exposure time was  $2$  min. The gain in integrated flux is  $1.63$ . In other words, the same flux level is reached in closed-loop in  $61\%$  of the time needed in open-loop.

### 5.1 AO guide stars

CRIRES wavefront sensing is done in the R band. The performance of the adaptive optics system depends on the distance to the science target and on the brightness of the selected guide star.

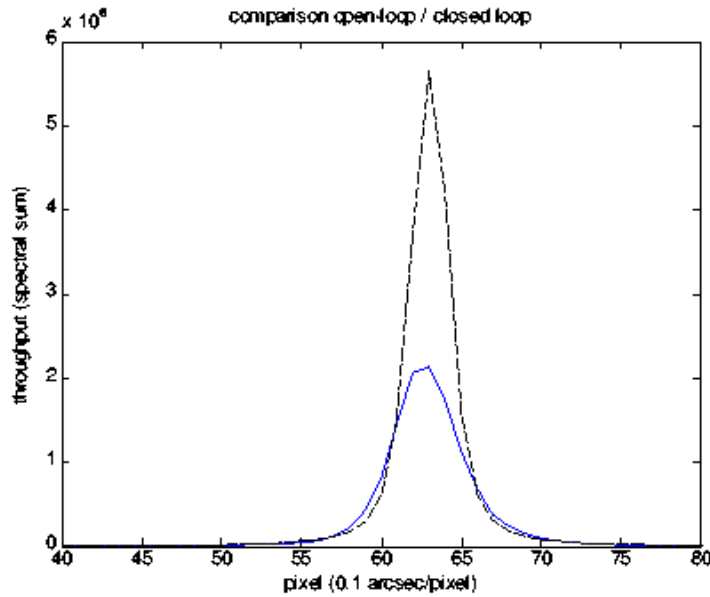


Figure 11: Improved throughput thanks to the use of the MACAO. Flux measured along the slit, measured in open-loop (blue, solid line) and in closed loop (black, dashed line), in the K band.

### 5.1.1 The distance of the AO star

Although the field selector allows the selection of the AO star within 25 " from the nominal position of the science target, the AO star should be as close as possible to the scientific target, usually closer than 10 ": ideally, it is the science target itself. Depending on the atmospheric conditions, in particular, on the isoplanatic angle,  $\theta_0$ , mild improvement in the amount of encircled energy can still be obtained if a bright ( $R < 11$ ) AO star is used 20 – 30 " from the scientific target.

It is important to recall that the isoplanatic angle decreases with zenith distance  $z$  as  $\theta_0 \propto (\sec z)^{-8/5}$  and increases with wavelength as  $\theta_0 \propto \lambda^{6/5}$ . On the other hand, the Strehl ratio decreases with the angular distance to the AO star  $\theta$  as  $SR \propto \exp(-(\theta/\theta_0)^{5/3})$ .

### 5.1.2 The brightness of the AO star

The intra- and extra-focal pupil of the AO star is imaged on a lenslet array. Each lenslet feeds an avalanche photo-diode (APD) that ultimately forwards its signal to the Real Time Computer (RTC) (Sect. 3).

The flux on an APD is limited to 1 million counts in order not to damage the devices. The optimal brightness of the AO star is  $R \sim 11$  mag. Brighter stars up to a bright magnitude limit of  $R \sim 0.2$  mag can be dimmed using neutral density filters. Depending on the B-R colour, some stars with slightly brighter R magnitude can be used.

Good correction is still obtained with stars as faint as  $R \sim 14$  mag under average seeing condi-

tions, while moderate image quality improvement is seen with stars as faint as  $R \sim 16-17$  mag under good seeing ( $\leq 0.6''$ ) conditions. Stars fainter than  $R \sim 17$  mag will not result in any improvement.

### 5.1.3 The color of the AO star

The B-R color is important for precise atmospheric refraction compensation. The AO system takes into account the differential atmospheric refraction between the wavelength used for the AO and the central wavelength of the spectrograph set-up in the calculation of the tip-tilt mirror orientation. A correct B-R is *crucial* for accurate centering of the target in the slit for airmass  $> 1.2$  when guiding with the slit viewer is not possible, as for example, if the AO star is outside the field-of-view of the slit viewer detector.

## 5.2 Limiting magnitude of slit viewer

Target centering in the NIR is optimized by slit viewing. The slit viewer (SV) is sufficiently sensitive that any emitting point source for which one aims to obtain a spectrum should be seen on the SV image. In particular in AO mode, stars of  $J \approx 14$  or  $H \approx 14$  are easily detected in a 10 s exposure, a typical time scale for guiding.

In NoAO mode,  $J=16.5$ ,  $H=16.0$ , or  $Ks=15.4$  stars are barely detected ( $3\sigma$ ) in a similar 10 s integration under  $0.9''$  seeing when located away from the slit. For guiding on target in NoAO mode, the limiting magnitude is much brighter as only a small fraction of the light is reflected by the slit jaws to the slit viewer detector. Under  $0.9''$  seeing and a slit of  $0.4''$ , reasonable guiding was possible with stars of  $J = 14.1$ ,  $H = 13.8$ ,  $Ks = 13.3$ .

Table 1: Summary of detector parameters.

Parameter	Detector			
	# 1	# 2	# 3	# 4
Dark current ( $e^-/s$ )	0.053	0.32	0.37	0.34
Gain ( $e^-/ADU$ )	6.97	6.89	6.92	7.27
Quantum efficiency ( $e^-/\gamma$ )	0.92	0.97	0.83	0.73
Read-out-noise ( $e^-$ RMS)	9.9	9.7	9.6	10
Saturation level ( $e^-$ )	120000	120000	120000	120000
Operating Temperature (K)	27.5	27.5	27.5	27.5

## 6 Detector characteristics

The focal plane of CRIFES is equipped with four  $1024 \times 1024$  pixel InSb Aladdin III,  $27 \mu$  pixel detector arrays. However, only the bottom half of each detector is actually illuminated by the slit, so that the useful mosaic actually consists of  $4 \times 1024 \times 512$  pixels (Fig. 2). The observer needs to specify the detector read-out mode (FowlerNsamp or FowlerNsampGrstWin). In both read-out modes, the following two detector parameters must be specified: the detector integration time (DIT) and the number of individual exposures (NDIT) to be averaged in a single exposure, whose total integration time is therefore  $NDIT \times DIT$ . Both parameters should be adjusted with help of the ETC (Sect. 10.2). Bright objects or observations in the L or M bands require short DITs to avoid saturation; in particular, heavily saturated spectra lead to detector remanence that affects subsequent observations. On the other hand, faint targets in the J, H or even K bands may require DITs up to 900s to decrease the readout-noise contribution. Long DITs are strongly affected by the detector glow which can be corrected by nodding (Sect. 9.2).

All other detector settings such as bias, voltages, operating temperature, etc. are automatically set by the system.

The default read-out mode is *Fowler Sampling* (Fowler & Gatley 1990 ApJ 353, L33; abbreviated as FowlerNsamp for use in templates): the detector is first reset, then each pixel is non-destructively read  $NDSAMPLES/2$  times at the start of the exposure, then again  $NDSAMPLES/2$  at the end of the exposure of exposure time DIT. The slope of the relation provides the intensity of the given pixel. The value of NDSAMPLES is 2 for DITs strictly smaller than 10 s, 4 for DITs at least equal to 10 s but strictly smaller than 20 s, etc... up to a maximum of 128. The value of NDSAMPLES for a given frame is available in the FITS header (DET.NDSAMPLES).

The intensity of a pixel corresponds to an exposure time of one DIT. If NDIT is larger than 1, the reading process is repeated NDIT times and the values for a given pixel are averaged. Therefore, the value saved always corresponds to an exposure time of one DIT. If the number of exposures (SEQ.NEXPO) is larger than 1 in the template, each individual exposure is saved independently.

In case of very bright targets, the *Fowler Sampling with Global Reset and Windowing* can be

used. The name of this mode is abbreviated to FowlerNsampGRstWin for use in templates. This mode only reads detector #2 and #3. It executes a global reset of the detector before applying the Fowler Sampling on two small stripes that fully cover detector #2 and #3 in the spectral direction but only a user selected number of pixels (64, 128 or 256) in the spatial direction. As only a small fraction of the detector is read, shorter DITs can be used. On the other hand, for comparable DITs, this mode allows to reduce the read-out noise by a factor  $\sim 2$  compared to the FowlerNsamp read-out mode: consequently, observations of faint targets are less affected by the read-out noise. This improvement is not yet implemented in the ETC.

## 6.1 Dark and gain

In Fig. 12 dark current and conversion gain of detector # 2 are shown. The dark current is estimated from the slope of the signal (in ADU or  $e^-$ ) as a function of integration time (s) for the linear region. Dark current, gain, read-out-noise, saturation of the four detectors # 1, # 2, # 3, and # 4 as well as the operating temperature are given in Table 1. Note that the raw gain values (cf. Fig 11) have been corrected by a factor of 0.9 to take into account the interpixel capacitance (see Finger et al. 2006, SPIE 6276, 62760F).

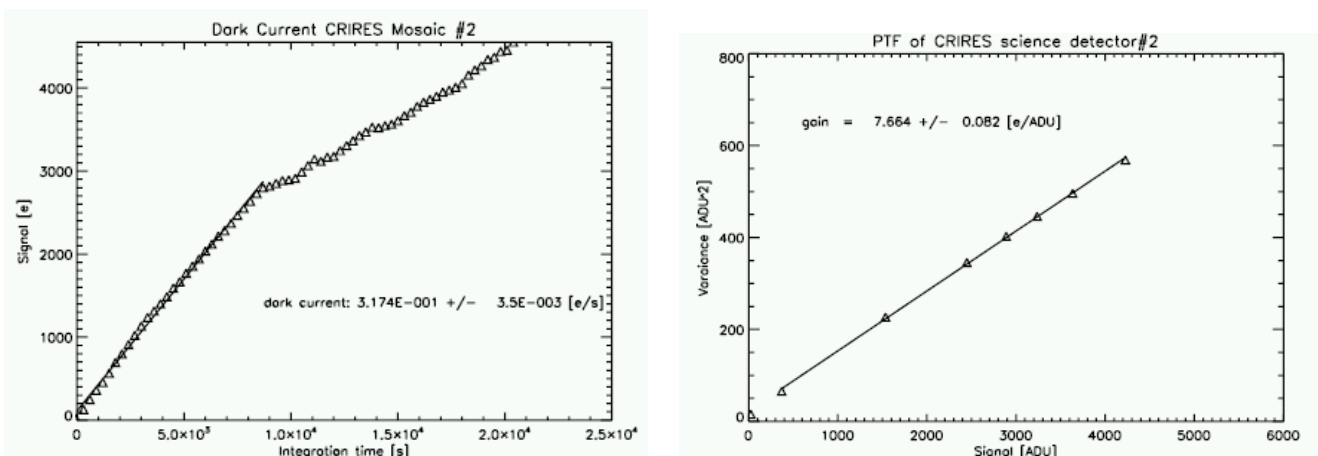


Figure 12: Dark current (left) and conversion gain (right) of detector # 2.

## 6.2 Glow

The detectors show glow over areas close to the amplifiers, as clearly visible in Fig.13. It is stable and can be subtracted by an exposure obtained with the same DIT. The glow increases with DIT. Therefore, in order to best remove it as well as other detector systematics, it is recommended that observations in any given wavelength setting should include at least one nodding cycle. Note however that areas affected by the glow suffer from increased Poisson noise.

## 6.3 Fringes

No detector fringes are detected in the wavelength range useful for science observations. Fringes are only visible beyond  $5\mu\text{m}$ , outside the atmospheric window.

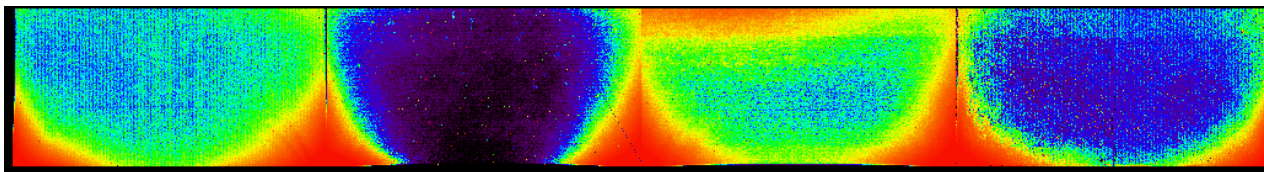


Figure 13: Example of the detector glow on a dark exposure. The detector glow (in red) is emerging from the bottom corners of each detector.

## 6.4 Odd-even effect

Images obtained with the science detectors show a pattern aligned with the reading direction. In other words, the pattern is aligned with the rows of the detectors, parallel to the spectral dispersion, for detectors # 2 and # 3. For detectors # 1 and # 4, the pattern is instead aligned with the columns, i.e. perpendicular to the spectral dispersion. This pattern consists of alternating rows or columns of larger and smaller intensities than the mean value.

This effect cannot be removed by simple flat fielding and is still visible after nodding. Figure 14 gives an example based on a sequence of flats obtained with different DIT settings. It shows that this “odd-even” effect depends on the signal level. A method to correct for the odd-even effect is described in the next paragraph.

## 6.5 Correcting for detector non-linearity

All common IR detectors suffer from non-linear effects. In the case of CRIRES, deviation from linearity is of the order of 3% of the detected flux at about 4,000 ADUs ( $\approx 32,000e^-$ ) and increases with flux.

The CRIRES team has developed a method that appears to efficiently correct for the non-linear behavior of the detector, *including the odd-even effect*. Results obtained at the date of issue of this manual indicates that a total signal (dark + sky + object) smaller than about 10,000 ADUs ( $\approx 70,000e^-$ ) can be corrected with good accuracy (residuals much smaller than 1%), providing *both* the science *and* the flat-fields are taken with DITs longer than 2 s. Data obtained with shorter DITs are affected by the finite reset time of the detector arrays.

The method is more detailed in the description of the [CRIRES pipeline](http://www.eso.org/observing/dfo/quality/CRIRES/pipeline/pipe_gen.html) at [http://www.eso.org/observing/dfo/quality/CRIRES/pipeline/pipe\\_gen.html](http://www.eso.org/observing/dfo/quality/CRIRES/pipeline/pipe_gen.html) and, in particular, in the section dealing with the [science recipes](#). Static calibration files necessary to correct for the non-linearity are available at [http://www.eso.org/observing/dfo/quality/ALL/ref\\_frames/ref\\_crires.html](http://www.eso.org/observing/dfo/quality/ALL/ref_frames/ref_crires.html).

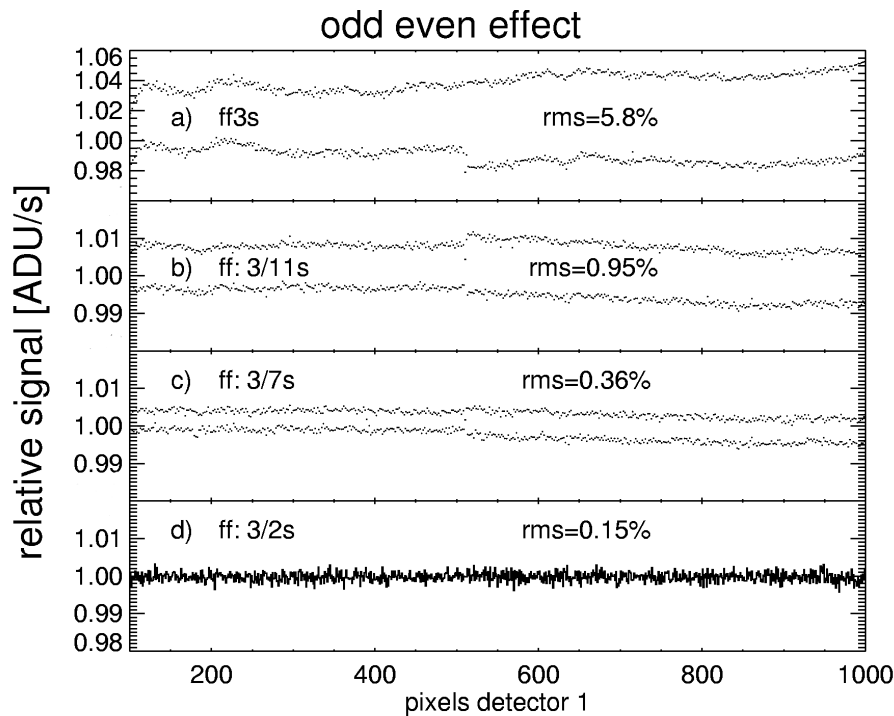


Figure 14: Flats obtained with the halogen lamp at different DITs, for detector 1. Each graph represents 1000 pixels of the image collapsed along the columns. A DIT=1s dark exposure has been subtracted from each image. From top to bottom: (a) a 3 s flat (ff3s) normalized to its median value shows a bimodal distribution of intensities, reflecting the odd–even effect. The measured RMS of the normalized flat is 5.8%. Panel (b) shows the ratio between two dark subtracted flats of 11s and 3s, respectively. The ratio shows an RMS of 0.95%. Panel (c) is similar to (b) but for flats with DITs of 3 and 7s, respectively. The RMS of the ratio is 0.36%. Panel (d) shows that the ratio for 2 flats obtained with DITs of 2s and 3s, respectively has an RMS of 0.15%. The decrease of the scatter in the ratio of flats when DITs tend to be similar demonstrates that the odd–even effect depends on the signal level.

## 7 Characteristics of the spectrograph

### 7.1 Wavelength settings

Wavelength settings are defined by a *reference wavelength* that corresponds to the wavelength at the middle of detector 3. In a few cases (see §7), this reference wavelength is not sufficient, and an additional number, the *grating order* is needed.

Set-ups are done by using the instrument model to position the spectrum with an absolute accuracy to better than 30 pixels and a reproducibility  $\approx 3$  pixels. Reproducibility to a fraction of a pixel is expected once the use of the metrology fibers is implemented end of December 2009.

Typically about 280 CRIRES settings are sufficient to cover the entire infrared spectrum in the range of  $955 \leq \lambda \leq 5248\text{nm}$ . Standard wavelength settings are detailed in Sect. 15. Wavelengths can also be set using free wavelength settings: allowed ranges for the reference wavelength are listed in Tab. 6a.

Tables 4a - 4k (Tables 5a - 5k) therefore now provide under the columns *Unvignetted range* the wavelength (wavenumber) ranges for which reproducibility of the illumination is estimated to be better than 1 % for a 0.4'' slit. Wavelength outside of these ranges but still covered by a detector are subject to contamination from adjacent orders. The wavelength range for which the reproducibility of the illumination is better than 1% is smaller for a wider slit. For an 0.8'' slit, the whole spectral range covered by the mosaic is likely affected by contamination by adjacent orders. *As a consequence, slit widths larger than 0.4'' should be avoided in general.*

*Vacuum wavelengths are used throughout this manual.*

### 7.2 Wavelength calibration

#### 7.2.1 Standard means: ThAr lamp and N<sub>2</sub>O and CO gas-cells

Wavelength calibration of CRIRES spectra is difficult. Depending on the wavelength and on the required accuracy, different methods can be used. For an accuracy corresponding to 3 pixels, the start and end wavelengths and the derived dispersion assumed to be linear for each detector is sufficient, in particular for the standard settings.

If present in raw data, either emission or absorption sky lines can be used in the data reduction to improve the absolute wavelength calibration. The CRIRES team has started to obtain data to quantify the absolute accuracy of such a method. However, the number of sky lines is insufficient to achieve a high precision absolute wavelength calibration for many settings, in particular those below 2500 nm.

The density of lines provided by arc lamps is usually small in the IR. However, the Thorium-Argon lamp can provide a large number of lines up to about 2500 nm. The ESO Calibration and Instrument Modelling group in Garching together with the US National Institute of Standards and Technology have collaborated to increase the number of identified Thorium and Argon lines in the NIR. This collaboration to support the wavelength calibration of CRIRES lead to a paper available in the **Tools section** in the CRIRES web page. Users whose science has benefitted from the ThAr calibration should cite Kerber, F., Nave, G. & Sansonetti, C.J., *ApJS*, 2008, 178, 374.

The atlas and line catalogue is available through <http://physics.nist.gov/PhysRefData/ThArLampAtlas/ThArLampAtlas.html>. It is also included in the static *CRIRES calibra-*

tion data page at [http://www.eso.org/observing/dfo/quality/CRIRES/pipeline/pipe\\_calib.html](http://www.eso.org/observing/dfo/quality/CRIRES/pipeline/pipe_calib.html).

An additional high-precision method is provided by the use of a N<sub>2</sub>O gas-cell in front of a halogen lamp, as the N<sub>2</sub>O lines are recognized wavelength standards beyond 3500 nm. However, they are only present in a limited number of settings. The list of N<sub>2</sub>O lines is also available at [http://www.eso.org/observing/dfo/quality/CRIRES/pipeline/pipe\\_calib.html](http://www.eso.org/observing/dfo/quality/CRIRES/pipeline/pipe_calib.html) and is also part of the CRIRES pipeline distribution.

The following guidelines should be considered in case high precision absolute wavelength calibration is required. Section 18 details the recommended method to carry-out an accurate wavelength calibration for each order.

1. *Sky lines*: A possible output of the ETC is the emission sky spectrum for the requested reference wavelength. Its examination should provide enough information as to decide if the required wavelength accuracy can be achieved.
2. *ThAr lamp*: For wavelengths below 2300 nm the Thorium–Argon lamp provides enough lines for a good wavelength calibration. Since April 2008, the ThAr spectra are obtained by means of a set of fibers. This method allows to avoid strong scattered light sometimes mimicking real lines and making the identification difficult. The several spectra obtained also provide a way to determine the distortion of the spectrograph. An example of a ThAr wavelength calibration frame can be seen in Fig 15.
3. *N<sub>2</sub>O gas-cell*: For wavelengths longer than 3500 nm, N<sub>2</sub>O is a strict (National Institute of Standards and Technology, NIST) wavelength standard. For shorter wavelengths, the available line list originates from the HITRAN database, itself based on Toth et al. (see <http://cfa-www.harvard.edu/hitran/>). Unfortunately, N<sub>2</sub>O has no lines below 1650 nm and only weak lines between 1650–2100 nm. Their distribution over the detectors for a given wavelength setting can be seen by using the ETC. A line list can be accessed from the Tools section in the CRIRES web page.
4. *CO gas-cell*: A CO gas-cell has been available since April 2008. The line list is also available at the NIST web site and will soon be available at the Tools section of the CRIRES web page.

It is also possible to use the N<sub>2</sub>O or CO gas-cell *during the observations themselves*, that is to have the gas-cell on the light-path of the astronomical object. First results from science verification or commissioning data or regular science observations indicate that a radial velocity accuracy of the order of  $\sim 20$  to  $30 \text{ m s}^{-1}$  can be reached. A monitoring programme has started to determine the long-term behavior.

It is important to note that the atmosphere itself contains N<sub>2</sub>O. Therefore, it is difficult to disentangle the origin of N<sub>2</sub>O lines originating in the gas-cell from the ones originating in the atmosphere, at least in the L or M band. In the K band, N<sub>2</sub>O lines originating from the atmosphere are weaker but still present. Similarly, the CO gas-cell can also be used for observations. Its use is particularly recommended in the K band (order 24).

The CRIRES team is actively working on alternative solutions for wavelength calibration, such as an accurate instrument model or the use of additional gas-cells. In particular, it is currently testing an OCS gas-cell in the laboratory.

Note that the temperature of the gas-cells is not controlled, but is left to fluctuate with the temperature within the telescope enclosure.

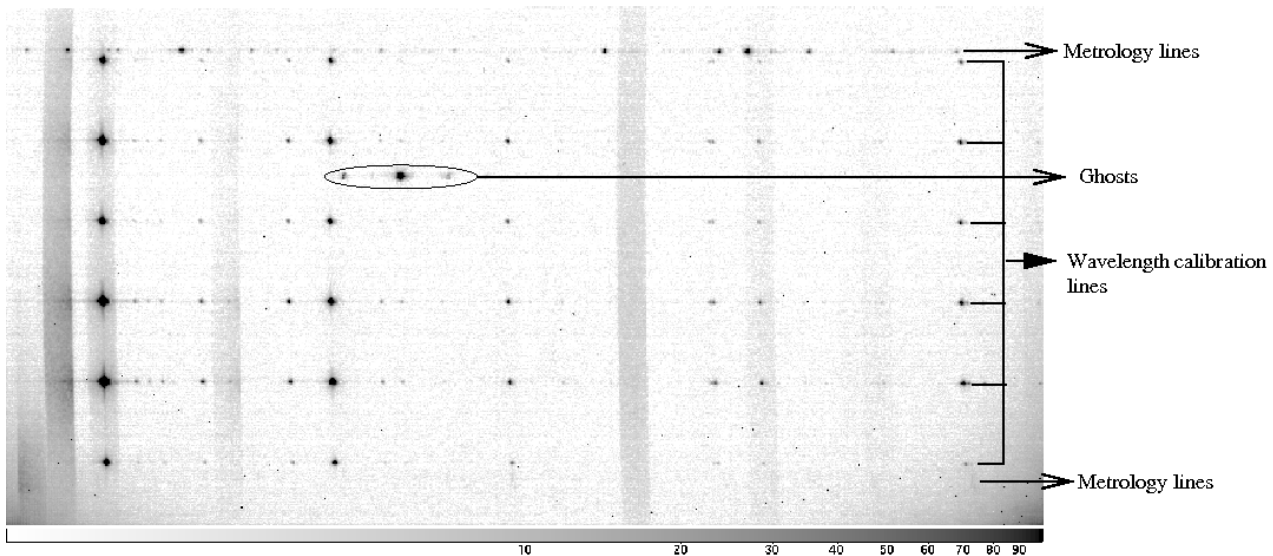


Figure 15: Example of a ThAr wavelength calibration exposure, corresponding to a reference wavelength of 1090.4 nm, detector #3. In addition to the lines to be used for wavelength calibration, the ThAr lines that will be used for metrology are visible at the top and bottom of the frame. In this setting and in a few other ones, ghosts are also visible.

### 7.2.2 Radial velocity measurements

Huelamo et al. (2008, A&A 489, 9), Seifahrt & Kaeufl (2008, A&A 491, 929), Figueira et al. 2009 (arXiv:0912.2643v1) and Bean et al. 2009 (arXiv:0912.0003v1) have demonstrated that accurate radial velocity measurements to better than  $\approx 35 \text{ ms}^{-1}$ , even possibly to  $10 \text{ ms}^{-1}$ , are feasible with CRIRES. The Seifahrt & Kaeufl (2008) study covered data over only  $\approx 4\text{h } 30\text{m}$ , while the Huelamo et al. (2008) study extends over slightly less than 7 days. Bean et al. (2009) find a typical internal precision of the measurements of  $\sim 10 \text{ ms}^{-1}$  with the use of an ammonia gas-cell over several months, with the Figueira et al. study providing a similar precision over a week without the gas cell (in NoAO mode).

Wavelength calibration is of course the critical aspect of all radial velocity measurements: a  $10 \text{ ms}^{-1}$  precision corresponds to a mean error on the solution of  $\approx 0.007$  science detector pixel. Some fundamental parameters regarding radial velocity measurements can be found in Bouchy, F., Pepe, F., & Queloz, D. (2001, A&A, 374, 733). However, this paper mainly deals with measurements in the optical regime though, and some results are not valid in the CRIRES accessible spectral range.

Regarding CRIRES observations, the following aspects require particular attention: (1) number of (absorption) lines of the star within the spectral range of interest; (2) number of lines used for wavelength calibration; (3) spectral resolution; (4) slit illumination and photocenter error; (5) flat-fielding error. These are briefly discussed in the following:

1. in general, the number of absorption lines should be as high as possible; however, blending or presence of broad lines should be avoided;
2. the number of lines used for wavelength calibration should also be as high as possible; here also, the presence of broad lines should be avoided. In the spectral range of CRIRES, telluric lines offer a natural choice of wavelength calibration lines. However, the following caveats regarding telluric lines and attached ThAr spectra have to be taken into account:

- (a) over the long term, a fundamental limitation is the overall motion of clouds giving rise to telluric lines. The fastest coherent cloud motion is caused by the jet-stream, which can reach velocities exceeding  $55 \text{ ms}^{-1}$  (during the Seifahrt & Kaeuffl 2008 study, it reached  $\approx 29 \text{ ms}^{-1}$ ); it can therefore possibly induce a shift of up  $\cos(\text{zenithal distance}) \times \cos(\text{difference of azimuth between jet-stream direction and direction of observation}) \times \text{jet-stream speed}$  for lines that are only produced at the jet stream altitude, and some possible line shape changes for lines that are partially produced at this altitude. However, the largest contribution to most telluric absorption lines (except  $\text{O}_3$ ) arise in the first scale height of the atmosphere above the telescope;
- (b) many settings of CRIRES cover spectral ranges that include water vapor lines: the column density of water vapor can change on a time scale of a few minutes. In addition, since water vapor is mainly located at low altitude, its column density dependence on airmass can be different from the one of other molecules. Presence of weak water vapor lines can subtly change the centroid of other telluric lines with which they are blended;
- (c) ThAr spectra are now produced using a set of fibers that illuminate the entrance slit. Currently, ESO cannot guarantee that the photo-center of the light coming out of the fibers is reproducible to the level of accuracy required for reaching a precision better than  $100 \text{ m/s}$ ;
3. for a discussion on spectral resolution see [Bouchy, F., Pepe, F., & Queloz, D. \(2001, id\)](#)). One should note that in the case of CRIRES, the choice of resolution is intimately related to the choice of slit width in the case that the PSF FWHM is larger than the slit width. If it is smaller, the resolution actually depends on the FWHM of the PSF and on the centering error caused by the secondary guiding algorithm;
4. the location of the star photocenter on a slit not uniformly illuminated is a crucial aspect. A mean precision of  $10 \text{ ms}^{-1}$  requires a mean error on the centering of the target of  $\approx 0.015$  slit-viewer detector pixel, from one observation to the next. This precision must be reached in spite of various seeing and transparency conditions. In the case of AO observations, this precision must also be reached despite variations on the quality of the AO corrections, which depends on atmospheric turbulence, airmass,... There is no guarantee that the algorithm used for the secondary guiding on the slit viewer can reach such a level of accuracy on a constant basis with so many variable parameters. Two solutions can be adopted:
- observations in NoAO mode with the narrowest slit in bad seeing conditions (FWHM *at the observing wavelength* larger than at least  $\approx 4 - 5$  times the slit width). In this case, the slit illumination is likely to be uniform enough that the exact location of the photocenter is not a problem. Clearly with this approach the throughput is reduced.;
  - in case of AO observations, it is important that the light path includes one of the offered gas-cells so that the reference lines it offers are fixed relative to the spectrograph. Note that some problems listed in point (2) above are also valid here: (a) line blending of the gas-cell lines with the star absorption lines as the star radial velocity changes with the Earth motion around the Sun, or by the presence of planet around the star under study; (b) line blending with telluric lines of varying

intensity depending on airmass or varying atmospheric conditions. However, in any case, the use of a gas-cell appears as a solution offering a very high radial velocity accuracy.

5. the shape of the absorption lines can be changed subtly if the flat-fielding was done with a slit width slightly different from the one obtained during the observations. It is therefore important to attach a flat-field in the corresponding OB.
6. It is always useful to observe a radial velocity standard star together with the science target in order to eliminate possible systematics.

### 7.2.3 Visitor gas-cells

For ultra precise radial velocity work users may wish to employ a special gas-cell in absorption during their scientific observations, similar to the Iodine Cell method employed in the optical. For the moment users have to supply their own gas-cell(s) at their own risk. In this context one should keep in mind the problem of pressure shift (c.f. Fig. 2b in [Glenar et al. ADV. HELIO- AND ASTEROSEISMOLOGY: I.A.U. SYMP.123 P.481, 1988](#) which gives a practical example of the associated error). *The use of gas-cells not part of the observatory standard set (which currently only includes N<sub>2</sub>O and CO gas-cells) is limited to runs executed in visitor mode, as their use would interfere with regular service mode observations.*

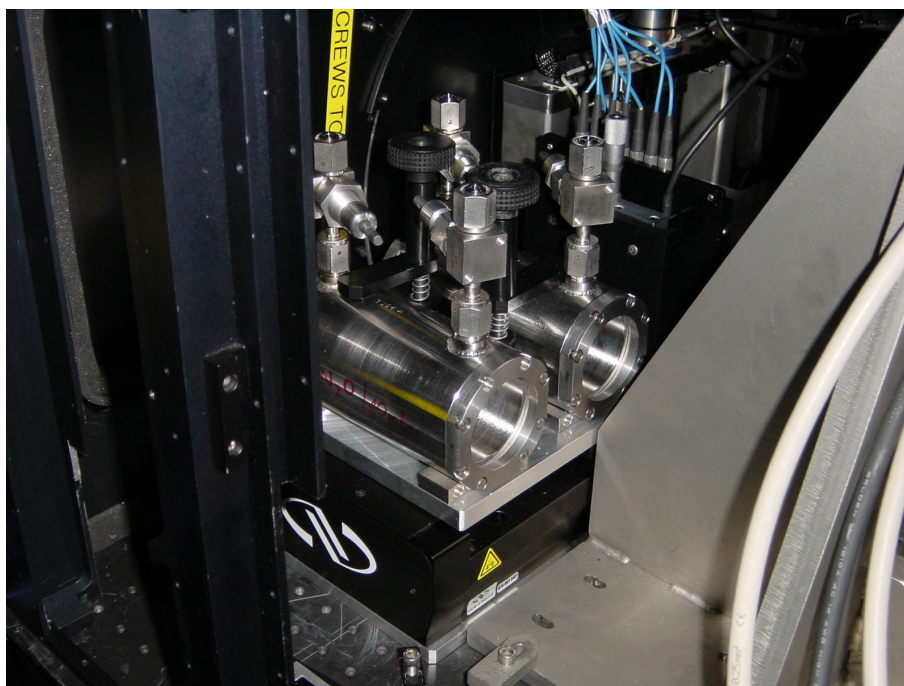


Figure 16: The N<sub>2</sub>O and CO gas-cells mounted on the carriage

**Mechanical lay-out** Figure 16 shows the way the present ESO's gas-cells are mounted on the carriage. Figure 17 illustrates their mechanical lay-out. In principle the cells are held in place by a bar pressed down with a knurled nut. Any mechanical design which is compatible with the overall design space and this very generic fixation method is acceptable.

The minimum optical clear diameter should be 22mm to have sufficient field for acquisition and nodding.

The optical quality of the entrance windows has to be sufficient to allow for diffraction limited imaging. Low order aberrations (e.g. spherical aberration or astigmatism) are acceptable, as the MACAO adaptive optics system would correct for them. The windows have to be transmitting and of good quality for both the AO-reference wavelength (600-1000nm) as well as for the spectral region of interest to be covered by CRIRES.

One of the windows is very close to the telescope focus, so it is important that at least one of the two windows is scratch free and clean! If relevant, the preferred orientation of the gas-cell needs to be indicated.

The gas-cell will operate in an f/15 beam so that fringing in the windows is not a big issue. Still if slightly wedged windows are used, they have to be aligned such that the net prismatic deflection is close to zero to avoid differential refraction effects.

**Logistics** As part of the proposal process all relevant information as to the properties of the visitor gas cell have to be submitted to ESO. In addition the fill-gas has to be described and if relevant handling and safety procedures have to be clarified. The cell(s) have to be sent to ESO Garching at least 4 weeks prior to the observing run properly packed for overseas shipment by airfreight. ESO takes the responsibility of shipping the cells to and from the observatory.

At this stage, only non-toxic gases are allowed in gas-cells.

**Operations** At the beginning of the visitor run ESO will remove one of the two observatory gas cells and mount one of the user's gas cells to the instrument. A change of the cells during one observing night is not possible.

Cells are kept in the warm part of the instrument. Their temperature is not controlled.

### 7.3 Flat fields

Dedicated flats are best taken with the Halogen lamp. DIT and NDIT are automatically determined by the template. In particular, DITs are always longer than 2 s for the reason given in §6.4.

There is *a priori* no need to take flat fields at night time, as the detector characteristics are sufficiently stable in time, and the spectrograph wavelength setting sufficiently accurate. However, flat-fields may be important for very accurate radial velocity measurements. They may also be important when the interesting lines appear at the blue or red edge of a spectral setting, where possible vignetting by the intermediate slit may affect the detector illumination (see §8.4).

Flat-fields that are part of the calibration plan (see Sect. 12) have a signal-to-noise ratio per pixel larger than 200 at the peak efficiency of a given setting. A systematic atlas of the S/N/pixel of the flat-fields for each standard wavelength setting has started and will be made available through a link in the instrument web page. Users requiring flat-fields with larger S/N should contact ESO through the email addresses listed in §1.4.

## 7.4 Spectrograph field-of-view, slit width and seeing

The field-of-view of the spectrograph is *slit width*  $\times 40''$ . The appearance of a spectrum on the science detector is illustrated in Figure 18. Note in particular that the default centering position is not at the center of the slit.

A slit width of  $0.4''$  offers a close to maximal throughput in most AO observations. For non-AO observations, the optimal slit width would in principle be given by the external seeing at the wavelength of observations. *However, it is not recommended to use a slit width larger than  $0.4''$ , as the spectral range for which the illumination is reproducible to better than 1% shrinks considerably (see §7.1).* In addition, for faint targets, not enough light is reflected by the slit jaws for proper secondary guiding.

It is worth to recall that the seeing FWHM  $\epsilon$  depends on the wavelength  $\lambda$  following

$$\epsilon(\lambda) = \epsilon(\lambda = 500\text{nm}) \left( \frac{\lambda(\text{nm})}{500\text{nm}} \right)^{-1/5}, \quad (1)$$

and on the zenith distance,  $z$ , following

$$\epsilon(z) = \epsilon(z = 0) (\sec z)^{0.6}. \quad (2)$$

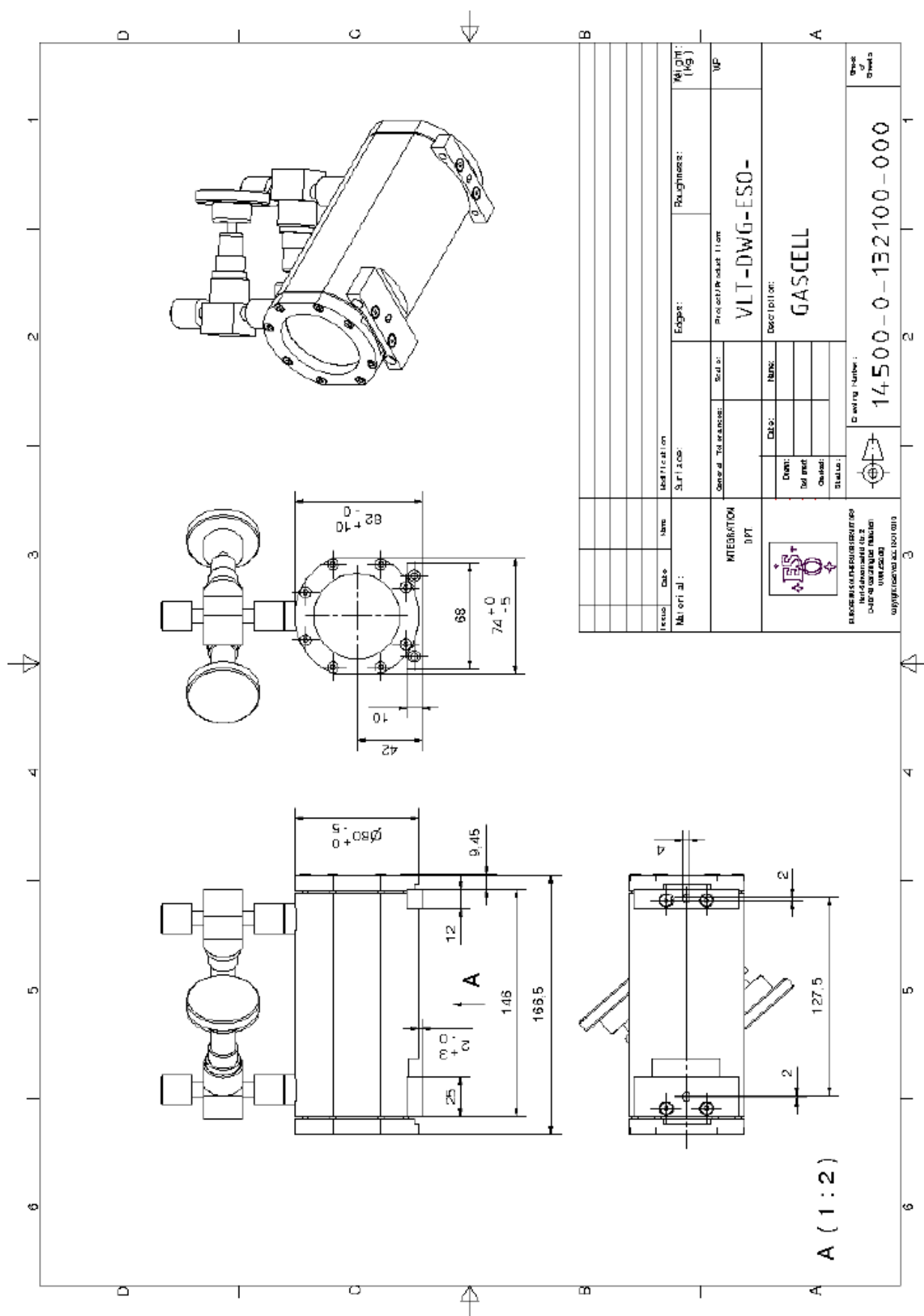


Figure 17: Mechanical lay-out of a gas-cell

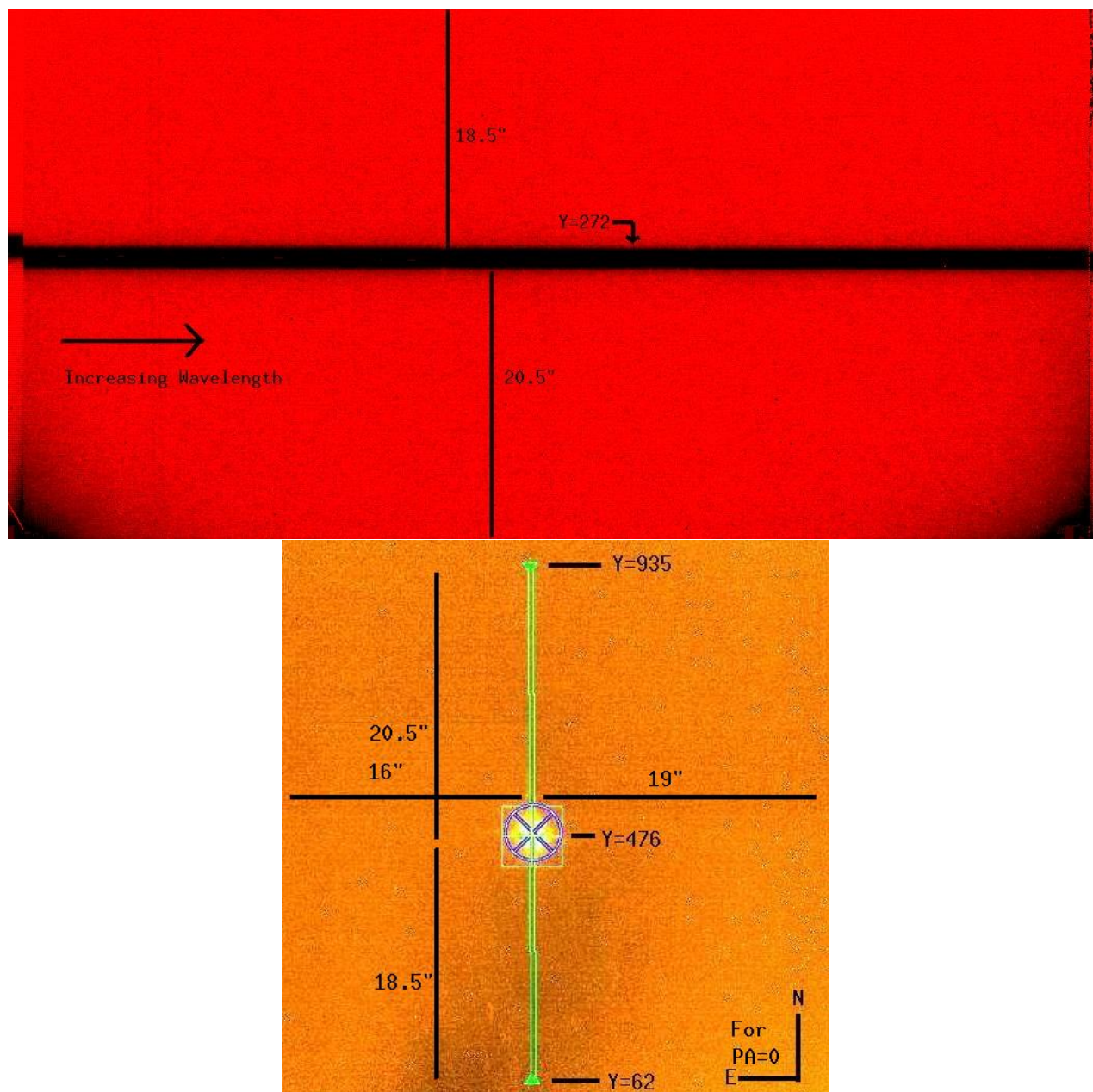


Figure 18: Illustration of the geometry of the science and slit viewer detectors for a position angle of 0 deg on sky. On the science detector, North is to the bottom and East to the left, while North is to the top and East to the left on the slit viewer detector. The centering position of the science target in the SV detector is the center of the slit in  $x$  and pixel  $y = 476$  along the slit. This position corresponds to pixel  $y \approx 293$  on the science mosaic; the exact value depends on the detector and the wavelength setting. With the templates `CRIRES_spec_obs_AutoNodOnSlit` and `CRIRES_spec_obs_SpectroAstrometry`, nodding is done symmetrically along the slit around the centering position. For nodding position A, the image of the target appears at larger  $y$  values on the slit-viewer and lower  $y$  value on the science detector, at half the nod throw from the centering position. In other words, for a position angle of 0 deg, the telescope position at nodding position A is South of the centering position. Conversely, for nodding position B, the image of the target appears at smaller  $y$  values on the slit-viewer and larger  $y$  value on the science detector. On the science detector, wavelengths increase from left to right.

## 7.5 Spectral resolving power

A spectral resolution of 96,000 has been measured with a slit width of  $0.2''$  at 2172 nm. Similarly, a spectral resolution of 60,000 has been measured with a slit width of  $0.3''$ . Currently, the relation slit-width to spectral resolution  $R$  is such that  $R \times \text{slit width (in } ''\text{)}/0.2'' \approx 100,000$ , which is valid for slit width between  $0.2$  and  $\approx 0.8''$ . However, this relation is only valid in the case that the whole slit width is uniformly illuminated by the light source, such as in the case of NoAO with narrow slit width. In the case of good AO corrections, the resolution may be partly determined by the width of the PSF at the entrance width and the stability of the PSF location in the slit during the observations.

Starting December 2008, the entrance slit width reproducibility showed peak-to-peak variation of up to  $\approx 25\%$ . A method to force the repeatability of the slit width to better than around  $10\%$  is now in place.

Figure 19 shows the optical depth profile obtained from the combination of 5  $^{12}\text{CO}$  lines seen in absorption toward the young star DG CrA, using a  $0.2''$  slit width. A Gaussian fit to this profile, taking into account the finite pixel width, gives a FWHM of  $3.18 \text{ km s}^{-1}$ , corresponding to a resolution of 94,300. This value is therefore a lower limit to the spectral resolving power of CRIRES.

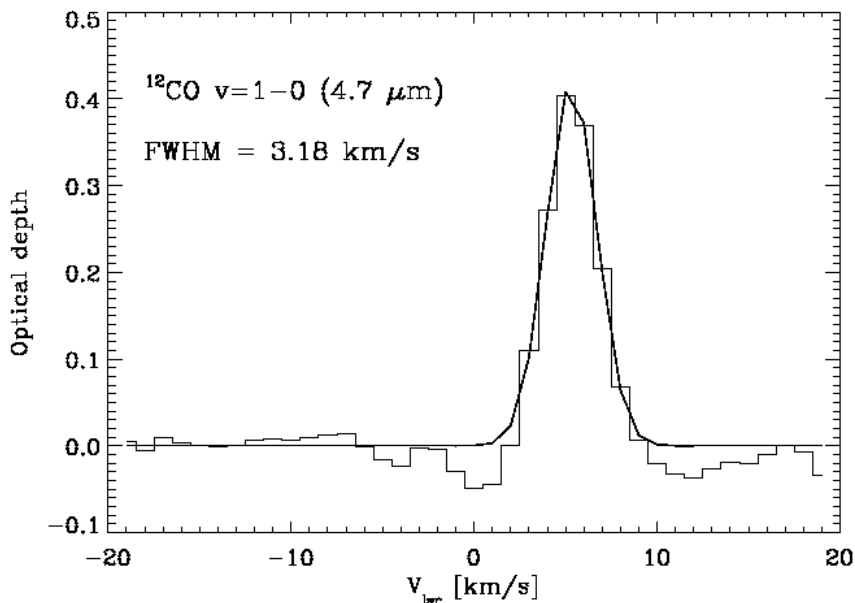


Figure 19: Optical depth profile obtained from the combination of 5  $^{12}\text{CO}$  lines seen in absorption toward the young star DG CrA. Courtesy Klaus Pontoppidan.

A slit width narrower than  $0.2''$  is possible, in particular, in the case of observations of very bright targets. However, there is no guarantee that the requested slit width can be achieved for a slit width parameter smaller than  $0.2''$ , due to the limitations of the slit mechanism. Also, there is no guarantee that the spectral resolution can be larger than 100,000.

## 8 System efficiency and throughput

The overall efficiency of CRIRES has been measured on spectrophotometric standard stars. The flux,  $F_\nu$ , of such a star, expressed in Jy, is converted to the flux,  $N_\gamma$ , in photons/s/pixel by

$$N_\gamma = \frac{c}{\lambda^2} F_\nu \cdot \frac{A_{\text{Tel}}}{E_\gamma} \cdot \Delta\lambda \quad (3)$$

where  $E_\gamma = hc/\lambda$  is the photon energy,  $A_{\text{Tel}}$ , the telescope collecting area. The dispersion  $\Delta\lambda$  is output by the ETC.

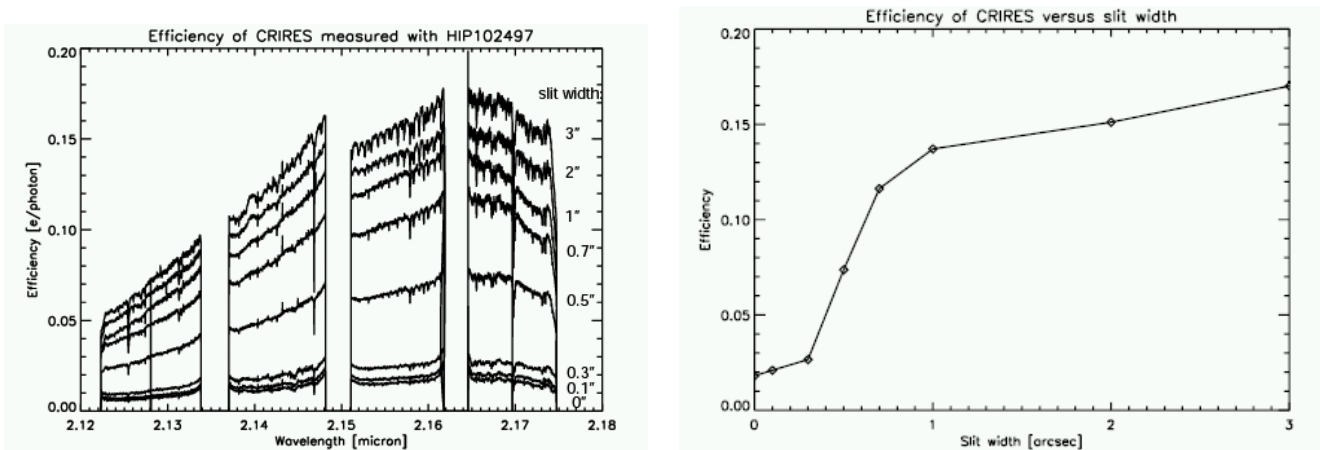


Figure 20: Overall system efficiency, also called throughput. The wavelength dependence of the efficiency for a particular wavelength setting is shown for different slit widths on the left. The peak efficiency as a function of slit width is shown on the right.

The overall efficiency or throughput  $\tau$ , is defined as the ratio of  $e^-/s/pixel$  as measured on the detector divided by the theoretical expected photon flux (photons/s/pixel) arriving above the Earth's atmosphere (Eq. 3). In Fig. 20 the overall efficiency as a function of slit width for order 26 at 2150 nm is shown together with the peak efficiency versus slit width. During these observations, atmospheric conditions were rather bad (seeing of  $\geq 1.6''$  and coherence time of 2 ms, see Sec. 3) so that the AO could not work effectively, leading to significant slit loss.

### 8.1 Transmission of the entrance window

The transmission of the dichroic window which also serves as entrance window for the spectrograph has been measured in the laboratory in Garching for  $\lambda > 1000\text{nm}$ . It is shown as a function of wavelength in Fig. 21. For shorter wavelengths, only manufacturer measurements exist: they indicate that the blue wavelength cut-off (transmission smaller than 50%) occurs at  $\approx 950\text{nm}$ .

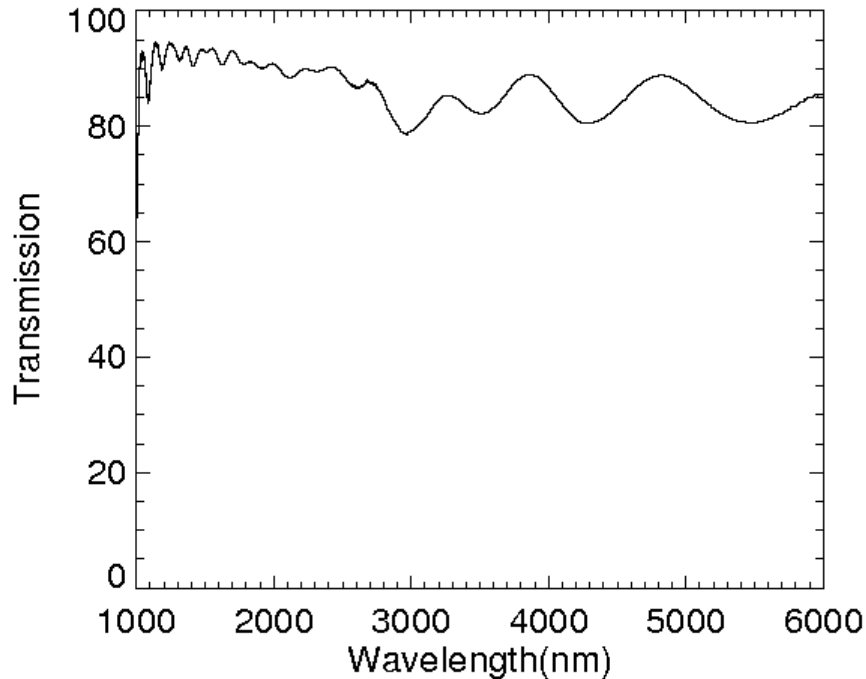


Figure 21: Transmission curve of the entrance window.

## 8.2 Sensitivity

Table 2 lists the instrument sensitivities. The table is intended as a quick reference only. Proposers should refer to the Exposure Time Calculator (Sect. 10.2) for more precise estimates. In particular, one should note that the grating blaze function introduces a large sensitivity variation within any given order.

Table 2: Point source sensitivities determined using a 0.4 "slit, adaptive optics, optical seeing of 0.8 ". The values listed correspond to a S/N of 10 for a 1h on-source integration in one spectral dispersion element. They are obtained by integrating the profile along the spatial direction.

Band	Sensitivity (mJy)	Magnitude
J	1.1	15.4
H	1.1	15.1
K	1.1	14.6
L	9.5	11.2
M	26	9.4

Short-ward of 1100 nm, the spectral range accessible to CRIRES overlaps with the one accessible to UVES. For the observations of specific spectral features in this region, it is interesting to compare the efficiency of the two spectrographs. Figure 22 shows the S/N of two spectra of the  $J = 1.3$  star  $\beta$  Col obtained nearly simultaneously with CRIRES and UVES on February 7, 2007, while the star was at an airmass  $< 1.07$ , with very similar seeing conditions.

In both cases, the slit was constantly aligned along the parallactic angle (ELEV mode). The first spectrum (in red) was obtained with UVES with a slit width of  $0.3''$ , providing a resolution  $R \approx 110,000$ . The other one (in blue) was obtained with CRIRES using AO and a slit width of  $0.2''$ , providing a resolution  $R \approx 100,000$ . For observations of specific lines accessible in one setup, CRIRES was clearly more efficient red-ward of  $\approx 970\text{nm}$ . Future observations are planned to determine the relative efficiencies of the two instruments after the UVES red CCD upgrade in July 2009.

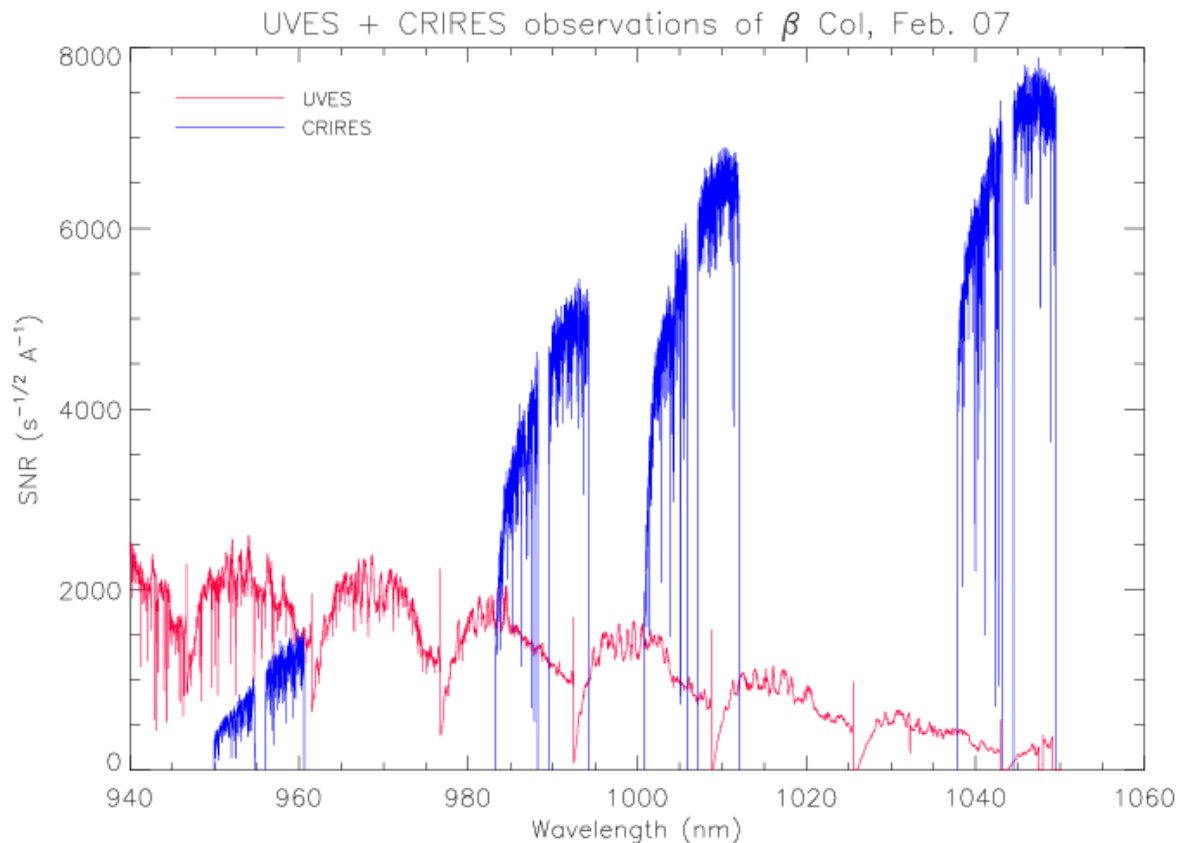


Figure 22: Comparison of  $S/N/\text{\AA}$  per second $^{1/2}$  of integration time obtained during nearly simultaneous CRIRES and UVES observations of  $\beta$  Col. Courtesy S. Uttenthaler. New observations are planned to compare the two systems after the UVES red CCD upgrade in July 2009.

### 8.3 Optical ghosts

Occasionally, especially when using the CRIRES Echelle grating in high order, a quasi white – light ghost is visible on the science data or calibrations. It results from a retro-reflection from the detector onto the grating, which is redirected onto the detector in a different order and with reduced dispersion. Ghosts cancel out by nodding, as sky emission lines do. One example of a ghost visible in a staring image is given in Fig. 23.

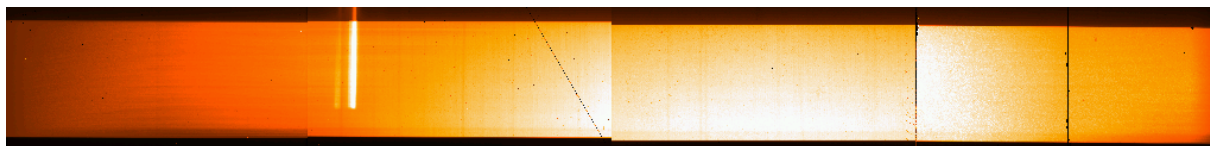


Figure 23: Example of a quasi-white light ghost observed with a reference wavelength of 1153.8 nm. The ghost is visible in staring frames top left on the second detector. Also, diagonal (middle) and vertical (right) detector scratches are also visible.

## 8.4 Stability and reproducibility

For wavelength calibration the stability and reproducibility of the different mechanical functions (grating, prism, slit) are important. The absolute setting of the prism and grating guarantees that a given standard wavelength setting is accurate to better than 30 pixels, even possibly after a minor intervention. A model of the instrument currently achieves a wavelength calibration of  $\approx 3$  pixels without simultaneous wavelength calibration.

A measurement of the stability of the instrument has been obtained by measuring the location of an emission line in short exposures spread over a span of  $\approx 10$  minutes. A preliminary value is 1/20 pixel. Such tests need to be repeated for different wavelength settings.

The reproducibility problem previously reported with the intermediate slit<sup>1</sup> has now been solved since the installation of a new intermediate slit mechanism in May 2009. The intermediate slit width is now reproducible to a few microns.

---

<sup>1</sup>This element is not shown in Figure 1. It is located between the collimator (the concave mirror located after the prism) and the small flat mirror located before the TMA.

## Part III

# Observing with CRIRES at the VLT

## 9 Introduction

### 9.1 Atmospheric transmission

The transmission of the Earth's atmosphere in the J, H, K, L and M bands is shown in Fig. 24. The amount of telluric absorption varies non-linearly with zenith distance and precipitable water vapor. In order to facilitate the identification of sky regions affected by water vapor absorption lines, Fig. 25 shows the atmospheric transmission spectrum only including water vapor absorption lines.

The transmission spectrum of the sky for a particular setting is an optional output provided by the ETC. This tool allows one to select spectra based on different amounts of precipitable water vapor.

### 9.2 Background removal

#### 9.2.1 Sky emission spectrum

The sky background emission can be divided in two regimes depending on the wavelength. Below 2200 nm, the sky emission is dominated by OH lines, formed at an altitude of 80 km. Detailed sky spectra with OH line identifications are available on

<http://www.eso.org/instruments/isaac/tools/>.

Beyond 2200 nm, the thermal background dominates with contributions from both atmospheric and telescope emission.

The sky emission spectrum for a particular setting is an optional output provided by the ETC.

#### 9.2.2 Nodding

The purpose of *nodding* is to correct or remove sky emission, detector dark current and glow (Fig. 13), and some ghosts. In a simple application of this technique a spectrum is taken at telescope position A, after which the telescope is moved along the direction of the slit to position B and another spectrum is taken. By subtracting the A and B images, dark and sky subtractions are performed. The number of nodding cycles and the nodding throw are free observing parameters. Because of the extended wings of the PSF a nodding throw greater than 5 " is recommended, preferably 10 ".

#### 9.2.3 Jittering

The purpose of *jittering* is to correct for bad pixels and decrease systematics due to the detector. This is particularly important for CRIRES observations. Indeed, the detectors suffer

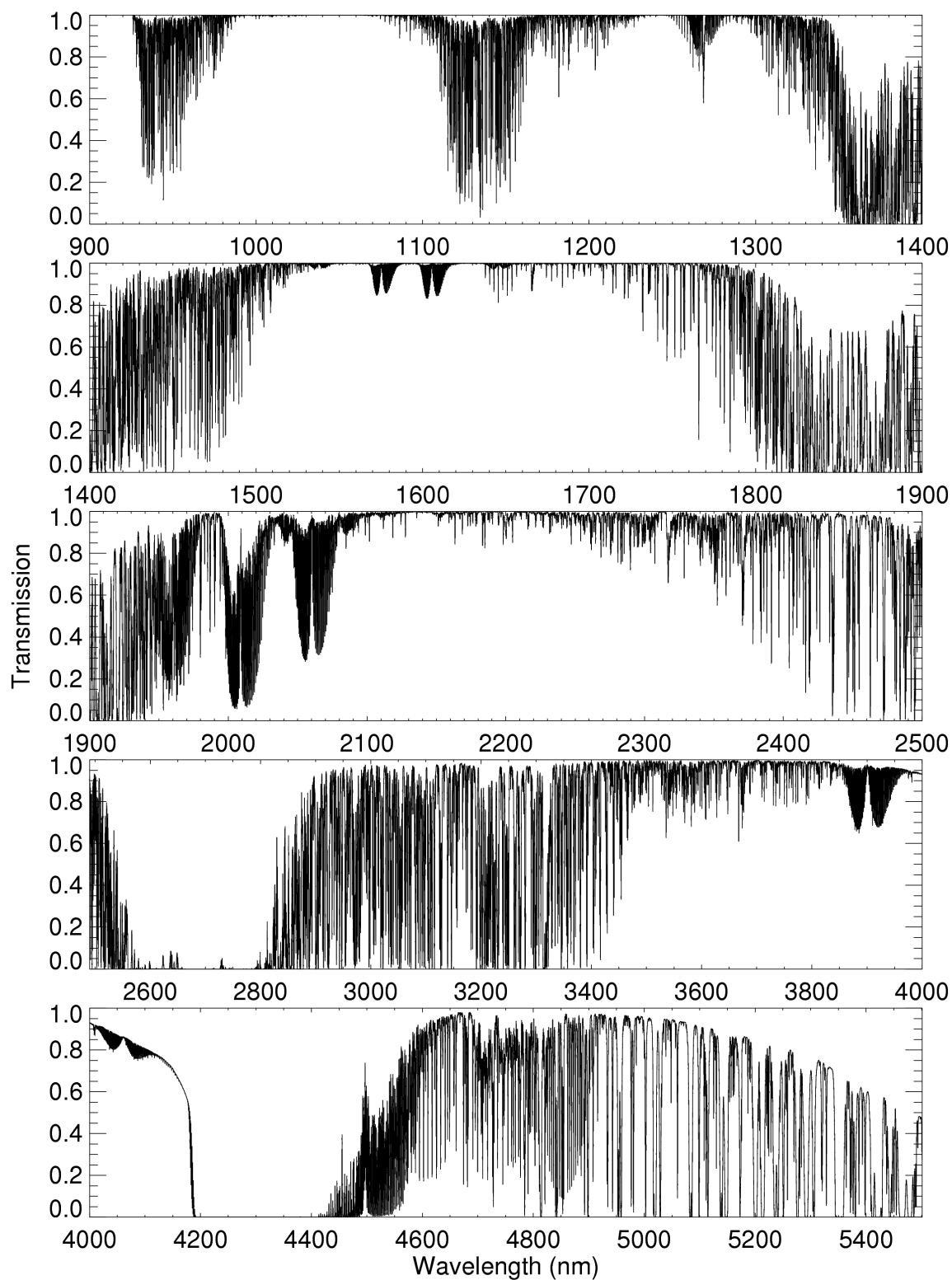


Figure 24: Atmospheric transmission from 900 – 5500nm computed with PCLnWin/HITRAN for a Paranal atmosphere, precipitable water vapor (PWV) of 2.5mm, at zenith and smoothed to a resolution of  $\lambda/\Delta\lambda = 10^4$ .

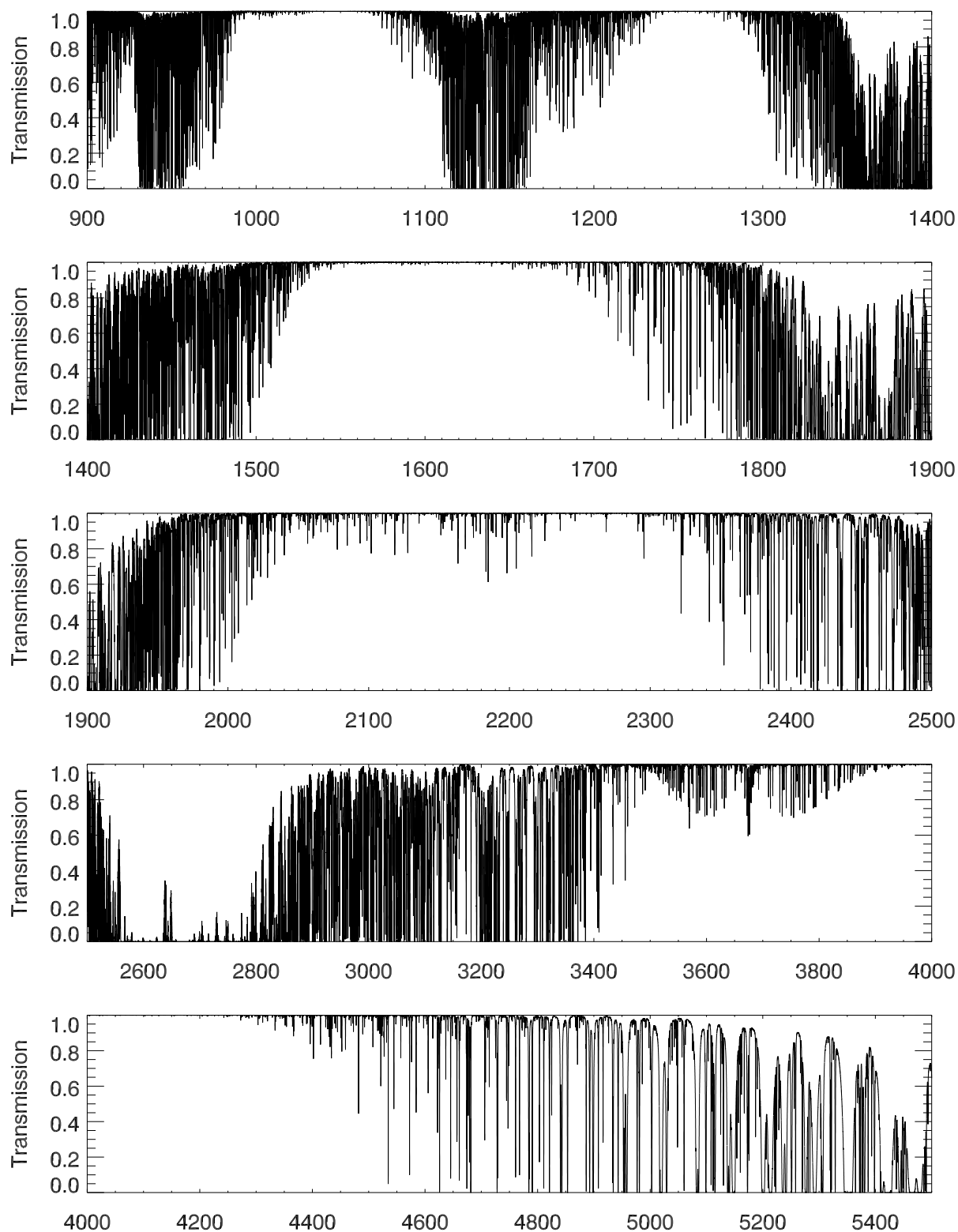


Figure 25: Water-vapor only atmospheric transmission from 900 – 5500nm computed with RFM/HITRAN for a Paranal atmosphere, precipitable water vapor (PWV) of 2.5mm, at zenith at a resolution of  $\lambda/\Delta\lambda = 100000$ .

from a relatively large number of bad pixels. In addition, the spatial extent of a spectrum is at most a few pixels in nominal conditions with AO. Jittering is obtained by adding a small, random offset to the telescope in addition to the nodding offset. The recommended maximum size of the jitter offset is a free parameter. It must be smaller than half the nodding offset but larger than the spatial extent of the minimum feature that one hopes to detect; for point sources, it should be larger than the width of the spatial profile.

## 9.3 Flux calibration and telluric correction

### 9.3.1 General procedure

Flux calibration and telluric correction are generally carried out in three steps. The first step removes telluric absorption features of the extracted, wavelength calibrated science spectrum by dividing it by the one of a telluric standard. The second step removes the intrinsic spectral features of the telluric standard that are imprinted onto the science spectrum because of the first step. The third step uses a spectro-photometric standard to set the absolute flux scale.

The spectro-photometric standard and the telluric standard can be the same star. Note that CRIRES, as spectrometers in general, is not meant to provide high absolute spectro-photometric accuracy.

The Observatory does not offer observations of telluric or spectro-photometric standard stars. Observers who wish to correct for telluric features or flux calibrate their spectrum therefore need to supply a standard star OB. Observing time needed to execute telluric or spectro-photometric standard stars is charged to the observer and must be taken into account in the amount of time requested during Phase 1.

### 9.3.2 Telluric correction

The most prominent features in IR spectra are telluric lines created by the Earth's atmosphere. Unfortunately, many telluric absorption lines are saturated and do not scale linearly with airmass. Therefore, it is necessary to observe a telluric standard as close as possible in airmass and with the same instrument setup as that used for the science target. Furthermore, the strength of some telluric lines varies with time, so it is also necessary to observe the standard soon after or soon before the science target. Thereafter, the spectrum of the science target is directly divided by the one of the telluric standard.

Ideally, the spectrum of the telluric standard should be known, so that features belonging to it can be removed (step 2 above). However, this is usually not the case, so one has to use standards in which the spectrum is approximately known. At present no high precision IR atlas of standard stars with bona fide spectra exists. The CRIRES Team will compile such a list of spectro-photometric standard stars and, once it is available, will put it on the CRIRES home page <http://www.eso.org/instruments/crIRES/>.

### 9.3.3 Hot stars as telluric standards

Usually either hot stars or solar analogs should be used as telluric standards. Spectra of stars hotter than B4 are well fitted by a black-body, with the exception of a few lines (for example, neutral hydrogen Brackett lines). So, by knowing its spectral type, the continuum of a star

can be fitted by a Planck function with the appropriate temperature. On the other hand, the spectra of stars cooler than A0 show molecular features.

Some hot stars also have emission lines or are in dusty regions, and should therefore be avoided. A positive value of the V-I color of a star can be used as an indicator of reddening due to the presence of dust on its line-of-sight.

Hot stars tend to lie near the galactic plane. Correction of telluric features for objects close to the galactic pole may therefore require a different strategy.

### 9.3.4 Late-type stars or G stars as telluric standards

Unfortunately, spectra of hot stars do contain some features, usually lines of hydrogen and helium, that can be difficult to remove. If the region around the hydrogen and helium lines is of interest, then a late type star could instead be observed, as its spectrum only show weak hydrogen and helium lines.

Solar analogs, for the purpose of removing telluric features, are stars with spectral type G0V to G4V. These stars have many absorption lines in the IR, particularly in the J band. These features can be removed by dividing the solar analog spectrum by the solar spectrum at the resolution of the observations.

In addition to hot stars and solar analogs, IR astronomers have used other stellar types as telluric standards. For example, F dwarfs are commonly used.

### 9.3.5 Catalogs

The CRIRES tools web page <http://www.eso.org/instruments/crises/tools> provides a number of catalogs of stars that can be used as telluric standards.

## 9.4 The influence of the Moon

Moonlight does not noticeably increase the background in any of the CRIRES modes, so there is no need to request dark or grey time for this reason. However, it is recommended not to observe targets closer than 30° to the Moon to avoid problems linked to the telescope guiding or active optics system.

On the other hand, the Moon may affect the quality of the adaptive optics correction if the source used for wavefront sensing is fainter than R=15 mag. In these cases, reducing the lunar illumination constraint to approximately 0.7 and increasing the distance to the Moon to approximately 50 degrees is generally adequate.

Observers in visitor mode are encouraged to carefully check their target positions with respect to the Moon at the time of their scheduled observations. Backup targets are recommended whenever possible, and users are encouraged to contact ESO in case of severe conflict, i.e. when the distance to the Moon is closer to 30°. Visitors can use the tools that are available at

<http://www.eso.org/observing/support.html>

Select the link “airmass” which is under “User Support Tools” to help to determine the distance between targets and the Moon for given dates.

## 10 Observing in Visitor and Service Mode

### 10.1 Overview

For CRIRES there are no deviations from standard VLT operational procedures. As for all ESO/VLT instruments, CRIRES users must prepare their observations with the P2PP tool, available at

<http://www.eso.org/sci/observing/phase2/P2PP/P2PPTool.html>.

Acquisitions, observations and calibrations are coded via templates. Two or more templates make up one observation block (OB), which then contains all information necessary for the execution of an observing sequence. CRIRES and the telescope are setup according to the content of the OB. There is one Real-Time Display (RTD) for the slit viewer and one RTD for the spectrometer. Daytime calibrations, as described in the calibration plan (see Sect. 12) are executed the following morning by the Observatory staff.

In particular for service mode observers, it is important to properly take into account the amount of time required for telluric corrections. The execution time of a science OB is typically 1 hour. Therefore, at the time of submitting a proposal, an observer has to already foresee that the observing time will be split in a number of OBs, each of which usually requires an associated OB of a telluric star.

Service mode observers should submit their OBs before the Phase 2 deadline whose date is announced in the web-letters.

*The most important points for successful observations are listed in § 20 at the end of this manual.*

### 10.2 The Exposure Time Calculator

The CRIRES exposure time calculator can be found at:

<http://www.eso.org/observing/etc/>

It returns an estimate of the on-source integration time necessary to achieve a given S/N as a function of different input parameters:

- The input magnitude can be specified for a point or an extended source. For the latter, the input parameter corresponds to the magnitude per square ". Also input flux can be specified as surface brightness. If the 'single line' option is chosen, it corresponds either to the total line flux, for a point source, or to the surface brightness for an extended source.
- If the observing date is known it may be used together with the target coordinates to compute the radial velocity shift due to orbital and rotational movement of the Earth. Alternatively, this tool allows the user to select the best time of the year to observe an object so that the targeted feature avoids a specific telluric line.
- If an AO guide star is used, R mag and spectral type must be specified. They can be obtained from online catalogs available at Simbad/Vizier.

- Requested output can be either exposure time to achieve a given signal-to-noise ratio (SNR) or SNR achieved in a given exposure time. In both cases the DIT needs to be specified (see Sect. 11.3).

The following items should be remembered:

- **ETC** outputs the on-source integration time. Depending on observing technique and accounting for overheads, the total execution time will be longer (Sect.10.3).
- It is always useful to ask the **ETC** to show the SNR as a function of wavelength due to the presence of numerous telluric features: a small difference in the requested wavelength may lead to very different SNR for a given total integration time or, alternatively, very different integration time for a requested SNR. In addition, it helps to visualize the wavelength coverage of each detector.
- For a point source, the SNR corresponds to the one obtained by integration over the spatial diffraction profile and is given per pixel in the spectral dispersion and not per resolution element. To compute the SNR for a resolution element the right number of pixels needs to be combined; typically 2 pixels for the 0.2 " slit.
- For an extended source, the SNR calculated corresponds to the one obtained by integrating the signal over 1" per pixel in the dispersion direction (and not per resolution element).
- When the NGS (AO mode) is selected, the **ETC** also outputs the estimated Strehl ratio in the K band. This value is needed in the constraint set of an OB. For extended objects, only FWHM should be entered.
- The user can specify the vertical amount of precipitable water vapour (PWV) in the atmosphere: the ETC therefore uses the appropriate emission and transmission spectra for the PWV and airmass chosen. This functionality allows one to determine if the SNR will be or not affected by water vapor. One should note that the effect of water vapor lines also depend on the temperature at the time of observation, as well as the altitude of the layers where the water vapor is concentrated, therefore limiting the accuracy of the SNR determination to a few 10%. Since Period 82, when relevant, users are suggested to group wavelength settings in OBs requiring similar PWV values; USD will flag OBs requiring low PWV so that the night time astronomers observe them in appropriate conditions. ESO considers the possibility to add a constraint on the water vapor in the P2PP constraint set for future periods.

For more detailed information, see the online help provided on the **ETC** page.

### 10.3 Overheads

Estimated overheads are listed in Table 3.

Table 3: Telescope and instrument overheads. The overhead for change of derotator position angle applies to the CRIRES\_spec\_obs\_SpectroAstrometry template. The coefficient  $c$  for the read-out overhead is 0.9 for the FowlerNsamp and 0.45 for the FowlerNsampGRstWin modes, respectively. For the change of wavelength setting, DifEnc represents the difference between the grating encoder of the requested wavelength setting and the one for the previous wavelength setting. Grating encoder values for standard settings are given in Table 4a – 4k and 5a – 5k. For free wavelength settings, the grating encoder values can be obtained by linear interpolation between the closest standard wavelength settings. There is no overhead for change of wavelength setting during acquisition, as the spectrograph configuration is done at the same time as the telescope preset. Until the intervention that will take place December 2009, overheads due to change of wavelength setting are smaller if settings with large encoder values are executed first; such difference of overheads between decreasing and increasing grating encoder values is not reflected in this table.

Action		Time (s)
Telescope	Preset	360
CRIRES	Acquisition without AO	180
CRIRES	Acquisition with AO	300
CRIRES	Read-out (DIT in s)	$2.3 + c \text{ NDIRIT} + 0.1 \text{ NDIRIT DIT}$
CRIRES	Nodding cycle	24
CRIRES	Change of wavelength setting	$82 + 1.71 \cdot 10^{-4} \text{ DifEnc} - 1.56 \cdot 10^{-10} \text{ DifEnc}^2$
CRIRES	Attached wavelength calibration	150
CRIRES	Attached lamp flat	120
CRIRES	Change of derotator position angle	60

### 10.4 Differential effects

A cause of the complexity of the CRIRES observation software is the need to correct for chromatic effects: differential refraction between the slit viewer filter effective wavelength and the reference wavelength of the observations; chromatic effect introduced by the entrance window.

If the reference wavelength is in the M band while the slit viewer filter effective wavelength is in the J or H band, the differential refraction can reach 0.18 arcsec at very high airmass, while the chromatic effect of the entrance window can introduce a shift of 1.5 slit viewer pixels. A differential refraction of 0.17 arcsec can also be reached at high airmass between a reference wavelength at  $1\mu$  and the effective wavelength of the J band slit viewer filter. It can therefore be surprising to receive a slit viewer image that shows a target that is apparently off the slit. An example is given in Fig 26.

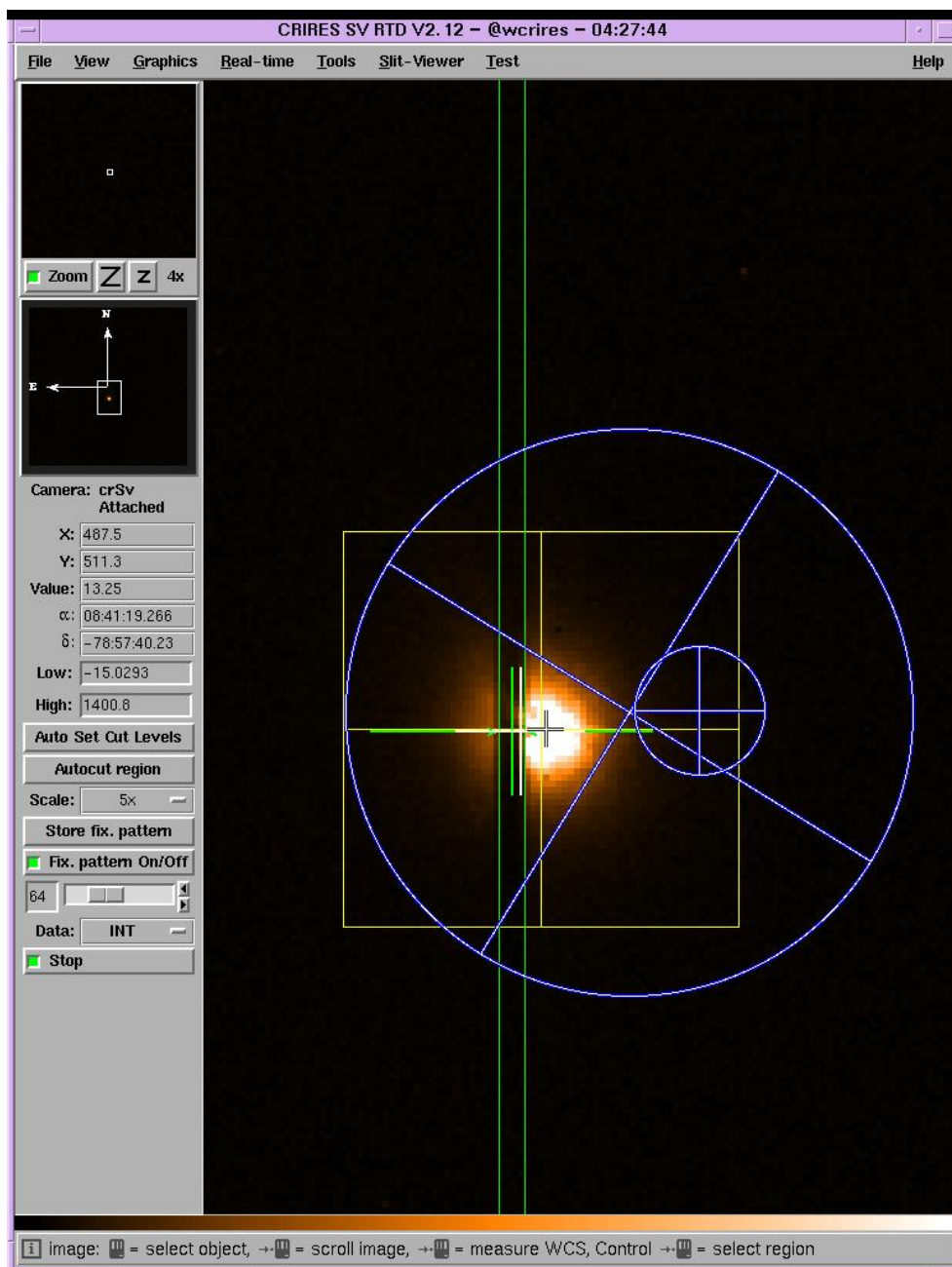


Figure 26: Differential chromatic effects: the target shown in the figure is observed close to the Celestial South Pole (airmass of 1.8). The reference wavelength is in the M band while the slit viewer is seen through a neutral density filter in the H band. The aim of the acquisition is to make sure that the target is at the center of the slit for the wavelength for which a spectrum must be obtained: the location of the image at that wavelength is represented by the green cross, which must be centered in the middle of the slit (two green vertical lines). The separation between this green cross and the white cross is caused by the chromatic effect of the entrance window ( $\approx 1.4$  slit viewer detector pixels). The separation between the white cross and the guiding window (yellow square with a yellow cross at the center) is caused by the differential refraction effect between the reference wavelength and the slit viewer effective wavelength ( $\approx 0.16$  arcsec). The little white and black cross represents the centroid of the target as calculated by the IRACE, the detector controller. The little blue circle with a + represents the calculated position of the star at the effective wavelength of the MACAO; the actual position of the field selector (big blue circle with a X) is different, likely because the AO star color is incorrect.

## 11 Preparation of Observation Blocks

This section provides some guidelines on how to prepare CRIRES observation blocks. A CRIRES Tutorial with a more detailed description has been prepared and it is available at:

<http://www.eso.org/sci/observing/phase2/CRIRES/P2PPTutorialCRIRES.html>.

### 11.1 Information required

The following are important considerations for a successful creation of CRIRES observation blocks.

- CRIRES acquisition templates may involve 3 different stars observed in 3 different wavelengths:
  1. the adaptive optics guide star, usually referred to as NGS, for natural guide star, which is used to determine the shape of the wave front; only the R band magnitude and B-R color of this star matters;
  2. the slit viewer guide star (SVGS) which is used for fine guiding using the slit viewer in one of 3 bandpasses, J, H or K. This star is also used as a reference star, which can be acquired before a blind offset is made to center the target into the slit;
  3. the target object itself, with a relevant wavelength between 940 and 5400 nm.

To be complete, the user can provide coordinates for a 4th star, which is the telescope guide star. This should ideally have R-band magnitude in the range 11 to 13 and be isolated. Fainter guide stars may work in good conditions. If no GS is contained in the OB the best one available will be selected by the telescope operator

- Target coordinates should be as accurate as possible. VLT absolute pointing accuracy is better than 3 " RMS;
- If any of the science target, the SVGS and NGS are different objects, it is important that their coordinates have been determined in the same coordinate system;
- In particular, if the SVGS is different from the target, it is *crucial* that their separation *at the time of observation* is known with high accuracy, ideally to better than 1/4 of the slit width. In this respect, proper motions of both the target and the SVGS must be taken into account.
- For observations without AO guide star, the acquisition template allows one to specify an offset between the SVGS and the target that is larger than half the width of the slit viewer (up to 40 "). In this case, guiding on the SVGS is therefore actually not possible. The SVGS is then only a reference star.
- Nodding in the case of extended objects larger than  $\approx 30''$  may require observations of offset fields to obtain sky measurements. Their frequency depends on the band (more frequent in J, H, less in K) and on the accuracy with which one wants to subtract them. Significant sky variations occur on timescales of a few minutes. The `CRIRES_spec_obs_GenericOffset` is recommended in this case.

- For moving targets, ephemeris files must be attached to each OB. Slit Viewer guiding can only be done on the target.
- *Differential tracking* is offered both in visitor and service mode in P85. Differential tracking allows to use the MACAO or secondary guiding on a moving guide 'star' while observing another, moving, target. For example, a satellite of a planet can be used for MACAO while observing a specific feature on the planet. Alternatively, it allows to use MACAO on a satellite while observing a feature on the satellite itself which moves as the satellite rotates. A third example is to use a background star in the field of a comet for MACAO while observing the comet itself.

Severe restrictions on this mode apply: in order to protect the MACAO APDs, MACAO can only be used at a safe distance from the parent planet. For example, using a Galilean satellite for MACAO is only possible if it lies at more than 4'' of Jupiter; fainter satellites can be used but must be located correspondingly further away from the planet as to avoid its glow.

Details regarding the differential tracking can be found in §19.

## 11.2 Observation Blocks and Templates

An Observation Block is the smallest scheduling unit. It consists of different templates, which are described in more details below. **Science** OBs must contain one and only one acquisition template. It is followed by a number of science and possibly calibration templates used to obtain wavelength calibration exposures or flat-fields. **Calibration** OBs are intended for observations of telluric/spectro-photometric standard stars. They must contain one acquisition template, followed by the template used for telluric standard stars.

### 11.2.1 Acquisition

The objective of the acquisition template is to preset the telescope and to center the target in the slit. Point sources should preferably be observed in ELEV mode where the slit is constantly aligned with the parallactic angle, in other words, along the atmospheric refraction direction. For specific needs to align the slit on the sky at some position angle, the SKY mode should be used. CRIRES offers two types of acquisitions:

1. The target itself or a star angularly close to it (closer than 30'') can be used to determine the shape of the wave front and therefore can be used to drive the adaptive optics system;
2. No adaptive optics is possible (or requested), because there is only an extended or a faint science target without a bright, compact object in the field.

The acquisition templates allow to distinguish between the acquisition modes:

AO :        CRIRES\_spec\_acq\_NGS CRIRES\_spec\_acq\_NGS\_difftrack  
 No AO :    CRIRES\_spec\_acq\_noAO CRIRES\_spec\_acq\_noAO\_difftrack.

AO correction is always performed on an NGS <sup>2</sup>.

---

<sup>2</sup>NGS is an AO natural guide star contrary to a LGS which is laser guide star using the LGS facility. This is not available for CRIRES.

In both acquisition methods, a sky frame can be taken in an offset field. The slit viewer detector control system subtracts this sky from each new image used for guiding in order to enhance the contrast in the SV image. It is crucial for faint targets.

Two acquisition images are usually delivered to the user in the final data package: the sky frame as well as the final centering of the target in the slit at the end of the execution of the acquisition template. However, for bright objects, a sky frame is not required for good guiding, and therefore, may not be taken.

In crowded fields, the choice of a good slit viewer guide star (SVGS) is important. It must not be too close to another star, in particular, to a brighter star; the latter should be chosen instead. No object should contribute significant flux within the area limited by the guiding box, whose width is optimally set by the instrument operator. The guiding box has a minimum width of  $\approx 0.4''$ . Note that if the SVGS is also the target – and therefore also partially hidden by the slit –, the width of the guiding box will typically be at least  $0.2''$  wider than the slit width. Also especially in crowded fields it is very important to choose carefully the WFS sky offsets.

The use of a slit width larger than  $0.4''$  should be avoided in general, as it would cause a significant contamination of the whole spectral range by adjacent spectral orders. A few exceptions can be made for (a) estimate of a slit loss (providing the measurement is only done at the very center of the observed spectral range); (b) observations of emission line only objects for which the identification of the lines (in particular for the ones produced by the adjacent orders) can be made without doubt.

### 11.2.2 Acquisition sequences with AO

In this section, we briefly describe the sequence of events taking place during the execution of the acquisition templates.

**General case:  $\text{NGS} \neq \text{SVGS} \neq \text{Target}$**  The most general acquisition for observation with AO takes place when the science target, the SV guide star and the AO guide star (NGS) are all different. Its sequence is the following:

1. preset the telescope to the NGS, possibly recenter it;
2. acquire the NGS with MACAO and close the AO loop;
3. offset the telescope to the SVGS;
4. interactively re-center the SVGS;
5. start guiding;
6. offset the telescope to the target; if the target is bright enough, recenter it.

**Case  $\text{NGS} = \text{SVGS} \neq \text{Target}$**  If the same star is used for slit viewing and for the AO, but is different from the target, this sequence becomes:

1. preset the telescope to the NGS, possibly recenter it;
2. acquire the NGS with MACAO and close the AO loop;

3. start guiding;
4. offset the telescope to the target; if the target is bright enough, recenter it.

**Case Target = SVGS  $\neq$  NGS** If the target is used for guiding using the slit viewer, but another star is needed for the AO, the sequence becomes:

1. preset the telescope to the NGS, possibly recenter it;
2. acquire the NGS with MACAO and close the AO loop;
3. offset the telescope to the target;
4. interactively re-center the target;
5. start guiding.

**Case Target = NGS  $\neq$  SVGS** If instead the target can be used for the AO but is too faint for guiding using the slit viewer so that another star is needed as a SVGS, the sequence becomes:

1. preset the telescope to the target, possibly recenter it;
2. acquire the target with MACAO and close the AO loop;
3. offset the telescope to the SV guide star;
4. interactively re-center the SVGS;
5. start guiding;
6. offset the telescope back to the target; if the target is bright enough, recenter it.

**Case Target = NGS = SVGS** If the same star is the target, the AO star and the SVGS, the sequence simplifies to:

1. preset the telescope to the target, possibly recenter it;
2. acquire the target and close the AO loop;
3. start guiding.

**Required information regarding the NGS** Acquisition with AO requires the following information:

- The coordinates of the AO guide star at equinox J2000 and at the epoch of the observations, unless the science target is also the AO Guide Star.
- The B-R color of the star used for AO (AO star or NGS). This is used to compute the guiding wavelength for the field selector holding the AO guide star, which in turn is used to correct for atmospheric refraction effects.

- The FWHM of the NGS in order to optimize a diaphragm in the AO system. This diaphragm is set as a function of the seeing such that it optimizes the amount of light received from the object with respect to the amount of background light from the sky. If the NGS is a point source, the FWHM is best left to zero (then only the seeing will be taken into account). Only if your AO guide star is significantly extended with respect to the seeing should this parameter be set to a value different from zero.

### 11.2.3 Acquisition sequences without AO

The most general acquisition sequence for observation without AO is the following:

1. preset the telescope to the slit viewer guide star (SVGS);
2. interactively re-center the SVGS in the slit;
3. start guiding;
4. offset to the target.

Of course, if the SVGS and the target are the same object, the sequence simplifies to:

1. preset the telescope to the target;
2. interactively re-center the target in the slit;
3. start guiding.

### 11.2.4 Science

Three templates are offered in P85. The `CRIRES_spec_obs_AutoNodOnSlit` is the preferred observing template for point-like sources. It allows staring or nodding observations with a fixed nodding throw along the slit, with optional jittering. The `CRIRES_spec_obs_SpectroAstrometry` essentially does the same as `CRIRES_spec_obs_AutoNodOnSlit`, but for each value of a list of slit position angles. This template is particularly suitable for applying the spectro-astrometry technique (Beckers, J., 1982, Opt. Acta, 29, 361; Bailey, J., 1998, MNRAS 301, 161 and references therein). First results using this technique with CRIRES are described in [Pontoppidan et al. 2008](#). Note that this template can only be used if the target is also the slit viewer guide star (but the AO star can be different).

The `CRIRES_spec_obs_GenericOffset` allows generic offsets suitable for observations of very extended objects.

The observing templates are described in Sect. 14.

### 11.2.5 Calibration

Darks, flat fields and wavelength calibrations are taken during daytime as part of the calibration plan (see Sect. 12). A Halogen lamp is used for flat fields. Fiber-fed ThAr spectra or the N<sub>2</sub>O or CO gas cell in front of the halogen lamp are used for wavelength calibration.

Observed sky lines which can be identified by HITRAN have the advantage that wavelength calibration is done from the science observations themselves. Unfortunately, sufficient sky lines are not necessarily available for all settings, sometimes because they are saturated. General

recommendations on absolute wavelength calibration is given in Sect. 7.1. *However, observers are strongly advised to use the ETC with the output options Sky Emission Spectrum and Sky Absorption Spectrum and to check for themselves if enough unsaturated telluric lines are available for a proper wavelength calibration in the spectral range of interest.*

Dedicated OBs for wavelength calibration shall be attached immediately before or after the science template so that prism and grating are not moved in between. Most observers wish to correct for telluric features and therefore need to supply a standard star OB. Observing time needed to execute telluric or spectro-photometric standard stars is charged to the observer.

### 11.3 Detector read-out mode and DIT setting

The choice of the detector read-out mode and DIT setting depends on the science to be performed.

- For the commonly used *FowlerNsamp* readout mode, it is strongly recommend to choose one of the DITs listed below. A first reason to limit the set of DITs is that the dark which depends on a particular DIT is taken during day time calibration for all settings used during the previous night: if a too large set of different and long DITs is used, there is a risk that daytime calibrations cannot be performed entirely. In addition, the method to correct for non-linear detector effects (including the 'odd-even' effect; see Sect. 6.4) requires a large number of calibrations: at this stage, the CRIRES team can only aim at providing the necessary information to apply such a method for the following DIT values.

Short exposures on objects brighter than J,H,K  $\sim$  8–10 mag, or in the L or M bands, should use DITs of 1 s, 1.5 s, 2 s, 3 s, 5 s, 7 s, 10 s, 15 s, 20 s, 30 s or 45 s. However, note that optimal flat-fielding correction requires that DIT is at least 2 s (§6.4).

Long exposures on faint targets *must* select DITs of 60 s, 90 s, 120 s, 180 s, 300 s or 600 s. For a longer DIT (typically 900 s), a waiver is required due to the problem of detector glow.

- Starting in P84, the new readout mode *FowlerNsampGRstWin* is offered. In this mode, the 2 central detectors of the mosaic are windowed permitting the use of DITs as short as 0.15s. Detector 1 and 4 are not read: the spectrum falling on detectors 1 and 4 are therefore lost. This read-out mode should also be more efficient for faint targets as the detectors are read more often, decreasing the effective read-out noise: however, the gain in sensitivity for faint targets has not yet been determined.

For the `CRIRES_spec_obs_AutoNodOnSlit`, `CRIRES_spec_cal_AutoNodOnSlit` and `CRIRES_spec_obs_SpectroAstrometry` templates, the window are actually 2 stripes separated by 12 arcsec, covering the whole detectors #2 and #3 in the spectral direction. On the spatial direction, each window has a width given by half the value of `DET1.WIN.NY` (*P2PP: Number of pixels along Y axis*). The permitted values of 64, 128 and 256 correspond to individual stripe width of 2.7, 5.5 and 11.0 arcsec. These 2 stripes are symmetrically located at 6 arcsec from the centering location (i.e, the location of the spectrum at the end of the acquisition). The nodding throw must be set to 12 arcsec. The jitter width must be set to 0 if `DET1.WIN.NY` is 64, smaller than 1 and 2 arcsec

if DET1.WIN.NY is 128 and 256 respectively, otherwise the spectrum can fall outside the stripes: indeed, distortion introduced by the spectrograph and the mis-alignment between detector #2 and 3 cause the spectrum to be slightly displaced in the spatial direction depending on the grating orientation (cf. Fig 18). *This is particularly the case if ‘the number of pixels along Y axis’ is set to 64 with the CRIRES\_spec\_obs\_AutoNodOnSlit template: this combination should be avoided as the spectrum in at least one of the 2 detectors may suffer significant loss in each nodding position.*

For the CRIRES\_spec\_obs\_GenericOffset template, the window corresponds to a single stripe covering detector #2 and #3 in the spectral direction and of width in the spatial direction given by DET1.WIN.NY (*P2PP: Number of pixels along Y axis*), corresponding to 5.5, 11.0 and 22.0 arcsec. The center of this stripe in the Y direction is located at the centering location, in other words, at the location of the spectrum following the acquisition template (cf. Fig 18).

The minimum DIT are 0.15, 0.25 and 0.50 s for DET1.WIN.NY = 64, 128 and 256, respectively.

NDIT is specified by the observer to reach the required SNR as computed with the ETC.

Overheads for the FowlerNsamp and FowlerNsampGRstWin are different (see Table 3).

In P85, the same read-out mode must be used for all the acquisition, science and calibration templates in a given OB for which the choice is possible<sup>3</sup>. If the FowlerNsampGRstWin is used, the same number of pixels in the Y direction must be used for all relevant templates in a same OB.

## 11.4 README and finding charts

General instructions on the README file and finding charts are given at:

<http://www.eso.org/observing/p2pp>

while CRIRES-specific requirements can be found at:

<http://www.eso.org/observing/p2pp/CRIRES/CRIRES-P2PP.html>

Appropriate and detailed finding charts are *crucial* for the success of observations, especially in crowded fields.

- The field of view of the finding chart should be 50'' by 50'' in size, with a clear indication of field orientation. The target should be clearly marked by an arrow. If observations are performed with the derotator in SKY mode, the slit orientation should be clearly drawn.
- For high proper motion stars (> 1''/year) the present day position should be indicated by an arrow pointing from the target in the chart to the present day position (especially if similar bright sources are around).
- The finding chart has to show the field in the NIR band closest to the observing wavelength,  $\lambda_{\text{OBS}}$ :

---

<sup>3</sup>Although the CRIRES\_spec\_cal\_Wave template uses the FowlerNsamp, it can be used in an OB where other science and calibrations templates uses the FowlerNsampGRstWin read-out mode.

- in J band, if  $950 \text{ nm} < \lambda_{\text{OBS}} \leq 1300 \text{ nm}$ ,
- in H band, if  $1300 \text{ nm} < \lambda_{\text{OBS}} \leq 2000 \text{ nm}$ , or for very bright targets;
- in K band, if  $2000 \text{ nm} < \lambda_{\text{OBS}} \leq 5400 \text{ nm}$ .

Note that the ESO infrared digitized sky II actually correspond to the I band and should not be used if other infrared images are available (e.g. 2MASS).

- In crowded fields, a second finding chart should be attached to the corresponding OB, with a zoom-in on the science target(s).
- In case of binary or multiple stars, the target must be clearly indicated, in particular, (a) in case of large proper motion, including relative proper motion; (b) in case the finding chart was obtained in a band-pass that does not include the observing wavelength.
- AO, SVGS and science target should be clearly marked. If the AO star or SVGS are less than  $15''$  from the edge of the finding chart (centered on the target), another  $2' \text{ by } 2'$  finding chart should be provided.

The magnitude of the AO and SV guide stars, of the science target, and of the standard stars should be explicitly given in the **Instrument Comments** field of each OB. Please check the CRIRES P2PP-related information at :

<http://www.eso.org/observing/p2pp/CRIRES/CRIRES-P2PP.html>

for more details.

## 11.5 Constraints

### 11.5.1 Moon

As stated above (§9.4), an FLI of 1.00 is suitable for most observations. However, telescope guiding and active optics can be compromised for moon distance smaller than 30 deg. A smaller FLI value is recommended only in the case of AO observations with an AO star fainter than  $R = 15 \text{ mag}$ . In this case, a value 0.7 and a moon distance larger than 50 deg is generally adequate.

### 11.5.2 Seeing and Strehl ratio for adaptive optics observations

For closed loop AO observations, the users must specify in the constraint set the desired on-axis Strehl ratio, i.e. the ratio of the maximal intensity of the PSF to the maximal intensity expected for the theoretical PSF with no turbulence. This is the main parameter regarding atmospheric turbulence. It should be set for the K band; this value is produced by the **ETC**. In addition, all closed loop AO observations should enter also the FWHM of the seeing, although this constraint is less relevant. The constraint on the seeing refers to the seeing measured by the DIMM or by the guide probe, as they are the most relevant for the MACAO system. It is used as a guide, together with the coherence time, in order to estimate the achievable Strehl ratio.

If the AO star is not the science target, it is worth noting that the isoplanatic angle  $\theta_0$  depends on airmass<sup>-8/5</sup>, and on the wavelength as  $\lambda^{6/5}$ . On the other hand, the Strehl ratio, SR, decreases with the angular distance to the AO star  $\theta$  as  $SR \propto \exp(-(\theta/\theta_0)^{5/3})$ .

For an extended source, the Strehl ratio has no meaning and only the constraint on the FWHM should be entered.

### 11.5.3 Seeing for seeing limited observations, no adaptive optics

For NoAO observations, only the seeing at the wavelength of observations is relevant. The user should therefore specify the FWHM for the respective bands of the science observations. The constraints set and definitions are the same as for all other seeing limited VLT instruments. The input field for the Strehl ratio should remain unchanged (i.e., N/A).

The classification of each observation will be based either (a) on the measured spatial profile of the spectrum if the object is a point source, or (b) on FWHM of a star seen on the Slit Viewer if there are more stars available, or (c) on the seeing measured on the guide probe otherwise, using the Roddier formula to convert it to the seeing at the observed wavelength.

### 11.5.4 Transparency

Thin clouds (THN) usually do not hamper CRIRES observations for bright objects. Clear (CLR) conditions are justified for observations requiring stable Strehl ratios, for example to study the close environment of the target, as clouds could otherwise adversely affect the adaptive optics. For the same reason, CLR conditions should be requested for AO observations using AO stars fainter than  $R \approx 14$ .

AO observations must not be carried with thick (THK) clouds as the likely rapid changes of transparency can damage APDs.

### 11.5.5 Airmass

In addition to the influence of airmass on the quality of the adaptive optics correction mentioned above, observations in SKY mode can be strongly affected by differential refraction effects. Some guide lines are given in §8.2.

## 11.6 Water vapor

Observations in the NIR can be severely affected by the presence of water vapor in the atmosphere: large amount of water vapor can significantly decrease the sky transmission, and, in particular, in the L and M bands increase the sky emission background.

The ETC offers the possibility to select sky spectra calculated with a set of representative amounts of water vapor in the atmosphere. Service mode users with the help of USD can then indicate in the README file which observations can be adversely affected by large amount of water vapor. ESO considers the possibility to add a constraint on the water vapor in the P2PP constraint set for future periods.

## 11.7 Offset conventions and definitions

CRIRES follows the standard astronomical offset conventions and definitions.

Position angles (PAs) are measured from 0 to 360 degrees. North corresponds to a PA of 0 degree, East, to a PA of 90 degrees.

All offsets are given in arc seconds.

Proper motions must be given in " per year.

For solar system objects, additional tracking velocities are given in arcsec per second.

For a position angle of 0 in SKY mode, the reconstructed slit viewer image shows North up and East left.

## Part IV

# Reference material

## 12 CRIRES calibration plan

The calibration plan defines the default calibrations obtained and archived for the user by the Paranal Science Operations. The CRIRES science calibration plan includes the following measurements:

- *daily*: 3 darks obtained with the same DITs as the science, telluric or spectro-photometric standard star observations, as well as for any flat-fields or wavelength calibrations. Note that the frequency may change to *weekly* if darks are found to be stable enough;
- *daily*: 3 flat-fields obtained with the same wavelength setting as the science and telluric or spectro-photometric standard star observations;
- *daily*: 3 wavelength calibration frames obtained with the same wavelength setting as the science and telluric or spectro-photometric standard star observations, for reference wavelengths shorter than 2400 nm. Currently, the reproducibility of the wavelength setting between night-time observations and day-time calibrations is  $\approx 3$  pixels.
- *daily*: bad-pixel maps, derived from darks and flat-fields. Note that the frequency may change to *weekly* or *monthly* these quantities are found to be stable enough;
- approximately *monthly*: linearity.
- *yearly or after instrument warm-up*: distortion map and photon transfer function;
- typically once per night CRIRES is used: radial velocity standard.
- at least once per night CRIRES is used: precipitable water vapour measurements.
- at least once per night CRIRES is used: measurements of column densities of a few molecular species.

Flats and wavelength calibration are only obtained with a slit width of 0.2 " and  $\text{DIT} \geq 2$  s.

## 13 Data format and reduction

### 13.1 Format

The SV image and the spectra recorded on the four science detectors are saved in extended FITS files. Each of the 4 extensions for the science images have format of  $1024 \times 512$  pixels (see Fig. 2).

### 13.2 Pipeline

ESO/SDD regularly updates the CRIRES pipeline. It uses the ESO/CPL library. The main observation and calibration templates are supported by an automatic version of the pipeline for quick-look analysis at the telescope. Raw images are combined, spectra extracted and calibrated in wavelength. Photometric conversion factors based on standard star observations are provided.

More information can be found at:

<http://www.eso.org/sci/data-processing/software/pipelines/>

and

[http://www.eso.org/observing/dfo/quality/index\\_crires.html](http://www.eso.org/observing/dfo/quality/index_crires.html)

## 14 Template parameters

All scientific and calibration observations with ESO instruments are prepared as observation blocks (OBs) and with the phase 2 proposal preparation tool (P2PP).

Observation blocks consist of the target information, a small number of user selected templates, the constraint sets and the scheduling information. The input parameters of the templates described below are list of keywords that define the telescope pointing and instrument configuration. One OB contains only one acquisition template and is followed by one or more science or calibration templates.

User accessible input parameters of CRIRES templates for acquisition, science, dark, flat, wavelength calibration and or standard star observation are described in the following sections. A pipeline recipe is triggered by a unique association of DPR (Data Product) keywords which are described in the pipeline user manual. They are given here for completeness.

### 14.1 Acquisition templates

All science and standard star OBs *must* start with an acquisition template. Four acquisition templates are available:

- CRIRES\_spec\_acq\_NGS,
- CRIRES\_spec\_acq\_NoAO,
- CRIRES\_spec\_acq\_NGS\_difftrack,
- CRIRES\_spec\_acq\_NoAO\_difftrack,

CRIRES\_spec\_acq\_NGS acquires the AO star with MACAO, which allows the user to make the following science or standard star observations with the adaptive optics system. On the other hand, observations following the CRIRES\_spec\_acq\_NoAO acquisition template will not be done with the adaptive optics system.

The CRIRES\_spec\_acq\_NGS\_difftrack and CRIRES\_spec\_acq\_NoAO\_difftrack allows acquisition of objects to be observed in differential tracking mode, i.e., the acquisition of a target using as reference an object moving relative to the target, either using the reference object for the MACAO and possibly slit viewer guiding (CRIRES\_spec\_acq\_NGS\_difftrack) or for slit viewer guiding alone without AO corrections (CRIRES\_spec\_acq\_NoAO\_difftrack). In P85, differential tracking is offered both in service and visitor mode.

The acquisition templates contain the parameters required for the pointing and tracking of the telescope, centering of the target in the slit, setting of the derotator mode which includes the orientation of the slit on the sky. CRIRES\_spec\_acq\_NGS also includes parameters used to acquire the natural guide star (NGS) and close the loop of the Adaptive Optics system. Finally, they also contain keywords that specify the science detector readout-mode.

#### 14.1.1 Target and SVGS parameters

**TEL.TARG.ALPHA**, **TEL.TARG.DELTA**, **TEL.TARG.EQUINOX** (P2PP: *RA*, *DEC*, *Equinox*) are the coordinates of the science target and the equinox for which these coordinates correspond to. In case of multiple objects in the slit or of extended objects, these coordinates correspond to the telescope pointing during the observations.

**TEL.TARG.PMA, TEL.TARG.PMD** (P2PP: *Proper Motion Alpha, Delta*) are proper motion values in RA and DEC and specified in units of "/year. If they are different from 0, the epoch, TEL.TARG.EPOCH (P2PP: *Epoch*), at which the coordinates were valid should be given.

**TEL.TARG.ADDVELALPHA, TEL.TARG.ADDVELDELTA** (P2PP: *Diff. in RA, DEC*) are additional velocities in  $\alpha$ ,  $\delta$  and in units of "/second. For solar system objects, the coordinates should be the J2000 ICRF, astrometric coordinates. In particular, the user should *not* provide the apparent coordinates!

*Note:* Starting with P2PP 2.12, the differential velocities for moving targets are to be specified directly in the target package, and not in the acquisition template as in previous versions (i.e., the fields *Telescope: Alpha/Delta additional tracking velocity* should be left blank). Please check Section 5.5.3 of the P2PP User Manual for more details.

**TEL.TARG.OFFSETALPHA and TEL.TARG.OFFSETDELTA:** (P2PP: *RA/DEC offset between target and SV guide star*). In some cases, such as:

- relatively faint targets observed through a relatively wide slit, for which not enough light is reflected from the slit jaws to the slit viewer detector; this situation may occur e.g. for  $H \simeq 14$  targets and slit wider than 0.3", in good seeing conditions,
- diffuse objects on which guiding is difficult or impossible,

the use of a brighter object in the field of the slit viewer is recommended. This object will be used as a reference object for initial centering and as a guide star for secondary guiding. It is referred to as slit viewer guide star (SVGS).

In this case, TEL.TARG.OFFSETALPHA and TEL.TARG.OFFSETDELTA correspond to the offsets in " between the SVGS and the target.

If  $\alpha(\text{SVGS})$  and  $\delta(\text{SVGS})$  are the coordinates of the slit viewer guide star, the sign conventions are as follows:

$$\text{TEL.TARG.ALPHA} + \text{TEL.TARG.OFFSETALPHA} = \alpha(\text{SVGS})$$

$$\text{TEL.TARG.DELTA} + \text{TEL.TARG.OFFSETDELTA} = \delta(\text{SVGS})$$

In other words, TEL.TARG.OFFSETALPHA and TEL.TARG.OFFSETDELTA are positive if the SVGS is located to the East and North of the target.

*Example:* one wishes to observe the target at  $\alpha_{2000}(\text{Target}) = 04\text{h}53\text{m}50.678\text{s}$ ,  $\delta_{2000}(\text{Target}) = -25^\circ25'56.017''$ . To center it in the slit, the nearby star at  $\alpha_{2000}(\text{SVGS}) = 04\text{h}53\text{m}49.690\text{s}$ ,  $\delta_{2000}(\text{SVGS}) = -25^\circ25'45.078''$  is used as a reference star as well as the slit viewer guide star. Both these objects have negligible proper motions. Then,

$$\text{TEL.TARG.OFFSETALPHA} = \Delta\alpha = \alpha_{2000}(\text{SVGS}) - \alpha_{2000}(\text{Target}), \quad (4)$$

$$\text{TEL.TARG.OFFSETDELTA} = \Delta\delta = \delta_{2000}(\text{SVGS}) - \delta_{2000}(\text{Target}). \quad (5)$$

Therefore, the relevant P2PP parameters are

$$\text{RA} = 04 : 53 : 50.678$$

	DEC = -25 : 25 : 56.017
RA offset between target and SV guide star =	-13.38,
DEC offset between target and SV guide star =	+10.94.

Notes:

1. the use of a SVGS different from the target is only possible if the derotator is set to SKY mode;

### 14.1.2 Gas cell

**INS.OPTI1.NAME** (P2PP: *Gas cell*) sets the gas cell to be used. The default value (FREE) should be set for observations without gas cell, while GAS\_N2O, GAS\_CO, GAS\_VISITOR should be set for observations with the N<sub>2</sub>O, CO or the visitor gas cell, respectively.

It should be set to the same value as the one in the first observing template.

### 14.1.3 NGS parameters

The following parameters are only required by the template CRIRES\_spec\_acq\_NGS.

**SEQ.NGS.ISTARGET** (P2PP: *Target = AO guide star*) is a flag. If set to 'T' (default) the natural guide star (NGS) used for the adaptive optics is also the science target of the observations. If this flag is set to 'F' then the user needs to provide the NGS coordinates SEQ.NGS.ALPHA and SEQ.NGS.DELTA. However, see also the note 3 below (§14.1.9) for a special case.

**SEQ.NGS.COLOR** (P2PP: *AO guide star: B-R color value*) gives the B-R color of the NGS. This parameter is needed for accurate correction of the differential refraction between the wavelength used for the observations and the effective wavelength of the wavefront sensor.

**SEQ.NGS.FWHM** (P2PP: *AO guide star: FWHM (arcsec)*) gives the FWHM (in ") of the object used as natural guide star. For a point source, a value of 0 is appropriate

**SEQ.NGS.SNR** (P2PP: *AO guide star: Minimum S/N*) gives the required signal-to-noise ratio that MACAO needs on the wavefront sensor to be able to close the loop. The default value is fine for most cases, except for the faintest objects that the MACAO can acquire, in which case a smaller value is to be given.

**SEQ.NGS.USELASTSKY** (P2PP: *Use the last sky measurement for the WFS*) is a flag. If set to 'T', the MACAO will not repeat the sky measurement for the wavefront sensor. The sky measurement is used to determine the signal-to-noise ratio of the wavefront sensor flux. The default value ('T') is adequate for bright AO stars ( $R < 10$ ). For fainter targets, it should be set to 'F'. In this case, the following parameters (SEQ.NGS.SKYALPHA and SEQ.NGS.SKYDELTA) should be **determined with care** if observations take place in crowded fields.

**SEQ.NGS.SKYALPHA** and **SEQ.NGS.SKYDELTA** (P2PP: *WFS Alpha/Delta sky offset (arcsec)*) gives the offsets of the location relative to the NGS where MACAO measures the sky.

If  $\text{SEQ.NGS.SKYALPHA} > 0$ , the sky is measured to the East of the NGS.

If  $\text{SEQ.NGS.SKYDELTA} > 0$ , the sky is measured to the North of the NGS.

Default values are usually fine, except in crowded fields.

**SEQ.NGS.ISSVGS** (P2PP: *SV Guide Star = AO Guide Star*) is a flag. If set to ‘T’ (default) the natural guide star (NGS) used for the adaptive optics is also the slit viewer guide star (SVGS). If this flag is ‘F’ then the user needs to provide the offsets **TEL.TARG.OFFSETALPHA** and **TEL.TARG.OFFSETDELTA**. However, see also the note 3 below (§14.1.9) for a special case.

#### 14.1.4 Parameters related to the slit viewer

**SEQ.SV.USELASTSKY** (P2PP: *Use the last sky measurement for the SV*). Generally one can use the last sky measurement and therefore leaves **SEQ.SV.USELASTSKY** = ‘T’ untouched from its default value. However, if one observes a faint target, a new sky should be obtained for the slit viewer. In this case set **SEQ.SV.USELASTSKY** = ‘F’.

**TEL.SKY.OFFSETALPHA**, **TEL.SKY.OFFSETDELTA**. (P2PP: *RA/DEC offset to sky*) are only relevant if **SEQ.SV.USELASTSKY** = ‘F’. By default sky exposures are taken 30 " in RA and DEC from the science target position. In crowded fields however, one has a high chance that the sky exposures is contaminated by some other source(s). Therefore these parameters offer freedom to specify RA and DEC offset positions. These offsets are usually executed early in the procedure, at the time of the acquisition of the NGS. The convention for these RA, DEC offsets are:

$$\begin{aligned}\text{TEL.SKY.OFFSETALPHA} &= \alpha_{\text{SKY}} - \alpha(\text{NGS}), \\ \text{TEL.SKY.OFFSETDELTA} &= \delta_{\text{SKY}} - \delta(\text{NGS}).\end{aligned}$$

#### 14.1.5 Telescope guide star parameters

Sometimes, the telescope operator may have difficulties to find an appropriate telescope guide star, which is also used to set-up the M1 active optics. This often happens in the Orion nebula, in other nebulae that appear as saturated in the Digital Sky Survey, or in extended dark nebulae. In these cases, it is useful to provide a telescope guide star.

**TEL.AG.GUIDESTAR** (P2PP: *Telescope guide star selection*): if set to ‘CATALOGUE’, the Telescope Control System semi-automatically searches for a telescope guide star. If the user wishes to provide the coordinates of the telescope guide star, then **TEL.AG.GUIDESTAR** should be set to ‘SETUPFILE’.

**TEL.GS1.ALPHA**, **TEL.GS1.DELTA** (P2PP: *RA/DEC of telescope guide star*) are only relevant if **TEL.AG.GUIDESTAR** = ‘SETUPFILE’. These parameters correspond to the J2000 coordinates, epoch of the observations, of the telescope guide star. Otherwise, both parameters should be kept to default 0.

#### 14.1.6 Derotator parameters

**INS.DROT.MODE** (P2PP label: *Derotator: Mode*) determines the derotator mode: SKY or ELEV. In ELEV mode, the slit is constantly aligned with the parallactic angle in order to reduce slit loss introduced by differential refraction. This is particularly important if slit viewer guiding has to be made in one band (e.g., in K) and the observations in another one (e.g., M). *However, in ELEV mode, guiding with a SVGS different from target is not implemented.*

The use of the **CRIRES\_spec\_obs\_SpectroAstrometry** and **CRIRES\_spec\_obs\_GenericOffset** templates is only possible if the derotator mode is set to SKY.

**INS.DROT.POSANG** (P2PP label: *Position angle*) determines the position angle (PA) of the slit if **INS.DROT.MODE** = SKY. The values must be set such that **INS.DROT.POSANG** = PA.

#### 14.1.7 Spectrograph parameters

**INS.SLIT.WID** (P2PP: *Entrance slit width*) determines the slit width in ". Recommended value is 0.2 – 0.4 " with AO. Without AO, the optimal S/N is obtained with a slit width equal to the seeing, however, a value larger than 0.4" is not recommended, as a large fraction of the spectral range can be affected by vignetting or lack of reproducibility (see §8.4). A value of 0.2 " gives the highest resolution.

**INS.WLEN.REF** (P2PP: *Reference wavelength*) is the reference wavelength. This wavelength corresponds to pixel 512 of detector # 3. Tables 4a to 4f provide the reference wavelengths of the standard settings. Tables 6a and 6b lists the allowed minimum and maximum ranges for a given order. For visual inspection of the start and end wavelengths of each detector, unvignetted spectral range, detector gaps (Fig. 2) or the appearance of sky lines, the ETC should be used. The reference wavelength is needed in the acquisition template to allow the spectrograph configuration to be carried out during telescope preset: it should therefore be set to the same value as in the first observation template.

**INS.GRAT.ORDER** (P2PP: *Grating order*) is the grating order. For most wavelength settings there is a unique relation between the reference wavelength and the grating order. In this case **INS.GRAT.ORDER** can be kept as its default value of 0. However, for some reference wavelengths in order 39–43 and 21–22 there is no unique relation and the grating order has to be specified by the user. Table 6a lists the orders and wavelength ranges for which this parameter must be given.

### 14.1.8 Science detector parameters

Since P84, the read-out mode of the science detector, `DET1.NCORRS.NAME` (P2PP *Detector Read-Out Mode*) can be selected between the 2 following possibilities:

- `FowlerNsamp`,
- `FowlerNsampGRstWin`.

See §6 for a description of these modes and restrictions on their use.

The default read-out mode is `FowlerNsamp`, which allows to read the whole mosaic with *recommended* DITs between 2 and 900s. It should be selected for most observations. See §11.3 for the list of possible DITs.

On the other hand, the `FowlerNsampGRstWin` readout mode reads only small windows of detector #2 and #3. As a smaller section of the detector is read, the read-out can be fastest, which allows observations of very bright targets. Since the read-out is fastest, more Fowler read-out samples can be obtained, therefore decreasing the read-out noise for an individual exposure (for a given DIT), which improves the signal-to-noise ratio of observations of read-out noise limited objects, such as faint targets.

If `FowlerNsampGRstWin` is selected, the total number of pixels in the Y direction for the detector window must be set using the parameter `DET1.WIN.NY` (P2PP: *Number of pixels along Y axis*).

See §11.3 for a description of the detector read-out modes.

Setting these parameters in the acquisition template is required to avoid saturating the detector in the case of observations of a very bright target, which could lead to possible remanence.

### 14.1.9 Notes

1. If both `SEQ.NGS.ISTARGET` and `SEQ.NGS.ISSVGS` are set to ‘T’, then the target is the AO guide star and the slit viewer guide star. Therefore, only the target coordinates `TEL.TARG.ALPHA` and `TEL.TARG.DELTA` must be provided.
2. If `SEQ.NGS.ISTARGET` is ‘T’ and `SEQ.NGS.ISSVGS` is ‘F’, then the target is the AO guide star but it is not used for guiding with the slit viewer. In this case, in addition to `TEL.TARG.ALPHA` and `TEL.TARG.DELTA`, `TEL.TARG.OFFSETALPHA` and `TEL.TARG.OFFSETDELTA` should be provided (see above for the convention).
3. If `SEQ.NGS.ISTARGET` is ‘F’ and `SEQ.NGS.ISSVGS` is ‘T’, then the slit viewer guide star is the AO guide star but not the target. In this case, of course, `TEL.TARG.ALPHA` and `TEL.TARG.DELTA` should be provided. On the other hand, the user can either enter the coordinates of the AO guide star (`SEQ.NGS.ALPHA` and `SEQ.NGS.DELTA`) or the offsets `TEL.TARG.OFFSETALPHA` and `TEL.TARG.OFFSETDELTA` (following the convention above).

## 14.2 Observation templates

This section describes the three observation templates offered in P85:

- `CRIRES_spec_obs_AutoNodOnSlit`,

- `CRIRES_spec_obs_GenericOffset`,
- `CRIRES_spec_obs_SpectroAstrometry`.

An observation template sets up the instrument, if different from the acquisition, as well as the detector integration time (DIT) and number of individual integrations averaged to create an exposure (NDIT). It defines the number of exposures taken at each nodding position as well as the nodding and, if needed, jittering offsets.

The following paragraphs describe only the parameters that are not defined in the previous sections.

### 14.2.1 Detector

**DET1.DIT** (P2PP: *DIT*) defines the exposure time of an individual integration, in seconds. For bright objects, saturation of the detector ( $120,000 e^-$ ) must be avoided. On the other hand, correction of the non-linearity of the detectors (incl. the odd-even effects; see Sect. 6.4) has so far been achieved to a reasonable accuracy only for a signal (dark + sky + object) smaller than about 10,000 ADUs ( $\approx 80,000 e^-$ ). DIT settings leading to stronger count rate should therefore be avoided. The **ETC** outputs a 'Max. intensity at central pixel per DIT (object+sky)' and therefore allows one to check if the chosen DIT is adequate. It is important to check that the **ETC** input parameter 'requested wavelength' does not correspond to a deep absorption line (either in the target spectrum or caused by the Earth's atmosphere). For faint objects in the J, H, and K bands, long DITs are recommended in order to decrease the contribution of the RON to the overall noise. See Sec. 11.3 for recommended and offered values.

**DET1.NDIT** (P2PP: *NDIT*) determines the number of individual integration averaged into one exposure. Therefore  $\text{DET1.NDIT} \times \text{DET1.DIT}$  sets the total integration time of one exposure.

**SEQ.NEXPO** (P2PP: *Number of exposures per nodding position*) is the number of exposures in any nodding or offset position. Therefore the integration time spend in one nodding position is given by:

$$\text{DET1.NDIT} \times \text{DET1.DIT} \times \text{SEQ.NEXPO}$$

### 14.2.2 Gas cell

**INS.OPTI1.NAME** (P2PP: *Gas cell*) sets the gas cell to be used. The default value (FREE) should be set for observations without gas cell, while `GAS_N2O` or `GAS_CO` should be set for observations with the N<sub>2</sub>O or CO gas cell, respectively.

### 14.2.3 `CRIRES_spec_obs_AutoNodOnSlit` and `CRIRES_spec_obs_SpectroAstrometry`: nodding and jittering

**SEQ.NABCYCLES** (P2PP: *Number of nodding cycles*) sets the number of AB or BA nodding cycles. Although the value of 0 is allowed (staring), it is not recommended because of detector glow and other systematic effects (Sect. 6.2). If set to a value  $\geq 1$ , the total integration time of the template, in seconds, is:

$DET1.NDIT \times DET1.DIT \times SEQ.NEXPO \times SEQ.NABCYCLES \times 2$ .

However, one should not confuse integration time with the total execution time of one OB caused by the various overheads which need to be added as described in Sec. 10.3.

*Examples:*

If  $SEQ.NABCYCLES = 1$ , the telescope first points to the A position: it is located to the South (if  $INS.DROT.POSANG = 0$ ) at a distance equal to  $SEQ.NODTHROW/2$  (see below) (and assuming  $SEQ.JITTER.WIDTH = 0$ ) from the centering position. After  $SEQ.NEXPO$  exposures, the telescope nods to the B position: it moves to the north by  $SEQ.NODTHROW$ , and takes  $SEQ.NEXPO$  additional exposures. Then the telescope moves back to its original position. The telescope has then executed one AB nodding cycle.

If  $SEQ.NABCYCLES = 3$ , the telescope first points to the A position, as defined in the previous paragraph, and takes  $SEQ.NEXPO$  exposures. It then moves to the B position, takes twice  $SEQ.NEXPO$  additional exposures. It then moves back to the A position, when it takes twice  $SEQ.NEXPO$  exposures. Then, it moves a last time to the B position for a last sequence of  $SEQ.NEXPO$  exposures before returning to the original position. The telescope had therefore executed 3 nodding cycles: AB BA AB.

**SEQ.NODTHROW** (P2PP: *Nod throw along the slit*) is the nodding throw, or telescope offset between two nodding positions (Sect. 9). It should be large enough so that the spatial profiles of the target in the two nodding positions do not overlap. The nodding positions are located symmetrically (at  $SEQ.NODTHROW/2$ ) around the centering location.

If the detector read-out mode is set to `FowlerNsampGRstWin`, the nodding throw *must* be set to 12 arcsec.

**SEQ.JITTER.WIDTH** (P2PP: *Jitter width*) A jitter is a small offset added to each nodding offset. It helps correcting for bad detector pixels (Sect. 9). `SEQ.JITTER.WIDTH` gives the width of the jitter box: the maximum offset from the nodding position is therefore given by half of this value. The successive values of the jitter offset in a given template are drawn from a set of 100 numbers determined from a Poisson random number generator. Jittering is currently not possible if  $SEQ.NABCYCLES = 0$  (staring mode).

If the detector read-out mode is set to `FowlerNsampGRstWin`, the jitter width is *restricted* to 0 if `DET1.WIN.NY` (P2PP: *Number of pixels along Y axis*) is 64, *limited* to values less than 1 or 2 arcsec if `DET1.WIN.NY` is 128 or 256, respectively.

**DET1.NCORRS.NAME** (P2PP *Detector Read-Out Mode*) and **DET1.WIN.NY** (P2PP: *Number of pixels along Y axis*) are described in § 11.3.

#### 14.2.4 CRIRES\_spec\_obs\_GenericOffset only: list of offsets

The `CRIRES_spec_obs_GenericOffset` allows the user to define a list of offsets, offering more flexibility for sky subtraction in case of extended objects. It only makes sense to use this template if `INS.DROT.MODE` (Derotator mode) is set to `SKY` in the acquisition template.

**SEQ.OFFSET.COORDS** (P2PP: *Offset coordinate type selection*) determines if the list of offsets given in `SEQ.OFFSET1.LIST` and `SEQ.OFFSET2.LIST` are given in `SKY` or `DETECTOR` coordinates.

**SEQ.OFFSET1.LIST, SEQ.OFFSET2.LIST** (P2PP: *Lists of offsets in RA or X, Lists of offsets in DEC or Y*)

In all cases, the list of offsets are in arcseconds.

If SEQ.OFFSET.COORDS is set to 'SKY', a positive value in SEQ.OFFSET1.LIST means that the new pointing of the telescope is to the east relative to the previous location; similarly, a positive value in SEQ.OFFSET2.LIST means that the new pointing of the telescope is to the north relative to its previous location. During the first exposure, the telescope points to the location given by (TEL.TARG.ALPHA, TEL.TARG.DELTA) + the first value given in (SEQ.OFFSET1.LIST, SEQ.OFFSET2.LIST). In other words, in this case, the offsets correspond to telescope offsets.

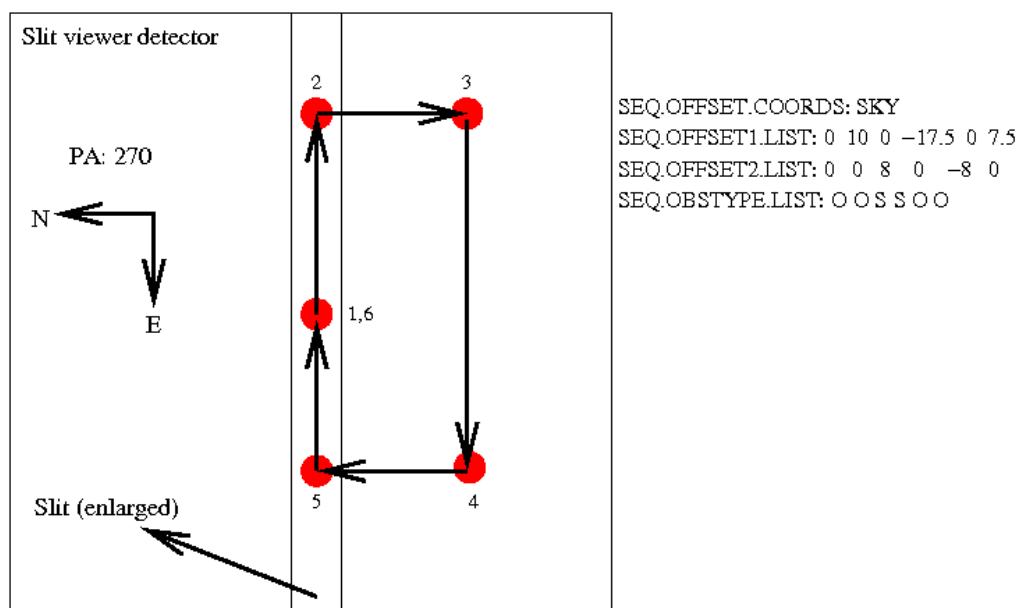


Figure 27: Illustration showing the apparent locations of a target as seen on the slit viewer detector for the given parameters, in the case of 'SKY' coordinate offsets.

If SEQ.OFFSET.COORDS is set to 'DETECTOR', the offsets correspond to the apparent motion of the target on the slit viewer detector, with X increasing from left to right (from E to W if the position angle is 0 deg) and Y increasing from bottom to top (from S to N if the position angle is 0 deg, see Fig. 18). In other words, in this case, a positive offset in both X and Y would bring the target to larger X and larger Y values as seen on the slit viewer. If the position angle is 0, this corresponds to a motion of the telescope to the East and South. Subsequent offsets are similarly made relative to the last telescope offset.

**SEQ.OBSTYPE.LIST** (P2PP: *List of observation types (O or S)*) is a list that determines if the exposure taken once the corresponding offset has been completed is an 'OBJECT' ('O') or a 'SKY' ('S') measurement. Therefore, the total integration time of one exposure in an 'OBJECT' location is DET1.NDIT.OBJECT  $\times$  DET1.DIT. Similarly, the total integration time of one exposure in 'SKY' location is DET1.NDIT.SKY  $\times$  DET1.DIT. Note that SEQ.NEXPO exposures can be obtained at each location.

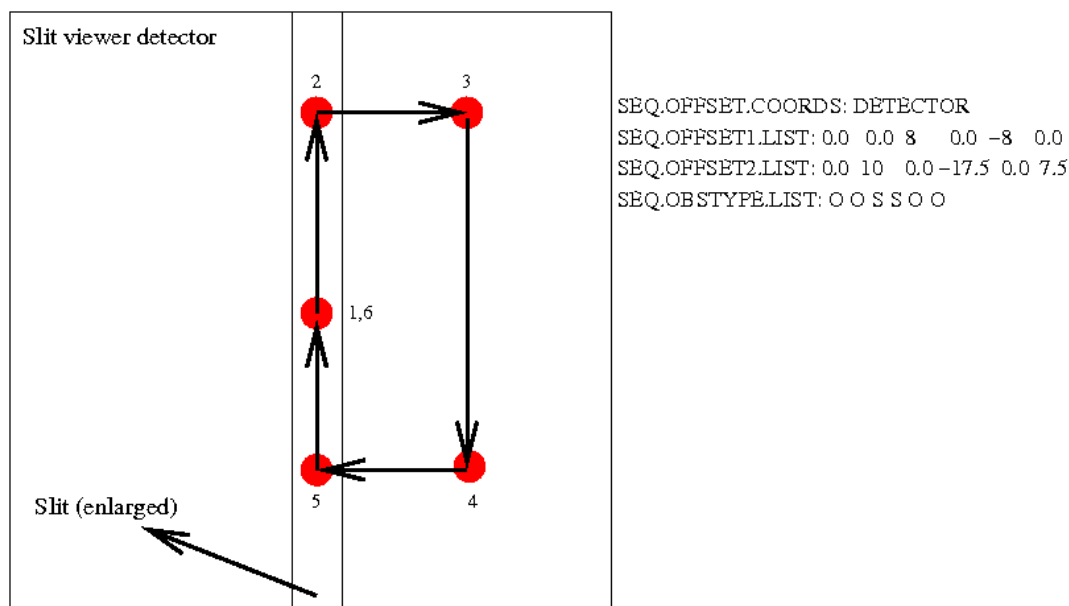


Figure 28: Illustration showing the apparent locations of a target as seen on the slit viewer detector for the given parameters, in the case of 'DETECTOR' coordinate offsets. Although the derotator mode must be set to 'SKY', the position angle is irrelevant since all the motions are made in detector coordinates.

**SEQ.NOFF** (P2PP: *Number of offset positions*) gives the total number of telescope positions that the telescope will have during the execution of the template. Minimum value is 1. If this value is larger than the number of values listed in SEQ.OFFSET1.LIST, or SEQ.OFFSET2.LIST then the list is started again.

For example, if SEQ.NOFF = 5, SEQ.OFFSET1.LIST = '0 0 0' and SEQ.OFFSET2.LIST = '0 10 -10', SEQ.OFFSET.COORDS = 'DETECTOR', the list of offsets will be '0 0 0 0 0' along the X direction, '0 10 -10 0 10' along the Y direction.

The telescope goes back to the centering location at the end of the template.

**DET1.NCORRS.NAME** (P2PP *Detector Read-Out Mode*) and **DET1.WIN.NY** (P2PP: *Number of pixels along Y axis*) are described in Sec. 11.3.

#### 14.2.5 CRIRES\_spec\_obs\_SpectroAstrometry only: list of derotator angles, jitter reset

The CRIRES\_spec\_obs\_SpectroAstrometry template allows one to apply the spectro-astrometry technique without having to re-acquire the target for each position angle. It only makes sense to use this template if INS.DROT.MODE (Derotator mode) is set to SKY in the acquisition template.

**INS.DROT.POSANG.LIST** (P2PP: *List of position angles*) is the list of position angles: the CRIRES\_spec\_obs\_SpectroAstrometry template allows one to repeat the same sequence of observations as the ones done for the CRIRES\_spec\_obs\_AutoNodOnSlit template but for each value of the list of slit position angles given by this parameter.

Best results are obtained by giving a list of pairs of position angles differing by 180 degrees.

**SEQ.JITTER.RESET** (P2PP: *Reset jitter for each DROT posang*). Only relevant if SEQ.JITTER.WIDTH (Jitter width) is larger than 0. If this parameter is set to T the list of jitter positions calculated by the observation software is repeated identically, in detector coordinates, for each value of the slit position angle. In other words, the location of the different spectra for each nodding position will be identically repeated for each position angle.

If set to F, each nodding position in the execution of the whole template will be given a different jitter value.

If the number of nodding cycles is small, it is probably better to set this parameter to T. For a large number of nodding cycles, any residual detector systematic effects may be further decreased by setting the parameter to F.

**DET1.NCORRS.NAME** (P2PP *Detector Read-Out Mode*) and **DET1.WIN.NY** (P2PP: *Number of pixels along Y axis*) are described in Sec. 11.3.

### 14.3 Calibration templates

This section describes the use of the calibration templates. Night-time calibration of science programs is charged to the user.

#### 14.3.1 Standard star or telluric observations

The calibration template CRIRES\_spec\_cal\_AutoNodOnSlit is used to measure a telluric or spectro-photometric standard star (Sect. 9). Its functionality is similar to the observing template CRIRES\_spec\_obs\_AutoNodOnSlit described above. The files produced here will be automatically recognized by the pipeline as standard star observations.

If the standard star is in the list of spectrophotometric standard in the pipeline static files, then the pipeline also output the sensitivity and throughput of the whole system (spectrograph, telescope, Earth atmosphere).

#### 14.3.2 Flat field

Flat-fields can be obtained with the template CRIRES\_spec\_cal\_LampFlats. However, there is no *a priori* necessity to obtain flat-fields during the night, unless possibly when observations aim at obtaining very high accuracy radial velocity or for observations of extended targets.

The following parameters must be defined in this template:

- the reference wavelength and, if needed, the grating order;
- the detector readout mode; cf. §11.3 for a description.
- the entrance slit width, which *must* be the same as the one defined in the acquisition template;
- the approximate maximum flux (in ADU) over the whole mosaic;

If the detector readout-mode is FowlerNsampGRstWin (cf. §11.3) two additional parameters must be given:

1. the total number of pixels in the Y direction, which should match the science observations;
2. the number of stripes:
  - 2 if the science observations are obtained with the CRIRES\_spec\_obs\_AutoNodOnSlit template
  - 1 if the science observations are obtained with the CRIRES\_spec\_obs\_GenericOffset template

### 14.3.3 Wavelength calibration

High precision absolute wavelength calibration can be either obtained with sky emission lines or through the use of an arc lamp spectrum (see Sect. 7.1): currently, the reproducibility of the wavelength setting between night-time observations and day-time calibrations is  $\approx 3$  pixels. If required for your science experiment than insert the CRIRES\_spec\_cal\_Wave template either before or after any new wavelength setting in order to perform a wavelength calibration. This must be taken with a 0.2 arcsecond slit.

The parameters required by this template are INS.LAMP, INS.WLEN.REF and possibly INS.GRAT.ORDER.

**INS.LAMP** (P2PP: *Wavelength calibration source*) determines the source used for the wavelength calibration. The values allowed are THAR for the Thorium-Argon lamp, HALOGEN+N2O\_CELL for the Halogen + the N<sub>2</sub>O gas-cell and HALOGEN+CO\_CELL for the Halogen + the CO gas-cell. See Sect. 18.

### 14.3.4 Darks

Darks are obtained during daytime calibration by the VLT observatory. There is no need to execute dark exposures during the night. *In particular, p2pp does not carry out any compatibility check regarding parameters in the darks templates.*

The parameters required by this template are DIT, NDIT and NEXPO, as well as the detector readout mode.

If the detector readout-mode is FowlerNsampGRstWin, two additional parameters must be given:

1. the total number of pixels in the Y direction, which should match the science observations;
2. the number of stripes:
  - 2 if the science observations are obtained with the CRIRES\_spec\_obs\_AutoNodOnSlit template
  - 1 if the science observations are obtained with the CRIRES\_spec\_obs\_GenericOffset template

Cf. §11.3 for a description of this readout-mode.

#### 14.3.5 Sky observation

The template `CRIRES_spec_cal_SkyObs` template allows to take a spectrum of the sky at the current telescope location without slit viewer guiding and with the AO loop open. It is unlikely to be needed in any science OB: its main use is for characterizing the atmospheric conditions (amount of water vapour...).

## 14.3.6 Template signatures

CRIRES_spec_acq_NGS		
<i>To be specified:</i>		
Parameter	Range (Default)	Label
DET1.NCORRS.NAME	FowlerNsamp FowlerNsampGRstWin (FowlerNsamp)	Detector Read-Out Mode
DET1.WIN.NY	64 128 256 (64)	Number of pixels along Y axis
SEQ.NGS.ISTARGET	T F (T)	Target = AO Guide Star
SEQ.NGS.ALPHA	(0)	RA of AO guide star
SEQ.NGS.DELTA	(0)	DEC of AO guide star
SEQ.NGS.COLOR	-1..5 (0)	AO guide star: B-R color value
SEQ.NGS.FWHM	0..10 (0.0)	AO guide star: FWHM (arcsec)
SEQ.NGS.SNR	0.0..10000.0 (1000)	AO guide star: Minimum S/N
SEQ.NGS.USELASTSKY	T F (F)	Use the last sky measurement for the WFS
SEQ.NGS.SKYALPHA	-30..+30 (4.0)	WFS Alpha sky offset (arcsec)
SEQ.NGS.SKYDELTA	-30..+30 (4.0)	WFS Delta sky offset (arcsec)
SEQ.NGS.ISSVGS	T F (T)	SV Guide Star = AO Guide Star
SEQ.SV.USELASTSKY	T F (T)	Use the last sky measurement for the SV
TEL.SKY.OFFSETALPHA	-120..120 (30.0)	RA offset to sky
TEL.SKY.OFFSETDELTA	-120..120 (30.0)	DEC offset to sky
TEL.AG.GUIDESTAR	NONE SETUPFILE CATALOGUE (CATALOGUE)	Telescope guide star selection
TEL.GS1.ALPHA	(0.0)	RA of telescope guide star
TEL.GS1.DELTA	(0.0)	DEC of telescope guide star
TEL.TARG.OFFSETALPHA	-22.5..22.5 (0.0)	RA offset between target and SV guidestar
TEL.TARG.OFFSETDELTA	-22.5..22.5 (0.0)	DEC offset between target and SV guidestar
INS.OPTI1.NAME	FREE GAS_N2O GAS_CO GAS_VISITOR (FREE)	Gas cell
INS.DROT.MODE	SKY ELEV (NODEFAULT)	Derotator: Mode
INS.DROT.POSANG	0.0..360.0 (0.0)	Position angle
INS.SLIT.WID	0.05..3.0 (0.2)	Entrance slit width
INS.WLEN.REF	958.3..5361.9 (NODEFAULT)	Reference wavelength
INS.GRAT.ORDER	0..59 (0)	Grating order
TEL.TARG.ALPHA	(NODEFAULT)	Right Ascension
TEL.TARG.DELTA	(NODEFAULT)	Declination
TEL.TARG.EQUINOX	-2000..3000 (2000)	Equinox
TEL.TARG.EPOCH	-2000..3000 (2000)	Epoch
TEL.TARG.PMA	-10..10 (0)	Proper Motion RA
TEL.TARG.PMD	-10..10 (0)	Proper Motion DEC
TEL.TARG.ADDVELALPHA	-15..15 (0.0)	Diff RA
TEL.TARG.ADDVELDELTA	-15..15 (0.0)	Diff DEC
<i>Fixed values:</i>		
Parameter	Value	Label
DPR.CATG	ACQUISITION	Data product category
DPR.TECH	IMAGE	Data product technique
DPR.TYPE	OBJECT	Data product type

CRIRES_spec_acq_NGS_difftrack		
<i>To be specified:</i>		
Parameter	Range ( <i>Default</i> )	Label
<b>DET1.NCORRS.NAME</b>	FowlerNsamp FowlerNsampGRstWin ( <i>FowlerNsamp</i> )	Detector Read-Out Mode
<b>DET1.WIN.NY</b>	64 128 256 ( <i>64</i> )	Number of pixels along Y axis
<b>SEQ.NGS.COLOR</b>	-1..5 ( <i>0</i> )	AO guide star: B-R color value
<b>SEQ.NGS.FWHM</b>	0..10 ( <i>0.0</i> )	AO guide star: FWHM (arcsec)
<b>SEQ.NGS.SNR</b>	0.0..10000.0 ( <i>1000</i> )	AO guide star: Minimum S/N
<b>SEQ.NGS.USELASTSKY</b>	T F ( <i>F</i> )	Use the last sky measurement for the WFS
<b>SEQ.NGS.SKYALPHA</b>	-30..+30 ( <i>4.0</i> )	WFS Alpha sky offset (arcsec)
<b>SEQ.NGS.SKYDELTA</b>	-30..+30 ( <i>4.0</i> )	WFS Delta sky offset (arcsec)
<b>SEQ.SV.USELASTSKY</b>	T F ( <i>T</i> )	Use the last sky measurement for the SV
<b>TEL.SKY.OFFSETALPHA</b>	-120..120 ( <i>30.0</i> )	RA offset to sky
<b>TEL.SKY.OFFSETDELTA</b>	-120..120 ( <i>30.0</i> )	DEC offset to sky
<b>TEL.AG.GUIDESTAR</b>	NONE SETUPFILE CATALOGUE ( <i>CATALOGUE</i> )	Telescope guide star selection
<b>TEL.GS1.ALPHA</b>	( <i>0.0</i> )	RA of telescope guide star
<b>TEL.GS1.DELTA</b>	( <i>0.0</i> )	DEC of telescope guide star
<b>INS.OPTI1.NAME</b>	FREE GAS_N2O GAS_CO GAS_VISITOR ( <i>FREE</i> )	Gas cell
<b>INS.DROT.POSANG</b>	0.0..360.0 ( <i>0.0</i> )	Position angle
<b>INS.SLIT.WID</b>	0.05..3.0 ( <i>0.2</i> )	Entrance slit width
<b>INS.WLEN.REF</b>	958.3..5361.9 ( <i>NODEFAULT</i> )	Reference wavelength
<b>INS.GRAT.ORDER</b>	0..59 ( <i>0</i> )	Grating order
<b>TEL.TARG.EQUINOX</b>	-2000..3000 ( <i>2000</i> )	Equinox
<b>TEL.TARG.EPOCH</b>	-2000..3000 ( <i>2000</i> )	Epoch
<b>TEL.TARG.PMA</b>	-10..10 ( <i>0</i> )	Proper Motion RA
<b>TEL.TARG.PMD</b>	-10..10 ( <i>0</i> )	Proper Motion DEC
<b>SEQ.TRACK.REF</b>	*.track ( <i>)</i>	Reference star tracking table file
<b>SEQ.TRACK.TARG</b>	*.track ( <i>)</i>	Target tracking table file
<i>Fixed values:</i>		
Parameter	Value	Label
<b>DPR.CATG</b>	ACQUISITION	Data product category
<b>DPR.TECH</b>	IMAGE	Data product technique
<b>DPR.TYPE</b>	OBJECT	Data product type

CRIRES_spec_acq_NoAO		
<i>To be specified:</i>		
Parameter	Range (Default)	Label
<b>DET1.NCORRS.NAME</b>	FowlerNsamp FowlerNsampGRstWin (FowlerNsamp)	Detector Read-Out Mode
<b>DET1.WIN.NY</b>	64 128 256 (64)	Number of pixels along Y axis
<b>SEQ.SV.USELASTSKY</b>	T F (T)	Use the last sky measurement for the SV
<b>TEL.SKY.OFFSETALPHA</b>	-120..120 (30.0)	RA offset to sky
<b>TEL.SKY.OFFSETDELTA</b>	-120..120 (30.0)	DEC offset to sky
<b>TEL.AG.GUIDESTAR</b>	NONE SETUPFILE CATALOGUE (CATALOGUE)	Telescope guide star selection
<b>TEL.GS1.ALPHA</b>	(0.0)	RA of telescope guide star
<b>TEL.GS1.DELTA</b>	(0.0)	DEC of telescope guide star
<b>TEL.TARG.OFFSETALPHA</b>	-40..40 (0.0)	RA offset between target and SV guidestar
<b>TEL.TARG.OFFSETDELTA</b>	-40..40 (0.0)	DEC offset between target and SV guidestar
<b>INS.OPTI1.NAME</b>	FREE GAS_N2O GAS_CO GAS_VISITOR (FREE)	Gas cell
<b>INS.DROT.MODE</b>	SKY ELEV (NODEFAULT)	Derotator: Mode
<b>INS.DROT.POSANG</b>	0.0..360.0 (0.0)	Position angle
<b>INS.SLIT.WID</b>	0.05..3.0 (0.2)	Entrance slit width
<b>INS.WLEN.REF</b>	958.3..5361.9 (NODEFAULT)	Reference wavelength
<b>INS.GRAT.ORDER</b>	0..59 (0)	Grating order
<b>TEL.TARG.ALPHA</b>	(NODEFAULT)	Right Ascension
<b>TEL.TARG.DELTA</b>	(NODEFAULT)	Declination
<b>TEL.TARG.EQUINOX</b>	-2000..3000 (2000)	Equinox
<b>TEL.TARG.EPOCH</b>	-2000..3000 (2000)	Epoch
<b>TEL.TARG.PMA</b>	-10..10 (0)	Proper Motion RA
<b>TEL.TARG.PMD</b>	-10..10 (0)	Proper Motion DEC
<b>TEL.TARG.ADDVELALPHA</b>	-15..15 (0.0)	Diff RA
<b>TEL.TARG.ADDVELDELTA</b>	-15..15 (0.0)	Diff DEC
<i>Fixed values:</i>		
Parameter	Value	Label
<b>DPR.CATG</b>	ACQUISITION	Data product category
<b>DPR.TECH</b>	IMAGE	Data product technique
<b>DPR.TYPE</b>	OBJECT	Data product type

CRIRES_spec_acq_NoAO_difftrack		
<i>To be specified:</i>		
Parameter	Range (Default)	Label
<b>DET1.NCORRS.NAME</b>	FowlerNsamp FowlerNsampGRstWin ( <i>FowlerNsamp</i> )	Detector Read-Out Mode
<b>DET1.WIN.NY</b>	64 128 256 ( <i>64</i> )	Number of pixels along Y axis
<b>SEQ.SV.USELASTSKY</b>	T F ( <i>T</i> )	Use the last sky measurement for the SV
<b>TEL.SKY.OFFSETALPHA</b>	-120..120 ( <i>30.0</i> )	RA offset to sky
<b>TEL.SKY.OFFSETDELTA</b>	-120..120 ( <i>30.0</i> )	DEC offset to sky
<b>TEL.AG.GUIDESTAR</b>	NONE SETUPFILE CATALOGUE ( <i>CATALOGUE</i> )	Telescope guide star selection
<b>TEL.GS1.ALPHA</b>	( <i>0.0</i> )	RA of telescope guide star
<b>TEL.GS1.DELTA</b>	( <i>0.0</i> )	DEC of telescope guide star
<b>INS.OPT11.NAME</b>	FREE GAS_N2O GAS_CO GAS_VISITOR ( <i>FREE</i> )	Gas cell
<b>INS.DROT.POSANG</b>	0.0..360.0 ( <i>0.0</i> )	Position angle
<b>INS.SLIT.WID</b>	0.05..3.0 ( <i>0.2</i> )	Entrance slit width
<b>INS.WLEN.REF</b>	958.3..5361.9 ( <i>NODEFAULT</i> )	Reference wavelength
<b>INS.GRAT.ORDER</b>	0..59 ( <i>0</i> )	Grating order
<b>TEL.TARG.EQUINOX</b>	-2000..3000 ( <i>2000</i> )	Equinox
<b>TEL.TARG.EPOCH</b>	-2000..3000 ( <i>2000</i> )	Epoch
<b>TEL.TARG.PMA</b>	-10..10 ( <i>0</i> )	Proper Motion RA
<b>TEL.TARG.PMD</b>	-10..10 ( <i>0</i> )	Proper Motion DEC
<b>SEQ.TRACK.REF</b>	*.track ()	Reference star tracking table file
<b>SEQ.TRACK.TARG</b>	*.track ()	Target tracking table file
<i>Fixed values:</i>		
Parameter	Value	Label
<b>DPR.CATG</b>	ACQUISITION	Data product category
<b>DPR.TECH</b>	IMAGE	Data product technique
<b>DPR.TYPE</b>	OBJECT	Data product type

CRIRES_spec_obs_AutoNodOnSlit		
<i>To be specified:</i>		
Parameter	Range (Default)	Label
<b>DET1.NCORRS.NAME</b>	FowlerNsamp FowlerNsampGRstWin (FowlerNsamp)	Detector Read-Out Mode
<b>DET1.WIN.NY</b>	64 128 256 (64)	Number of pixels along Y axis
<b>DET1.DIT</b>	0..900 (NODEFAULT)	DIT
<b>DET1.NDIT</b>	1..1000 (1)	NDIT
<b>SEQ.NEXPO</b>	1..100 (1)	Number of exposures per nodding position
<b>SEQ.NABCYCLES</b>	0..100 (1)	Number of nodding cycles
<b>SEQ.NODTHROW</b>	0..22.5 (10)	Nod throw along the slit
<b>SEQ.JITTER.WIDTH</b>	0.8 (0)	Jitter width
<b>INS.OPTI1.NAME</b>	FREE GAS_N2O GAS_CO	Gas cell
<b>INS.WLEN.REF</b>	GAS_VISITOR (FREE) 958.3..5361.9 (NODEFAULT)	Reference wavelength
<b>INS.GRAT.ORDER</b>	0.59 (0)	Grating order
<i>Fixed values:</i>		
Parameter	Value	Label
<b>DPR.CATG</b>	SCIENCE	Data product category
<b>DPR.TECH</b>	SPECTRUM,NODDING/DIRECT, [JITTER/OTHER]	Data product technique
<b>DPR.TYPE</b>	OBJECT	Data product type
CRIRES_spec_obs_SpectroAstrometry		
<i>To be specified:</i>		
Parameter	Range (Default)	Label
<b>DET1.NCORRS.NAME</b>	FowlerNsamp FowlerNsampGRstWin (FowlerNsamp)	Detector Read-Out Mode
<b>DET1.WIN.NY</b>	64 128 256 (64)	Number of pixels along Y axis
<b>DET1.DIT</b>	0..900 (NODEFAULT)	DIT
<b>DET1.NDIT</b>	1..1000 (1)	NDIT
<b>INS.DROT.POSANG.LIST</b>	0.0..360.0 ( )	List of position angles
<b>INS.GRAT.ORDER</b>	0.59 (0)	Grating order
<b>INS.OPTI1.NAME</b>	FREE GAS_N2O GAS_CO	Gas cell
<b>INS.WLEN.REF</b>	GAS_VISITOR (FREE) 958.3..5361.9 (NODEFAULT)	Reference wavelength
<b>SEQ.JITTER.RESET</b>	F T (T)	Reset jitter for each DROT posang
<b>SEQ.JITTER.WIDTH</b>	0.8 (0)	Jitter width
<b>SEQ.NABCYCLES</b>	0..100 (1)	Number of nodding cycles
<b>SEQ.NEXPO</b>	1..100 (1)	Number of exposures per nodding position
<b>SEQ.NODTHROW</b>	0..22.5 (10)	Nod throw along the slit
<i>Fixed values:</i>		
Parameter	Value	Label
<b>DPR.CATG</b>	SCIENCE	Data product category
<b>DPR.TECH</b>	SPECTRUM,NODDING,JITTER, ASTROMETRY	Data product technique
<b>DPR.TYPE</b>	OBJECT	Data product type

CRIRES_spec_obs_GenericOffset		
<i>To be specified:</i>		
Parameter	Range (Default)	Label
<b>DET1.NCORRS.NAME</b>	FowlerNsamp FowlerNsampGRstWin ( <i>FowlerNsamp</i> )	Detector Read-Out Mode
<b>DET1.WIN.NY</b>	64 128 256 (64)	Number of pixels along Y axis
<b>DET1.DIT</b>	0..900 (NODEFAULT)	DIT
<b>DET1.NDIT.OBJECT</b>	1..100 (1)	NDIT for the OBJECT positions
<b>DET1.NDIT.SKY</b>	1..100 (1)	NDIT for the SKY positions
<b>INS.GRAT.ORDER</b>	0..59 (0)	Grating order
<b>INS.OPTI1.NAME</b>	FREE GAS_N2O GAS_CO GAS_VISITOR ( <i>FREE</i> )	Gas cell
<b>INS.WLEN.REF</b>	958.3..5361.9 (NODEFAULT)	Reference wavelength
<b>SEQ.NEXPO</b>	1..100 (1)	Number of exposures on each position
<b>SEQ.NOFF</b>	1..100 (NODEFAULT)	Number of offset positions
<b>SEQ.OBSTYPE.LIST</b>	O S (NODEFAULT)	List of observation types (O or S)
<b>SEQ.OFFSET.COORDS</b>	SKY DETECTOR ( <i>SKY</i> )	Offset coordinate type selection
<b>SEQ.OFFSET1.LIST</b>	(NODEFAULT)	List of offsets in RA or X
<b>SEQ.OFFSET2.LIST</b>	(NODEFAULT)	List of offsets in DEC or Y
<i>Fixed values:</i>		
Parameter	Value	Label
<b>DPR.CATG</b>	SCIENCE	Data product category
<b>DPR.TECH</b>	SPECTRUM	Data product technique
<b>DPR.TYPE</b>	OBJECT or SKY	Data product type

CRIRES_spec_cal_AutoNodOnSlit		
<i>To be specified:</i>		
Parameter	Range (Default)	Label
<b>DET1.NCORRS.NAME</b>	FowlerNsamp FowlerNsampGRstWin ( <i>FowlerNsamp</i> )	Detector Read-Out Mode
<b>DET1.WIN.NY</b>	64 128 256 (64)	Number of pixels along Y axis
<b>DET1.DIT</b>	0..900 (NODEFAULT)	DIT
<b>DET1.NDIT</b>	1..1000 (1)	NDIT
<b>SEQ.NEXPO</b>	1..100 (1)	Number of exposures per nodding position
<b>SEQ.NABCYCLES</b>	0..100 (1)	Number of nodding cycles
<b>SEQ.NODTHROW</b>	0..22.5 (10)	Nod throw along the slit
<b>SEQ.JITTER.WIDTH</b>	0..8 (0)	Jitter width
<b>INS.OPTI1.NAME</b>	FREE GAS_N2O GAS_CO GAS_VISITOR ( <i>FREE</i> )	Gas cell
<b>INS.WLEN.REF</b>	958.3..5361.9 (NODEFAULT)	Reference wavelength
<b>INS.GRAT.ORDER</b>	0..59 (0)	Grating order
<i>Fixed values:</i>		
Parameter	Value	Label
<b>DPR.CATG</b>	CALIB	Data product category
<b>DPR.TECH</b>	SPECTRUM,NODDING/DIRECT, [JITTER/OTHER]	Data product technique
<b>DPR.TYPE</b>	STD	Data product type

CRIRES_spec_cal_LampFlats		
<i>To be specified:</i>		
Parameter	Range (Default)	Label
<b>DET1.NCORRS.NAME</b>	FowlerNsamp FowlerNsampGRstWin ( <i>FowlerNsamp</i> )	Detector Read-Out Mode
<b>DET1.WIN.NY</b>	64 128 256 (64)	Number of pixels along Y axis
<b>INS.WLEN.REF</b>	958.3..5361.9 (NODEFAULT)	Reference wavelength
<b>INS.GRAT.ORDER</b>	0..59 (0)	Grating order
<i>Fixed values:</i>		
Parameter	Value	Label
<b>DPR.CATG</b>	CALIB	Data product category
<b>DPR.TECH</b>	SPECTRUM	Data product technique
<b>DPR.TYPE</b>	FLAT	Data product type
CRIRES_spec_cal_Wave		
<i>To be specified:</i>		
Parameter	Range (Default)	Label
<b>INS.LAMP</b>	THAR HALOGEN+N2O.CELL HALOGEN+CO.CELL HALO- GEN+VISITOR.CELL (THAR)	Wavelength calibration source
<b>INS.WLEN.REF</b>	958.3..5361.9 (NODEFAULT)	Reference wavelength
<b>INS.GRAT.ORDER</b>	0..59 (0)	Grating order
<i>Fixed values:</i>		
Parameter	Value	Label
<b>DPR.CATG</b>	CALIB	Data product category
<b>DPR.TECH</b>	SPECTRUM	Data product technique
<b>DPR.TYPE</b>	WAVE,LAMP/ABSORPTION-CELL	Data product type
CRIRES_spec_cal_Darks		
<i>To be specified:</i>		
Parameter	Range (Default)	Label
<b>DET1.NCORRS.NAME</b>	FowlerNsamp FowlerNsampGRstWin ( <i>FowlerNsamp</i> )	Detector Read-Out Mode
<b>DET1.WIN.NY</b>	64 128 256 (64)	Number of pixels along Y axis
<b>DET1.DIT</b>	0..900 (60.)	DIT
<b>DET1.NDIT</b>	1..1000 (1)	NDIT
<b>SEQ.NEXPO</b>	1..100 (3)	Number of exposures
<i>Fixed values:</i>		
Parameter	Value	Label
<b>DPR.CATG</b>	CALIB	Data product category
<b>DPR.TECH</b>	IMAGE	Data product technique
<b>DPR.TYPE</b>	DARK	Data product type
CRIRES_spec_cal_SkyObs		
<i>To be specified:</i>		
Parameter	Range (Default)	Label
<b>DET1.DIT</b>	0..900 (60.)	DIT
<b>DET1.NDIT</b>	1..1000 (1)	NDIT
<b>INS.WLEN.REF</b>	958.3..5361.9 (NODEFAULT)	Reference wavelength
<b>INS.GRAT.ORDER</b>	0..59 (0)	Grating order
<b>INS.SLIT.WID</b>	0.05..3.0 (0.2)	Entrance slit width
<b>SEQ.NEXPO</b>	1..100 (3)	Number of exposures
<i>Fixed values:</i>		
Parameter	Value	Label
<b>DPR.CATG</b>	CALIB TESTCALIB	Data product category
<b>DPR.TECH</b>	SPECTRUM	Data product technique
<b>DPR.TYPE</b>	WAVE,SKY	Data product type

## 15 CRIFES standard wavelength settings

### 15.1 Wavelength ranges

Table 4a: Reference wavelengths,  $\lambda_{\text{ref}}$ , for the standard settings, defined as the wavelength at pixel 512 of the 3rd detector; order number ( $\mathcal{O}$ ), corresponding grating encoder, spectral range uncontaminated by adjacent orders and coverage for each of the four detectors are also given. The last column lists the mean dispersion,  $\delta\lambda$ , in  $10^{-3}$  nm/pixel, for detector 3. A <sup>c</sup> indicates that the order number *must* also be specified as a parameter. Illumination outside of the unvignetted spectral range is affected by lack of reproducibility at more than 1% level, for a 0.4 arcsec slit: wavelength values given in italic fall outside the uncontaminated range. *Wavelengths are vacuum expressed in nm*. The accuracy on the positioning of the reference wavelength is  $\approx 30$  pixels. Overheads due to wavelength setting changes are minimized by ordering the templates by decreasing grating encoder values. See Table 5a-5k for spectral ranges in wavenumber.

$\lambda_{\text{ref}}$	$\mathcal{O}$	Grating encoder	Unvign. range $\lambda_{\text{min}}$ $\lambda_{\text{max}}$	Det. 1 $\lambda_{\text{min}}$ $\lambda_{\text{max}}$	Det. 2 $\lambda_{\text{min}}$ $\lambda_{\text{max}}$	Det. 3 $\lambda_{\text{min}}$ $\lambda_{\text{max}}$	Det. 4 $\lambda_{\text{min}}$ $\lambda_{\text{max}}$	$\delta\lambda$
971.0	58	206561	961.8 974.6	955.7 <i>960.9</i>	962.3 967.3	968.6 973.4	974.6 <i>979.1</i>	4.6
974.0	58	194930	964.8 977.6	958.9 <i>964.0</i>	965.4 970.4	971.7 976.4	977.6 <i>982.0</i>	4.6
983.3	58	157901	974.3 987.0	968.8 <i>973.7</i>	975.1 979.8	981.0 985.6	986.7 <i>991.0</i>	4.4
986.3	58	145622	977.3 990.1	971.9 <i>976.8</i>	978.2 982.8	984.1 988.5	989.7 <i>993.9</i>	4.4
988.0	57	206690	978.6 991.7	972.5 <i>977.7</i>	979.2 984.2	985.6 990.4	991.7 <i>996.3</i>	4.7
991.0	57	195256	981.6 994.8	975.7 <i>980.9</i>	982.3 987.3	988.6 993.4	994.6 <i>999.2</i>	4.7
1000.6	57	157688	991.2 1004.6	985.8 <i>990.8</i>	992.2 997.0	998.3 1002.9	1004.1 <i>1008.5</i>	4.5
1003.6	57	145618	994.2 1007.7	989.0 <i>994.0</i>	995.3 1000.1	1001.3 1005.9	1007.0 <i>1011.3</i>	4.4
1005.6	56	206844	995.8 1009.6	989.8 <i>995.1</i>	996.6 1001.8	1003.1 1008.1	1009.3 <i>1014.0</i>	4.8
1008.7	56	195245	998.9 1012.7	993.1 <i>998.4</i>	999.8 1004.9	1006.3 1011.1	1012.4 <i>1017.0</i>	4.8
1018.6	56	157183	1009.0 1022.7	1003.6 <i>1008.7</i>	1010.1 1015.0	1016.3 1020.9	1022.1 <i>1026.6</i>	4.6
1021.6	56	145320	1012.0 1025.7	1006.7 <i>1011.8</i>	1013.2 1018.0	1019.3 1023.9	1025.1 <i>1029.5</i>	4.5
1023.8	55	207155	1013.8 1027.9	1007.7 <i>1013.2</i>	1014.7 1019.9	1021.3 1026.3	1027.6 <i>1032.4</i>	4.9
1026.9	55	195760	1016.9 1031.1	1011.0 <i>1016.4</i>	1017.9 1023.1	1024.4 1029.4	1030.7 <i>1035.4</i>	4.8
1037.1	55	157245	1027.1 1041.5	1021.8 <i>1027.0</i>	1028.4 1033.4	1034.7 1039.5	1040.7 <i>1045.2</i>	4.6
1040.2	55	145205	1030.2 1044.7	1025.1 <i>1030.2</i>	1031.6 1036.6	1037.9 1042.6	1043.8 <i>1048.2</i>	4.6
1042.7	54	207356	1032.3 1047.1	1026.3 <i>1031.9</i>	1033.4 1038.7	1040.1 1045.3	1046.6 <i>1051.4</i>	5.0
1045.9	54	195811	1035.5 1050.4	1029.7 <i>1035.2</i>	1036.7 1042.0	1043.4 1048.4	1049.7 <i>1054.5</i>	4.9
1056.4	54	156883	1046.1 1061.1	1040.8 <i>1046.1</i>	1047.6 1052.6	1054.0 1058.8	1060.1 <i>1064.7</i>	4.7
1059.6	54	144678	1049.3 1064.3	1044.2 <i>1049.4</i>	1050.9 1055.9	1057.2 1062.0	1063.2 <i>1067.8</i>	4.7
1062.3	53	207626	1051.6 1066.9	1045.6 <i>1051.3</i>	1052.8 1058.3	1059.7 1064.9	1066.2 <i>1071.2</i>	5.1
1065.6	53	195955	1055.0 1070.2	1049.1 <i>1054.7</i>	1056.2 1061.6	1063.0 1068.2	1069.5 <i>1074.4</i>	5.0
1076.4	53	156667	1066.1 1080.9	1060.5 <i>1065.9</i>	1067.4 1072.6	1073.9 1078.9	1080.1 <i>1084.8</i>	4.8
1079.6	53	144682	1069.4 1084.1	1063.9 <i>1069.3</i>	1070.7 1075.8	1077.2 1082.0	1083.3 <i>1087.9</i>	4.7
1082.7	52	207764	1072.1 1087.1	1065.7 <i>1071.5</i>	1073.1 1078.6	1080.1 1085.4	1086.7 <i>1091.8</i>	5.2
1086.0	52	196318	1075.5 1090.3	1069.2 <i>1074.9</i>	1076.5 1081.9	1083.4 1088.6	1090.0 <i>1095.0</i>	5.1

Table 4b: Reference wavelengths,  $\lambda_{\text{ref}}$ , for the standard settings, defined as the wavelength at pixel 512 of the 3rd detector; order number ( $\mathcal{O}$ ), corresponding grating encoder, spectral range uncontaminated by adjacent orders and coverage for each of the four detectors are also given. The last column lists the mean dispersion,  $\delta\lambda$ , in  $10^{-3}$  nm/pixel, for detector 3. A <sup>c</sup> indicates that the order number *must* also be specified as a parameter. Illumination outside of the unvignetted spectral range is affected by lack of reproducibility at more than 1% level, for a 0.4 arcsec slit: wavelength values given in italic fall outside the uncontaminated range. *Wavelengths are vacuum expressed in nm*. The accuracy on the positioning of the reference wavelength is  $\approx 30$  pixels. Overheads due to wavelength setting changes are minimized by ordering the templates by decreasing grating encoder values. See Table 5a-5k for spectral ranges in wavenumber.

$\lambda_{\text{ref}}$	$\mathcal{O}$	Grating encoder	Unvign. range		Det. 1		Det. 2		Det. 3		Det. 4		$\delta\lambda$
			$\lambda_{\text{min}}$	$\lambda_{\text{max}}$									
1097.2	52	156340	1087.2	1101.3	<i>1081.1</i>	<i>1086.5</i>	1088.1	1093.3	1094.7	1099.7	1101.0	<i>1105.8</i>	4.9
1100.5	52	144207	1090.6	1104.5	<i>1084.6</i>	<i>1090.0</i>	1091.5	1096.7	1098.0	1103.0	1104.2	<i>1109.0</i>	4.8
1103.9	51	207868	1093.4	1108.0	<i>1086.6</i>	<i>1092.5</i>	1094.1	1099.7	1101.2	1106.6	<i>1108.0</i>	<i>1113.1</i>	5.3
1107.2	51	196622	1096.6	1111.5	<i>1090.1</i>	<i>1095.9</i>	1097.5	1103.1	1104.5	1109.9	1111.2	<i>1116.3</i>	5.2
1118.8	51	155993	1108.0	1123.6	<i>1102.3</i>	<i>1107.9</i>	1109.5	1114.8	1116.2	1121.4	1122.7	<i>1127.5</i>	5.0
1122.1	51	144091	1111.2	1127.0	<i>1105.8</i>	1111.4	1112.9	1118.2	1119.6	1124.6	1125.9	<i>1130.7</i>	4.9
1125.9	50	208111	1114.5	1130.8	<i>1108.2</i>	<i>1114.2</i>	1115.9	1121.6	1123.1	1128.7	1130.1	<i>1135.3</i>	5.4
1129.3	50	196769	1118.0	1134.2	<i>1111.8</i>	<i>1117.7</i>	1119.4	1125.1	1126.6	1132.0	1133.4	<i>1138.6</i>	5.3
1141.2	50	155924	1130.1	1146.1	<i>1124.4</i>	<i>1130.1</i>	1131.7	1137.2	1138.6	1143.8	1145.1	<i>1150.1</i>	5.1
1144.6	50	143900	1133.6	1149.5	<i>1128.0</i>	1133.7	1135.2	1140.6	1142.0	1147.2	1148.5	<i>1153.4</i>	5.0
1148.8	49	208370	1137.3	1153.7	<i>1130.8</i>	<i>1136.9</i>	1138.6	1144.4	1146.0	1151.6	1153.1	<i>1158.4</i>	5.5
1152.3	49	196925	1140.8	1157.2	<i>1134.5</i>	<i>1140.5</i>	1142.2	1148.0	1149.5	1155.1	1156.5	<i>1161.8</i>	5.4
1164.6	49	155543	1153.2	1169.7	<i>1147.5</i>	1153.3	1154.9	1160.5	1161.9	1167.3	1168.6	<i>1173.7</i>	5.2
1168.1	49	143410	1156.8	1173.3	<i>1151.2</i>	1156.9	1158.5	1164.0	1165.5	1170.7	1172.1	<i>1177.1</i>	5.1
1172.7	48	208475	1160.8	1177.8	<i>1154.3</i>	<i>1160.5</i>	1162.3	1168.2	1169.8	1175.6	1177.0	<i>1182.5</i>	5.6
1176.2	48	197270	1164.3	1181.4	<i>1158.0</i>	<i>1164.2</i>	1165.9	1171.8	1173.4	1179.0	1180.5	<i>1185.9</i>	5.5
1188.9	48	155417	1177.1	1194.3	<i>1171.4</i>	1177.4	1179.0	1184.7	1186.2	1191.6	1193.0	<i>1198.2</i>	5.3
1192.5	48	143189	1180.8	1197.9	<i>1175.2</i>	1181.1	1182.7	1188.3	1189.8	1195.2	1196.6	<i>1201.6</i>	5.2
1197.5	47	208949	1185.2	1202.9	<i>1178.7</i>	<i>1185.1</i>	1186.8	1193.0	1194.6	1200.4	1201.9	<i>1207.5</i>	5.7
1201.2	47	197355	1189.0	1206.6	<i>1182.6</i>	<i>1188.9</i>	1190.7	1196.7	1198.3	1204.1	1205.6	<i>1211.1</i>	5.7
1214.3	47	155079	1202.3	1219.8	<i>1196.5</i>	1202.5	1204.2	1210.0	1211.5	1217.1	1218.5	<i>1223.8</i>	5.4
1217.9	47	143100	1205.9	1223.5	<i>1200.3</i>	1206.3	1207.9	1213.7	1215.2	1220.6	1222.0	<i>1227.2</i>	5.3
1223.5	46	209047	1210.9	1229.1	<i>1204.3</i>	<i>1210.8</i>	1212.6	1218.9	1220.5	1226.5	1228.0	<i>1233.8</i>	5.8
1227.2	46	197696	1214.6	1232.9	<i>1208.2</i>	1214.6	1216.4	1222.6	1224.2	1230.2	1231.7	<i>1237.3</i>	5.8
1240.7	46	155057	1228.0	1246.8	<i>1222.5</i>	1228.7	1230.4	1236.3	1237.9	1243.5	1245.0	<i>1250.4</i>	5.5
1244.4	46	143009	1231.7	1250.6	<i>1226.4</i>	1232.5	1234.2	1240.1	1241.6	1247.2	1248.6	<i>1253.9</i>	5.5

Table 4c: Reference wavelengths,  $\lambda_{\text{ref}}$ , for the standard settings, defined as the wavelength at pixel 512 of the 3rd detector; order number ( $\mathcal{O}$ ), corresponding grating encoder, spectral range uncontaminated by adjacent orders and coverage for each of the four detectors are also given. The last column lists the mean dispersion,  $\delta\lambda$ , in  $10^{-3}$  nm/pixel, for detector 3. A <sup>c</sup> indicates that the order number *must* also be specified as a parameter. Illumination outside of the unvignetted spectral range is affected by lack of reproducibility at more than 1% level, for a 0.4 arcsec slit: wavelength values given in italic fall outside the uncontaminated range. *Wavelengths are vacuum expressed in nm*. The accuracy on the positioning of the reference wavelength is  $\approx 30$  pixels. Overheads due to wavelength setting changes are minimized by ordering the templates by decreasing grating encoder values. See Table 5a-5k for spectral ranges in wavenumber.

$\lambda_{\text{ref}}$	$\mathcal{O}$	Grating encoder	Unvign. range		Det. 1		Det. 2		Det. 3		Det. 4		$\delta\lambda$
			$\lambda_{\text{min}}$	$\lambda_{\text{max}}$									
1250.6	45	209311	1237.3	1256.7	<i>1231.0</i>	1237.6	1239.5	1245.8	1247.5	1253.7	1255.2	<i>1261.1</i>	6.0
1254.4	45	197920	1241.2	1260.5	<i>1235.0</i>	1241.6	1243.4	1249.7	1251.4	1257.4	1259.0	<i>1264.8</i>	5.9
1268.4	45	154666	1255.5	1274.5	<i>1249.8</i>	1256.1	1257.9	1263.9	1265.5	1271.3	1272.8	<i>1278.3</i>	5.6
1272.2	45	142554	1259.4	1278.3	<i>1253.8</i>	1260.1	1261.8	1267.8	1269.4	1275.1	1276.5	<i>1281.9</i>	5.6
1279.0	44	209386	1265.5	1285.1	<i>1258.9</i>	1265.7	1267.6	1274.1	1275.9	1282.1	1283.7	<i>1289.7</i>	6.1
1282.9	44	197948	1269.5	1289.1	<i>1263.0</i>	1269.8	1271.6	1278.1	1279.8	1286.0	1287.6	<i>1293.5</i>	6.0
1297.3	44	154442	1284.0	1303.7	<i>1278.3</i>	1284.7	1286.5	1292.7	1294.3	1300.3	1301.8	<i>1307.4</i>	5.8
1301.2	44	142284	1287.9	1307.6	<i>1282.4</i>	1288.8	1290.6	1296.7	1298.3	1304.1	1305.6	<i>1311.2</i>	5.7
1299.2	43	236191	1285.2	1305.5	<i>1278.1</i>	1285.3	1287.2	1294.1	1295.9	1302.5	1304.2	<i>1310.5</i>	6.4
1303.2	43	225045	1289.2	1309.6	<i>1282.4</i>	1289.4	1291.4	1298.2	1299.9	1306.5	1308.1	<i>1314.3</i>	6.4
1318.1	43	182361	1304.4	1324.5	<i>1298.1</i>	1304.9	1306.8	1313.3	1315.0	1321.2	1322.8	<i>1328.7</i>	6.1
1322.1	43	170551	1308.5	1328.5	<i>1302.3</i>	1309.0	1310.9	1317.3	1319.0	1325.2	1326.8	<i>1332.6</i>	6.0
1337.0	43	125126	1323.6	1343.6	<i>1318.1</i>	1324.5	1326.3	1332.5	1334.1	1339.9	1341.4	<i>1347.0</i>	5.7
1340.9	43	112827	1327.5	1347.6	<i>1322.3</i>	1328.6	1330.4	1336.4	1338.0	1343.8	1345.3	<i>1350.7</i>	5.6
1330.0	42	236563	1315.7	1336.4	<i>1308.4</i>	1315.7	1317.8	1324.8	1326.6	1333.4	1335.1	<i>1341.5</i>	6.6
1334.1	42	225407	1319.9	1340.5	<i>1312.8</i>	1320.0	1322.0	1328.9	1330.8	1337.4	1339.1	<i>1345.5</i>	6.5
1349.5	42	182303	1335.3	1356.3	<i>1329.0</i>	1336.0	1337.9	1344.6	1346.3	1352.7	1354.3	<i>1360.4</i>	6.2
1353.5	42	170769	1339.3	1360.4	<i>1333.3</i>	1340.1	1342.0	1348.6	1350.4	1356.7	1358.3	<i>1364.3</i>	6.1
1368.9	42	124914	1354.7	1376.1	<i>1349.6</i>	1356.2	1358.0	1364.3	1365.9	1371.9	1373.4	<i>1379.1</i>	5.8
1373.0	42	112288	1358.9	1380.3	<i>1353.9</i>	1360.4	1362.2	1368.4	1370.1	1376.0	1377.5	<i>1383.1</i>	5.8
1362.3	41	236920	1347.2	1369.4	<i>1340.2</i>	1347.7	1349.8	1356.9	1358.9	1365.8	1367.5	<i>1374.1</i>	6.7
1366.4	41	226037	1351.3	1373.5	<i>1344.5</i>	1351.9	1354.0	1361.1	1363.0	1369.8	1371.6	<i>1378.1</i>	6.7
1382.4	41	182351	1367.6	1389.6	<i>1361.4</i>	1368.5	1370.5	1377.3	1379.1	1385.7	1387.3	<i>1393.6</i>	6.4
1386.5	41	170813	1371.7	1393.7	<i>1365.8</i>	1372.8	1374.7	1381.5	1383.3	1389.7	1391.4	<i>1397.5</i>	6.3
1402.5	41	124290	1388.0	1409.9	<i>1382.7</i>	1389.5	1391.3	1397.7	1399.4	1405.6	1407.1	<i>1413.0</i>	6.0
1406.6	41	111952	1392.2	1414.0	<i>1387.1</i>	1393.7	1395.6	1401.9	1403.6	1409.6	1411.2	<i>1416.9</i>	5.9

Table 4d: Reference wavelengths,  $\lambda_{\text{ref}}$ , for the standard settings, defined as the wavelength at pixel 512 of the 3rd detector; order number ( $\mathcal{O}$ ), corresponding grating encoder, spectral range uncontaminated by adjacent orders and coverage for each of the four detectors are also given. The last column lists the mean dispersion,  $\delta\lambda$ , in  $10^{-3}$  nm/pixel, for detector 3. A <sup>c</sup> indicates that the order number *must* also be specified as a parameter. Illumination outside of the unvignetted spectral range is affected by lack of reproducibility at more than 1% level, for a 0.4 arcsec slit: wavelength values given in italic fall outside the uncontaminated range. *Wavelengths are vacuum expressed in nm*. The accuracy on the positioning of the reference wavelength is  $\approx 30$  pixels. Overheads due to wavelength setting changes are minimized by ordering the templates by decreasing grating encoder values. See [Table 5a-5k](#) for spectral ranges in wavenumber.

$\lambda_{\text{ref}}$	$\mathcal{O}$	Grating encoder	Unvign. range		Det. 1		Det. 2		Det. 3		Det. 4		$\delta\lambda$
			$\lambda_{\text{min}}$	$\lambda_{\text{max}}$									
1396.2	40	237335	1380.7	1403.5	<i>1373.6</i>	1381.2	1383.3	1390.7	1392.7	1399.7	1401.6	<i>1408.3</i>	6.9
1400.5	40	226200	1385.1	1407.8	<i>1378.1</i>	1385.7	1387.8	1395.1	1397.0	1404.0	1405.8	<i>1412.5</i>	6.8
1417.0	40	182244	1401.8	1424.4	<i>1395.5</i>	1402.8	1404.8	1411.8	1413.7	1420.3	1422.1	<i>1428.4</i>	6.5
1421.2	40	170713	1406.0	1428.7	<i>1399.9</i>	1407.2	1409.2	1416.1	1417.9	1424.5	1426.2	<i>1432.5</i>	6.5
1437.7	40	123891	1422.7	1445.4	<i>1417.4</i>	1424.3	1426.2	1432.8	1434.6	1440.8	1442.5	<i>1448.4</i>	6.1
1441.9	40	111556	1427.0	1449.6	<i>1421.9</i>	1428.7	1430.6	1437.1	1438.8	1445.0	1446.6	<i>1452.5</i>	6.0
1431.9	39	237586	1415.9	1439.5	<i>1408.7</i>	1416.5	1418.7	1426.3	1428.3	1435.5	1437.4	<i>1444.3</i>	7.1
1436.2	39	226739	1420.3	1443.8	<i>1413.2</i>	1421.0	1423.1	1430.6	1432.6	1439.8	1441.6	<i>1448.5</i>	7.0
1453.3	39	182336	1437.6	1461.0	<i>1431.3</i>	1438.7	1440.8	1448.0	1449.9	1456.7	1458.5	<i>1465.0</i>	6.7
1457.7	39	170556	1442.0	1465.5	<i>1435.9</i>	1443.3	1445.4	1452.4	1454.3	1461.1	1462.8	<i>1469.3</i>	6.6
1474.7	39	123510	1459.3	1482.6	<i>1453.9</i>	1461.0	1463.0	1469.7	1471.5	1477.9	1479.6	<i>1485.7</i>	6.3
1479.1	39	110903	1463.8	1487.1	<i>1458.6</i>	1465.6	1467.5	1474.2	1475.9	1482.3	1483.9	<i>1489.9</i>	6.2
1469.4	38	238033	1452.9	1477.3	<i>1445.6</i>	1453.6	1455.9	1463.6	1465.7	1473.1	1475.0	<i>1482.2</i>	7.3
1473.9	38	226975	1457.5	1481.8	<i>1450.3</i>	1458.3	1460.5	1468.2	1470.2	1477.6	1479.5	<i>1486.5</i>	7.2
1491.5	38	182457	1475.3	1499.5	<i>1468.9</i>	1476.6	1478.7	1486.0	1488.0	1495.0	1496.8	<i>1503.5</i>	6.9
1496.0	38	170721	1479.9	1504.0	<i>1473.6</i>	1481.2	1483.3	1490.6	1492.5	1499.5	1501.3	<i>1507.9</i>	6.8
1513.6	38	123256	1497.8	1521.8	<i>1492.3</i>	1499.5	1501.5	1508.5	1510.3	1516.9	1518.6	<i>1524.9</i>	6.4
1518.1	38	110688	1502.3	1526.4	<i>1497.1</i>	1504.2	1506.2	1513.0	1514.9	1521.4	1523.0	<i>1529.2</i>	6.4
1509.0	37	238310	1492.0	1517.1	<i>1484.5</i>	1492.8	1495.1	1503.1	1505.2	1512.8	1514.8	<i>1522.1</i>	7.5
1513.6	37	227306	1496.7	1521.8	<i>1489.4</i>	1497.6	1499.8	1507.7	1509.8	1517.4	1519.3	<i>1526.6</i>	7.4
1531.9	37	182232	1515.2	1540.3	<i>1508.7</i>	1516.6	1518.7	1526.3	1528.3	1535.5	1537.4	<i>1544.3</i>	7.1
1536.4	37	170804	1519.7	1544.8	<i>1513.4</i>	1521.2	1523.4	1530.9	1532.8	1540.0	1541.8	<i>1548.6</i>	7.0
1554.7	37	122741	1538.3	1563.4	<i>1532.8</i>	1540.3	1542.3	1549.4	1551.3	1558.1	1559.8	<i>1566.3</i>	6.6
1559.3	37	110229	1543.0	1567.9	<i>1537.7</i>	1545.1	1547.1	1554.1	1556.0	1562.6	1564.4	<i>1570.7</i>	6.5
1550.8	36	238580	1533.1	1559.4	<i>1525.6</i>	1534.2	1536.5	1544.7	1546.9	1554.7	1556.8	<i>1564.3</i>	7.7
1555.5	36	227647	1537.9	1564.1	<i>1530.6</i>	1539.0	1541.4	1549.5	1551.6	1559.4	1561.4	<i>1568.8</i>	7.6

Table 4e: Reference wavelengths,  $\lambda_{\text{ref}}$ , for the standard settings, defined as the wavelength at pixel 512 of the 3rd detector; order number ( $\mathcal{O}$ ), corresponding grating encoder, spectral range uncontaminated by adjacent orders and coverage for each of the four detectors are also given. The last column lists the mean dispersion,  $\delta\lambda$ , in  $10^{-3}$  nm/pixel, for detector 3. A <sup>c</sup> indicates that the order number *must* also be specified as a parameter. Illumination outside of the unvignetted spectral range is affected by lack of reproducibility at more than 1% level, for a 0.4 arcsec slit: wavelength values given in italic fall outside the uncontaminated range. *Wavelengths are vacuum expressed in nm*. The accuracy on the positioning of the reference wavelength is  $\approx 30$  pixels. Overheads due to wavelength setting changes are minimized by ordering the templates by decreasing grating encoder values. See Table 5a-5k for spectral ranges in wavenumber.

$\lambda_{\text{ref}}$	$\mathcal{O}$	Grating encoder	Unvign. range		Det. 1		Det. 2		Det. 3		Det. 4		$\delta\lambda$
			$\lambda_{\text{min}}$	$\lambda_{\text{max}}$									
1574.4	36	182375	1557.3	1582.9	1550.5	1558.6	1560.9	1568.6	1570.7	1578.1	1580.0	1587.1	7.3
1579.1	36	170763	1562.2	1587.6	1555.5	1563.5	1565.7	1573.4	1575.4	1582.8	1584.7	1591.6	7.2
1598.0	36	122454	1581.7	1606.3	1575.6	1583.2	1585.3	1592.6	1594.5	1601.5	1603.3	1609.9	6.8
1602.7	36	110003	1586.3	1611.2	1580.5	1588.1	1590.2	1597.4	1599.3	1606.1	1607.9	1614.4	6.7
1595.0	35	238838	1577.3	1603.3	1569.1	1577.9	1580.3	1588.7	1591.0	1599.0	1601.1	1608.9	7.9
1599.9	35	227752	1582.3	1608.3	1574.3	1583.0	1585.4	1593.7	1595.9	1603.9	1606.0	1613.6	7.8
1619.4	35	182324	1601.6	1628.4	1594.9	1603.2	1605.5	1613.5	1615.6	1623.2	1625.2	1632.5	7.5
1624.2	35	170792	1606.4	1633.4	1599.9	1608.2	1610.5	1618.3	1620.4	1628.0	1629.9	1637.1	7.4
1643.7	35	122331	1625.8	1653.5	1620.6	1628.5	1630.6	1638.1	1640.1	1647.3	1649.1	1655.9	7.0
1648.6	35	109712	1630.7	1658.5	1625.8	1633.6	1635.7	1643.1	1645.1	1652.1	1653.9	1660.6	6.9
1641.8	34	239069	1622.5	1651.5	1615.2	1624.2	1626.7	1635.3	1637.6	1646.0	1648.1	1656.1	8.1
1646.8	34	228087	1627.5	1656.6	1620.4	1629.3	1631.8	1640.4	1642.7	1650.9	1653.0	1660.9	8.0
1667.0	34	182385	1647.8	1677.3	1641.7	1650.3	1652.7	1660.9	1663.1	1670.9	1673.0	1680.4	7.7
1672.0	34	170718	1652.8	1682.4	1647.0	1655.5	1657.8	1666.0	1668.1	1675.9	1677.9	1685.3	7.6
1692.2	34	121939	1673.0	1703.0	1668.4	1676.5	1678.8	1686.5	1688.5	1695.9	1697.8	1704.8	7.2
1697.2	34	109429	1678.2	1708.0	1673.8	1681.7	1683.9	1691.6	1693.6	1700.8	1702.7	1709.6	7.1
1691.5	33	239170	1670.9	1702.4	1664.0	1673.3	1675.9	1684.8	1687.2	1695.8	1698.0	1706.2	8.4
1696.6	33	228306	1676.1	1707.4	1669.4	1678.6	1681.2	1690.0	1692.4	1700.8	1703.0	1711.1	8.3
1717.5	33	182433	1697.6	1728.1	1691.5	1700.3	1702.7	1711.2	1713.5	1721.6	1723.6	1731.4	7.9
1722.7	33	170657	1703.0	1733.3	1697.0	1705.7	1708.1	1716.5	1718.7	1726.7	1728.8	1736.4	7.8
1743.6	33	121662	1724.7	1754.0	1719.1	1727.5	1729.8	1737.7	1739.8	1747.4	1749.3	1756.5	7.4
1748.7	33	109270	1729.8	1759.1	1724.6	1732.8	1735.0	1742.9	1745.0	1752.4	1754.4	1761.4	7.3
1744.3	32	239310	1723.8	1754.7	1716.0	1725.6	1728.2	1737.4	1739.9	1748.7	1751.0	1759.5	8.6
1749.6	32	228358	1729.2	1760.1	1721.6	1731.1	1733.7	1742.8	1745.2	1754.0	1756.2	1764.6	8.5
1771.2	32	182375	1751.0	1781.9	1744.4	1753.5	1756.0	1764.7	1767.0	1775.4	1777.5	1785.5	8.2
1776.5	32	170734	1756.4	1787.3	1750.0	1759.0	1761.5	1770.1	1772.4	1780.6	1782.7	1790.6	8.1

Table 4f: Reference wavelengths,  $\lambda_{\text{ref}}$ , for the standard settings, defined as the wavelength at pixel 512 of the 3rd detector; order number ( $\mathcal{O}$ ), corresponding grating encoder, spectral range uncontaminated by adjacent orders and coverage for each of the four detectors are also given. The last column lists the mean dispersion,  $\delta\lambda$ , in  $10^{-3}$  nm/pixel, for detector 3. A <sup>c</sup> indicates that the order number *must* also be specified as a parameter. Illumination outside of the unvignetted spectral range is affected by lack of reproducibility at more than 1% level, for a 0.4 arcsec slit: wavelength values given in italic fall outside the uncontaminated range. *Wavelengths are vacuum expressed in nm*. The accuracy on the positioning of the reference wavelength is  $\approx 30$  pixels. Overheads due to wavelength setting changes are minimized by ordering the templates by decreasing grating encoder values. *See Table 5a-5k for spectral ranges in wavenumber*.

$\lambda_{\text{ref}}$	$\mathcal{O}$	Grating encoder	Unvign. range		Det. 1		Det. 2		Det. 3		Det. 4		$\delta\lambda$
			$\lambda_{\text{min}}$	$\lambda_{\text{max}}$									
1798.1	32	121633	1778.3	1809.1	<i>1772.9</i>	1781.5	1783.8	1792.0	1794.2	1802.0	1804.0	<i>1811.4</i>	7.6
1803.4	32	109145	1783.7	1814.4	<i>1778.5</i>	1787.0	1789.3	1797.4	1799.6	1807.3	1809.2	<i>1816.5</i>	7.5
1800.5	31	239445	1779.0	1811.6	<i>1771.3</i>	1781.2	1783.9	1793.4	1795.9	1805.1	1807.4	<i>1816.1</i>	8.9
1806.0	31	228438	1784.6	1817.1	<i>1777.1</i>	1786.9	1789.6	1799.0	1801.5	1810.5	1812.8	<i>1821.5</i>	8.8
1828.4	31	182247	1807.6	1839.5	<i>1800.7</i>	1810.1	1812.7	1821.7	1824.1	1832.7	1834.9	<i>1843.1</i>	8.4
1833.8	31	170755	1813.2	1844.8	<i>1806.4</i>	1815.7	1818.3	1827.2	1829.5	1838.1	1840.2	<i>1848.4</i>	8.3
1856.2	31	121424	1836.2	1867.1	<i>1830.2</i>	1839.0	1841.5	1849.9	1852.2	1860.2	1862.3	<i>1870.0</i>	7.9
1861.6	31	109094	1841.7	1872.6	<i>1835.9</i>	1844.7	1847.1	1855.4	1857.6	1865.6	1867.6	<i>1875.2</i>	7.8
1860.5	30	239487	1838.7	1871.6	<i>1830.3</i>	1840.5	1843.4	1853.2	1855.8	1865.2	1867.6	<i>1876.7</i>	9.2
1866.1	30	228640	1844.4	1877.3	<i>1836.2</i>	1846.3	1849.1	1858.9	1861.4	1870.8	1873.2	<i>1882.1</i>	9.1
1889.3	30	182344	1867.9	1900.6	<i>1860.7</i>	1870.4	1873.1	1882.4	1884.9	1893.8	1896.0	<i>1904.5</i>	8.7
1894.9	30	170813	1873.6	1906.3	<i>1866.6</i>	1876.2	1878.9	1888.1	1890.5	1899.3	1901.6	<i>1909.9</i>	8.6
1918.1	30	121366	1897.2	1929.7	<i>1891.2</i>	1900.4	1902.9	1911.6	1913.9	1922.3	1924.4	<i>1932.3</i>	8.1
1923.7	30	108989	1902.9	1935.4	<i>1897.2</i>	1906.2	1908.7	1917.3	1919.6	1927.8	1929.9	<i>1937.7</i>	8.0
1924.6	29	239591	1901.8	1936.4	<i>1893.4</i>	1903.9	1906.9	1917.0	1919.7	1929.5	1932.0	<i>1941.3</i>	9.5
1930.4	29	228734	1907.7	1942.3	<i>1899.5</i>	1909.9	1912.8	1922.9	1925.6	1935.2	1937.7	<i>1946.9</i>	9.4
1954.5	29	182245	1932.2	1966.5	<i>1924.9</i>	1935.0	1937.7	1947.4	1949.9	1959.1	1961.5	<i>1970.2</i>	9.0
1960.3	29	170697	1938.1	1972.3	<i>1931.1</i>	1941.0	1943.7	1953.2	1955.8	1964.9	1967.2	<i>1975.9</i>	8.9
1984.3	29	121245	1962.6	1996.4	<i>1956.5</i>	1966.0	1968.6	1977.6	1980.0	1988.6	1990.8	<i>1999.0</i>	8.4
1990.1	29	108853	1968.5	2002.3	<i>1962.7</i>	1972.0	1974.6	1983.5	1985.9	1994.4	1996.5	<i>2004.6</i>	8.3
1993.3	28	239659	1969.6	2005.7	<i>1961.0</i>	1971.9	1974.9	1985.5	1988.3	1998.4	2000.9	<i>2010.6</i>	9.9
1999.4	28	228631	1975.9	2011.8	<i>1967.4</i>	1978.2	1981.2	1991.6	1994.4	2004.4	2007.0	<i>2016.5</i>	9.8
2024.3	28	182256	2001.3	2036.7	<i>1993.7</i>	2004.1	2006.9	2016.9	2019.5	2029.1	2031.5	<i>2040.6</i>	9.3
2030.3	28	170725	2007.5	2042.7	<i>2000.0</i>	2010.3	2013.1	2023.0	2025.6	2035.0	2037.4	<i>2046.4</i>	9.2
2055.2	28	121185	2033.1	2067.6	<i>2026.4</i>	2036.2	2038.9	2048.3	2050.7	2059.7	2062.0	<i>2070.4</i>	8.7
2061.2	28	108806	2039.2	2073.6	<i>2032.8</i>	2042.5	2045.1	2054.4	2056.8	2065.6	2067.9	<i>2076.2</i>	8.6

Table 4g: Reference wavelengths,  $\lambda_{\text{ref}}$ , for the standard settings, defined as the wavelength at pixel 512 of the 3rd detector; order number ( $\mathcal{O}$ ), corresponding grating encoder, spectral range uncontaminated by adjacent orders and coverage for each of the four detectors are also given. The last column lists the mean dispersion,  $\delta\lambda$ , in  $10^{-3}$  nm/pixel, for detector 3. A <sup>c</sup> indicates that the order number *must* also be specified as a parameter. Illumination outside of the unvignetted spectral range is affected by lack of reproducibility at more than 1% level, for a 0.4 arcsec slit: wavelength values given in italic fall outside the uncontaminated range. *Wavelengths are vacuum expressed in nm*. The accuracy on the positioning of the reference wavelength is  $\approx 30$  pixels. Overheads due to wavelength setting changes are minimized by ordering the templates by decreasing grating encoder values. See Table 5a-5k for spectral ranges in wavenumber.

$\lambda_{\text{ref}}$	$\mathcal{O}$	Grating encoder	Unvign. range $\lambda_{\text{min}}$ $\lambda_{\text{max}}$	Det. 1 $\lambda_{\text{min}}$ $\lambda_{\text{max}}$	Det. 2 $\lambda_{\text{min}}$ $\lambda_{\text{max}}$	Det. 3 $\lambda_{\text{min}}$ $\lambda_{\text{max}}$	Det. 4 $\lambda_{\text{min}}$ $\lambda_{\text{max}}$	$\delta\lambda$
2067.1	27	239709	2042.8 2079.8	2033.6 2044.9	2048.1 2059.0	2061.9 2072.3	2075.0 2085.0	10.2
2073.4	27	228727	2049.2 2086.2	2040.2 2051.4	2054.6 2065.4	2068.2 2078.6	2081.2 2091.2	10.1
2099.3	27	182210	2075.5 2112.2	2067.5 2078.3	2081.3 2091.6	2094.4 2104.2	2106.8 2116.2	9.7
2105.5	27	170718	2081.8 2118.5	2074.1 2084.8	2087.7 2097.9	2100.6 2110.4	2112.9 2122.2	9.5
2131.3	27	121222	2108.1 2144.4	2101.4 2111.6	2114.4 2124.1	2126.7 2135.9	2138.3 2147.1	9.0
2137.6	27	108687	2114.5 2150.8	2108.1 2118.2	2120.9 2130.5	2133.0 2142.2	2144.5 2153.2	8.9
2146.6	26	239717	2121.1 2160.2	2111.8 2123.6	2126.8 2138.2	2141.2 2152.0	2154.8 2165.2	10.6
2153.1	26	228807	2127.7 2166.7	2118.6 2130.3	2133.5 2144.8	2147.7 2158.5	2161.2 2171.5	10.5
2180.0	26	182289	2155.2 2193.6	2147.0 2158.2	2161.3 2172.0	2174.9 2185.1	2187.8 2197.6	10.0
2186.5	26	170686	2161.8 2200.1	2153.9 2165.0	2168.0 2178.6	2181.4 2191.6	2194.2 2203.8	9.9
2213.3	26	121171	2189.3 2226.9	2182.3 2192.8	2195.8 2205.8	2208.5 2218.1	2220.6 2229.7	9.4
2219.8	26	108720	2196.0 2233.4	2189.2 2199.6	2202.5 2212.4	2215.1 2224.5	2227.0 2236.0	9.3
2232.4	25	239822	2205.9 2246.6	2196.2 2208.4	2211.8 2223.6	2226.7 2238.1	2241.0 2251.8	11.0
2239.1	25	229012	2212.8 2253.3	2203.2 2215.4	2218.7 2230.4	2233.5 2244.7	2247.6 2258.3	10.9
2267.2	25	182293	2241.5 2281.4	2232.9 2244.5	2247.8 2258.9	2261.9 2272.5	2275.3 2285.5	10.4
2273.9	25	170794	2248.4 2288.1	2240.0 2251.5	2254.7 2265.7	2268.6 2279.2	2281.9 2291.9	10.3
2302.0	25	120870	2277.2 2316.2	2269.8 2280.7	2283.8 2294.2	2297.0 2307.0	2309.6 2319.0	9.8
2308.7	25	108524	2284.1 2322.9	2276.9 2287.7	2290.7 2301.1	2303.8 2313.6	2316.2 2325.5	9.6
2325.2	24	240159	2297.7 2340.0	2287.5 2300.2	2303.8 2316.1	2319.3 2331.1	2334.1 2345.4	11.5
2332.2	24	229321	2304.9 2347.0	2294.8 2307.5	2311.0 2323.2	2326.4 2338.0	2341.0 2352.2	11.4
2361.7	24	182240	2335.1 2376.4	2326.0 2338.1	2341.4 2353.1	2356.1 2367.3	2370.1 2380.7	10.9
2368.7	24	170706	2342.3 2383.4	2333.4 2345.4	2348.7 2360.2	2363.2 2374.2	2377.0 2387.5	10.7
2398.1	24	120552	2372.5 2412.8	2364.5 2376.0	2379.1 2390.0	2392.9 2403.3	2406.0 2415.8	10.2
2405.1	24	108163	2379.8 2419.7	2372.0 2383.3	2386.4 2397.1	2400.0 2410.2	2412.9 2422.6	10.0
2425.9	23	240745	2397.3 2441.4	2386.5 2399.8	2403.5 2416.4	2419.8 2432.1	2435.2 2447.0	12.0
2433.2	23	229919	2404.7 2448.8	2394.2 2407.4	2411.1 2423.8	2427.1 2439.3	2442.4 2454.1	11.9

Table 4h: Reference wavelengths,  $\lambda_{\text{ref}}$ , for the standard settings, defined as the wavelength at pixel 512 of the 3rd detector; order number ( $\mathcal{O}$ ), corresponding grating encoder, spectral range uncontaminated by adjacent orders and coverage for each of the four detectors are also given. The last column lists the mean dispersion,  $\delta\lambda$ , in  $10^{-3}$  nm/pixel, for detector 3. A <sup>c</sup> indicates that the order number *must* also be specified as a parameter. Illumination outside of the unvignetted spectral range is affected by lack of reproducibility at more than 1% level, for a 0.4 arcsec slit: wavelength values given in italic fall outside the uncontaminated range. *Wavelengths are vacuum expressed in nm*. The accuracy on the positioning of the reference wavelength is  $\approx 30$  pixels. Overheads due to wavelength setting changes are minimized by ordering the templates by decreasing grating encoder values. See [Table 5a-5k](#) for spectral ranges in wavenumber.

$\lambda_{\text{ref}}$	$\mathcal{O}$	Grating encoder	Unvign. range		Det. 1		Det. 2		Det. 3		Det. 4		$\delta\lambda$
			$\lambda_{\text{min}}$	$\lambda_{\text{max}}$									
2464.4	23	182212	2436.4	2480.2	<i>2427.1</i>	2439.8	2443.3	2455.4	2458.6	2470.2	2473.2	<i>2484.2</i>	11.3
2471.6	23	170845	2443.7	2487.5	<i>2434.7</i>	2447.3	2450.7	2462.7	2465.9	2477.3	2480.3	<i>2491.2</i>	11.2
2502.8	23	119818	2475.5	2518.9	<i>2467.8</i>	2479.7	2483.0	2494.4	2497.4	2508.2	2511.0	<i>2521.3</i>	10.6
2510.0	23	107598	2482.8	2526.2	<i>2475.5</i>	2487.2	2490.5	2501.7	2504.7	2515.4	2518.1	<i>2528.2</i>	10.4
2515.0	22	270172	2483.9	2532.3	<i>2472.7</i>	2487.0	2491.0	2504.7	2508.4	2521.6	2525.0	<i>2537.7</i>	12.9
2522.6	22	259705	2491.7	2539.8	<i>2480.7</i>	2494.9	2498.8	2512.4	2516.1	2529.1	2532.5	<i>2545.1</i>	12.8
2555.9	22	212504	2525.8	2573.0	<i>2515.8</i>	2529.4	2533.1	2546.2	2549.6	2562.2	2565.4	<i>2577.3</i>	12.2
2563.5	22	201401	2533.6	2580.6	<i>2523.8</i>	2537.3	2541.0	2553.9	2557.3	2569.7	2572.9	<i>2584.7</i>	12.1
2596.8	22	151096	2567.9	2613.8	<i>2559.0</i>	2571.9	2575.4	2587.7	2590.9	2602.7	2605.7	<i>2616.8</i>	11.5
2604.4	22	139204	2575.7	2621.3	<i>2567.1</i>	2579.8	2583.3	2595.4	2598.6	2610.2	2613.2	<i>2624.2</i>	11.3
2637.6	22	85198	2609.9	2654.5	<i>2602.4</i>	2614.4	2617.7	2629.1	2632.2	2643.1	2645.8	<i>2656.1</i>	10.6
2645.2	22	72315	2617.6	2662.1	<i>2610.5</i>	2622.3	2625.6	2636.9	2639.8	2650.6	2653.3	<i>2663.5</i>	10.5
2633.1	21	272346	2600.7	2651.2	<i>2588.8</i>	2603.7	2607.9	2622.3	2626.2	2640.0	2643.6	<i>2656.9</i>	13.6
2641.0	21	261983	2608.9	2659.0	<i>2597.1</i>	2611.9	2616.0	2630.3	2634.1	2647.9	2651.4	<i>2664.6</i>	13.4
2677.1	21	213212	2645.6	2695.2	<i>2635.1</i>	2649.3	2653.2	2666.9	2670.5	2683.7	2687.0	<i>2699.5</i>	12.8
2685.0	21	202203	2653.7	2703.2	<i>2643.4</i>	2657.5	2661.4	2674.9	2678.5	2691.5	2694.8	<i>2707.2</i>	12.7
2721.0	21	150290	2690.4	2739.3	<i>2681.5</i>	2694.9	2698.6	2711.5	2714.9	2727.1	2730.3	<i>2742.0</i>	12.0
2729.0	21	138329	2698.6	2747.4	<i>2689.9</i>	2703.2	2706.9	2719.6	2722.9	2735.1	2738.2	<i>2749.7</i>	11.8
2764.9	21	82465	2735.2	2783.5	<i>2728.1</i>	2740.6	2744.1	2756.1	2759.2	2770.6	2773.5	<i>2784.3</i>	11.1
2772.8	21	69634	2743.2	2791.6	<i>2736.5</i>	2748.9	2752.3	2764.1	2767.2	2778.4	2781.3	<i>2791.9</i>	10.9
2761.9	20	275889	2727.0	2782.0	<i>2715.2</i>	2731.0	2735.4	2750.6	2754.6	2769.2	2773.0	<i>2787.0</i>	14.3
2770.2	20	265556	2735.5	2790.3	<i>2723.9</i>	2739.6	2743.9	2759.0	2763.0	2777.4	2781.2	<i>2795.0</i>	14.1
2810.0	20	214467	2775.2	2831.1	<i>2765.8</i>	2780.8	2784.9	2799.3	2803.1	2816.9	2820.4	<i>2833.6</i>	13.5
2818.3	20	203465	2783.5	2839.6	<i>2774.6</i>	2789.4	2793.5	2807.7	2811.5	2825.1	2828.6	<i>2841.6</i>	13.3
2858.0	20	148939	2823.3	2880.2	<i>2816.5</i>	2830.6	2834.5	2848.0	2851.6	2864.4	2867.7	<i>2880.0</i>	12.6
2866.3	20	137104	2831.6	2888.8	<i>2825.3</i>	2839.3	2843.1	2856.4	2860.0	2872.7	2875.9	<i>2888.0</i>	12.4

Table 4i: Reference wavelengths,  $\lambda_{\text{ref}}$ , for the standard settings, defined as the wavelength at pixel 512 of the 3rd detector; order number ( $\mathcal{O}$ ), corresponding grating encoder, spectral range uncontaminated by adjacent orders and coverage for each of the four detectors are also given. The last column lists the mean dispersion,  $\delta\lambda$ , in  $10^{-3}$  nm/pixel, for detector 3. A <sup>c</sup> indicates that the order number *must* also be specified as a parameter. Illumination outside of the unvignetted spectral range is affected by lack of reproducibility at more than 1% level, for a 0.4 arcsec slit: wavelength values given in italic fall outside the uncontaminated range. *Wavelengths are vacuum expressed in nm*. The accuracy on the positioning of the reference wavelength is  $\approx 30$  pixels. Overheads due to wavelength setting changes are minimized by ordering the templates by decreasing grating encoder values. See Table 5a-5k for spectral ranges in wavenumber.

$\lambda_{\text{ref}}$	$\mathcal{O}$	Grating encoder	Unvign. range $\lambda_{\text{min}}$ $\lambda_{\text{max}}$	Det. 1 $\lambda_{\text{min}}$ $\lambda_{\text{max}}$	Det. 2 $\lambda_{\text{min}}$ $\lambda_{\text{max}}$	Det. 3 $\lambda_{\text{min}}$ $\lambda_{\text{max}}$	Det. 4 $\lambda_{\text{min}}$ $\lambda_{\text{max}}$	$\delta\lambda$
2906.0	20	78065	2871.3 2929.5	2867.6 2880.7	2884.3 2896.8	2900.1 2911.9	2915.0 2926.2	11.6
2914.3	20	65158	2879.8 2937.9	2876.4 2889.3	2892.9 2905.2	2908.5 2920.2	2923.1 2934.2	11.4
2902.8	19	281120	2862.3 2928.1	2853.4 2870.1	2874.7 2890.8	2895.1 2910.5	2914.5 2929.3	15.1
2911.5	19	270883	2871.2 2936.8	2862.6 2879.1	2883.7 2899.6	2903.8 2919.2	2923.1 2937.8	15.0
2956.4	19	216337	2917.1 2981.7	2909.8 2925.6	2930.0 2945.1	2949.1 2963.7	2967.4 2981.3	14.2
2965.1	19	205403	2926.0 2990.3	2919.0 2934.6	2938.9 2953.9	2957.9 2972.3	2976.0 2989.7	14.0
3009.9	19	146949	2972.0 3035.1	2966.4 2981.1	2985.2 2999.4	3003.1 3016.7	3020.1 3033.0	13.2
3018.6	19	135138	2981.0 3043.8	2975.6 2990.2	2994.2 3008.2	3011.9 3025.3	3028.7 3041.4	13.0
3063.4	19	71522	3023.2 3084.5	3023.2 3036.9	3040.7 3053.8	3057.2 3069.6	3072.8 3084.5	12.1
3072.1	19	58559	3032.5 3092.9	3032.5 3046.0	3049.8 3062.6	3066.0 3078.2	3081.3 3092.9	11.9
3057.2	18	288711	3013.9 3084.8	3004.7 3022.5	3027.4 3044.5	3049.0 3065.4	3069.6 3085.4	16.0
3066.3	18	278642	3023.2 3093.8	3014.3 3031.9	3036.7 3053.7	3058.2 3074.4	3078.6 3094.2	15.9
3118.3	18	219101	3075.0 3147.2	3069.0 3085.7	3090.3 3106.4	3110.6 3126.0	3129.9 3144.6	15.0
3127.5	18	208179	3084.2 3156.7	3078.7 3095.2	3099.8 3115.7	3119.9 3135.1	3139.0 3153.5	14.9
3179.4	18	144027	3133.6 3203.7	3133.6 3149.1	3153.4 3168.4	3172.3 3186.5	3190.2 3203.7	13.9
3188.6	18	132155	3143.3 3212.6	3143.3 3158.7	3163.0 3177.7	3181.6 3195.6	3199.2 3212.6	13.7
3240.4	18	61924	3198.5 3262.4	3198.5 3212.8	3216.7 3230.4	3233.9 3246.9	3250.2 3262.4	12.6
3249.6	18	48775	3208.3 3271.2	3208.3 3222.4	3226.3 3239.7	3243.2 3256.0	3259.2 3271.2	12.4
3226.5	17	299609	3170.4 3256.7	3170.4 3189.4	3194.6 3212.9	3217.7 3235.3	3239.8 3256.7	17.2
3236.2	17	289576	3180.6 3266.1	3180.6 3199.4	3204.6 3222.7	3227.5 3244.9	3249.4 3266.1	17.0
3298.3	17	222918	3245.9 3326.3	3245.9 3263.6	3268.6 3285.6	3290.1 3306.5	3310.7 3326.3	16.0
3307.9	17	212200	3256.0 3335.6	3256.0 3273.6	3278.5 3295.4	3299.8 3316.0	3320.1 3335.6	15.8
3369.9	17	139809	3321.6 3395.5	3321.6 3338.0	3342.5 3358.3	3362.4 3377.4	3381.2 3395.5	14.6
3379.6	17	127929	3331.9 3404.9	3331.9 3348.1	3352.6 3368.1	3372.2 3387.0	3390.8 3404.9	14.5
3441.5	17	47758	3397.8 3464.4	3397.8 3412.7	3416.8 3431.0	3434.8 3448.2	3451.7 3464.4	13.1
3451.1	17	34549	3408.1 3473.6	3408.1 3422.8	3426.8 3440.8	3444.5 3457.7	3461.1 3473.6	12.9

Table 4j: Reference wavelengths,  $\lambda_{\text{ref}}$ , for the standard settings, defined as the wavelength at pixel 512 of the 3rd detector; order number ( $\mathcal{O}$ ), corresponding grating encoder, spectral range uncontaminated by adjacent orders and coverage for each of the four detectors are also given. The last column lists the mean dispersion,  $\delta\lambda$ , in  $10^{-3}$  nm/pixel, for detector 3. A <sup>c</sup> indicates that the order number *must* also be specified as a parameter. Illumination outside of the unvignetted spectral range is affected by lack of reproducibility at more than 1% level, for a 0.4 arcsec slit: wavelength values given in italic fall outside the uncontaminated range. *Wavelengths are vacuum expressed in nm*. The accuracy on the positioning of the reference wavelength is  $\approx 30$  pixels. Overheads due to wavelength setting changes are minimized by ordering the templates by decreasing grating encoder values. See Table 5a-5k for spectral ranges in wavenumber.

$\lambda_{\text{ref}}$	$\mathcal{O}$	Grating encoder	Unvign. range		Det. 1		Det. 2		Det. 3		Det. 4		$\delta\lambda$
			$\lambda_{\text{min}}$	$\lambda_{\text{max}}$									
3426.3	16	301407	3366.6	3458.4	3366.6	3386.8	3392.4	3411.8	3416.9	3435.6	3440.5	3458.4	18.3
3436.6	16	291399	3377.4	3468.4	3377.4	3397.4	3403.0	3422.2	3427.3	3445.9	3450.6	3468.4	18.1
3503.8	16	223591	3448.1	3533.6	3448.1	3467.0	3472.2	3490.3	3495.1	3512.5	3517.0	3533.6	17.0
3514.0	16	212882	3458.9	3543.4	3458.9	3477.5	3482.7	3500.7	3505.4	3522.6	3527.0	3543.4	16.8
3581.2	16	139032	3529.9	3608.4	3529.9	3547.3	3552.2	3568.8	3573.2	3589.2	3593.2	3608.4	15.5
3591.4	16	127261	3540.7	3618.2	3540.7	3558.0	3562.7	3579.2	3583.6	3599.3	3603.3	3618.2	15.3
3658.4	16	45436	3612.1	3682.6	3612.1	3627.9	3632.3	3647.3	3651.3	3665.5	3669.2	3682.6	13.9
3668.6	16	32187	3623.0	3692.4	3623.0	3638.6	3642.9	3657.7	3661.6	3675.6	3679.2	3692.4	13.7
3696.7	15	262637	3635.2	3729.7	3635.2	3656.0	3661.7	3681.8	3687.1	3706.3	3711.3	3729.7	18.8
3707.5	15	252422	3646.5	3740.2	3646.5	3667.1	3672.9	3692.7	3698.0	3717.0	3721.9	3740.2	18.6
3778.7	15	182258	3721.6	3809.1	3721.6	3740.9	3746.3	3764.9	3769.8	3787.6	3792.2	3809.1	17.4
3789.5	15	171139	3733.0	3819.5	3733.0	3752.2	3757.5	3775.9	3780.7	3798.3	3802.8	3819.5	17.2
3860.5	15	94294	3808.3	3888.0	3808.3	3826.1	3831.0	3848.0	3852.4	3868.6	3872.7	3888.0	15.8
3871.3	15	81960	3819.8	3898.4	3819.8	3837.4	3842.2	3859.0	3863.4	3879.3	3883.3	3898.4	15.5
3874.4	14	335861	3804.3	3912.3	3804.3	3827.9	3834.5	3857.3	3863.4	3885.4	3891.1	3912.3	21.5
3885.9	14	326392	3816.3	3923.4	3816.3	3839.8	3846.3	3869.0	3875.0	3896.8	3902.4	3923.4	21.3
3961.5	14	261977	3895.6	3996.9	3895.6	3917.9	3924.1	3945.5	3951.2	3971.8	3977.1	3996.9	20.1
3973.0	14	251819	3907.7	4008.0	3907.7	3929.8	3935.9	3957.2	3962.8	3983.2	3988.5	4008.0	19.9
4048.6	14	182263	3987.4	4081.2	3987.4	4008.2	4013.9	4033.8	4039.1	4058.1	4063.0	4081.2	18.6
4060.1	14	171213	3999.5	4092.3	3999.5	4020.1	4025.8	4045.5	4050.7	4069.5	4074.4	4092.3	18.4
4135.5	14	95089	4079.5	4165.0	4079.5	4098.6	4103.9	4122.1	4126.9	4144.2	4148.6	4165.0	16.9
4147.0	14	82842	4091.8	4176.1	4091.8	4110.6	4115.8	4133.8	4138.5	4155.5	4159.9	4176.1	16.7
4174.6	13	334207	4099.2	4215.3	4099.2	4124.6	4131.7	4156.2	4162.8	4186.4	4192.5	4215.3	23.1
4186.9	13	324789	4112.0	4227.3	4112.0	4137.3	4144.3	4168.7	4175.1	4198.6	4204.7	4227.3	22.9
4267.4	13	261022	4196.5	4305.4	4196.5	4220.5	4227.1	4250.2	4256.3	4278.5	4284.2	4305.4	21.7
4279.6	13	251006	4209.3	4317.3	4209.3	4233.1	4239.7	4262.6	4268.6	4290.6	4296.2	4317.3	21.5

Table 4k: Reference wavelengths,  $\lambda_{\text{ref}}$ , for the standard settings, defined as the wavelength at pixel 512 of the 3rd detector; order number ( $\mathcal{O}$ ), corresponding grating encoder, spectral range uncontaminated by adjacent orders and coverage for each of the four detectors are also given. The last column lists the mean dispersion,  $\delta\lambda$ , in  $10^{-3}$  nm/pixel, for detector 3. A <sup>c</sup> indicates that the order number *must* also be specified as a parameter. Illumination outside of the unvignetted spectral range is affected by lack of reproducibility at more than 1% level, for a 0.4 arcsec slit: wavelength values given in *italic* fall outside the uncontaminated range. *Wavelengths are vacuum expressed in nm*. The accuracy on the positioning of the reference wavelength is  $\approx 30$  pixels. Overheads due to wavelength setting changes are minimized by ordering the templates by decreasing grating encoder values. See Table 5a-5k for spectral ranges in wavenumber.

$\lambda_{\text{ref}}$	$\mathcal{O}$	Grating encoder	Unvign. range $\lambda_{\text{min}}$ $\lambda_{\text{max}}$	Det. 1 $\lambda_{\text{min}}$ $\lambda_{\text{max}}$	Det. 2 $\lambda_{\text{min}}$ $\lambda_{\text{max}}$	Det. 3 $\lambda_{\text{min}}$ $\lambda_{\text{max}}$	Det. 4 $\lambda_{\text{min}}$ $\lambda_{\text{max}}$	$\delta\lambda$
4360.0	13	182289	4294.1 4395.1	<i>4294.1</i> 4316.4	4322.6 4344.1	4349.7 4370.3	4375.5 4395.1	20.0
4372.2	13	171407	4307.0 4406.9	<i>4307.0</i> 4329.1	4335.2 4356.5	4362.1 4382.4	4387.6 4406.9	19.8
4452.5	13	96182	4392.2 4484.3	<i>4392.2</i> 4412.7	4418.4 4438.0	4443.2 4461.8	4466.6 4484.3	18.2
4464.7	13	84134	4405.2 4496.0	<i>4405.2</i> 4425.5	4431.1 4450.4	4455.5 4473.9	4478.6 4496.0	18.0
4544.8	13	-53	4490.9 4572.9	<i>4490.9</i> 4509.3	4514.4 4531.9	4536.5 4553.1	4557.3 4572.9	16.2
4525.8	12	331867	4444.2 4569.8	<i>4444.2</i> 4471.7	4479.4 4505.9	4513.0 4538.6	4545.2 4569.8	25.0
4538.8	12	322660	4457.8 4582.5	<i>4457.8</i> 4485.1	4492.7 4519.1	4526.1 4551.5	4558.0 4582.5	24.8
4624.6	12	259824	4547.8 4665.8	<i>4547.8</i> 4573.8	4581.0 4606.0	4612.6 4636.6	4642.8 4665.8	23.4
4637.6	12	249961	4561.5 4678.4	<i>4561.5</i> 4587.2	4594.4 4619.2	4625.7 4649.5	4655.6 4678.4	23.2
4723.3	12	182313	4651.9 4761.3	<i>4651.9</i> 4676.1	4682.8 4706.1	4712.2 4734.4	4740.1 4761.3	21.7
4736.3	12	171611	4665.6 4773.9	<i>4665.6</i> 4689.6	4696.2 4719.2	4725.3 4747.3	4752.9 4773.9	21.5
4821.9	12	97662	4756.4 4856.4	<i>4756.4</i> 4778.7	4784.9 4806.2	4811.8 4832.0	4837.2 4856.4	19.8
4834.9	12	85837	4770.3 4868.9	<i>4770.3</i> 4792.3	4798.4 4819.4	4824.9 4844.9	4850.0 4868.9	19.5
4920.3	12	3261	4861.6 4950.8	<i>4861.6</i> 4881.7	4887.2 4906.3	4911.3 4929.3	4933.9 4950.8	17.6
4889.5	11	362306	4798.3 4938.8	<i>4798.3</i> 4829.0	4837.6 4867.3	4875.2 4903.8	4911.2 4938.8	28.0
4903.4	11	353526	4812.8 4952.3	<i>4812.8</i> 4843.3	4851.8 4881.3	4889.2 4917.6	4925.0 4952.3	27.8
4994.8	11	293999	4908.5 5041.2	<i>4908.5</i> 4937.7	4945.8 4973.8	4981.3 5008.3	5015.3 5041.2	26.4
5008.7	11	284651	4923.1 5054.7	<i>4923.1</i> 4952.0	4960.1 4987.9	4995.3 5022.1	5029.0 5054.7	26.2
5100.1	11	220949	5019.3 5143.3	<i>5019.3</i> 5046.6	5054.2 5080.5	5087.5 5112.7	5119.2 5143.3	24.6
5114.0	11	210890	5033.9 5156.8	<i>5033.9</i> 5061.0	5068.6 5094.6	5101.5 5126.5	5132.9 5156.8	24.4
5205.3	11	141944	5130.4 5245.0	<i>5130.4</i> 5155.9	5162.9 5187.3	5193.7 5216.9	5222.9 5245.0	22.7
5219.1	11	131041	5145.1 5258.3	<i>5145.1</i> 5170.3	5177.2 5201.3	5207.6 5230.6	5236.5 5258.3	22.4

## 15.2 Wavenumber ranges

Table 5a: Reference wavelengths,  $\lambda_{\text{ref}}$ , in nm for the standard wavelength settings, defined as the wavelength at pixel 512 of the 3rd detector; order number ( $\mathcal{O}$ ), corresponding grating encoder, spectral range uncontaminated by adjacent orders and coverage in vacuum wavenumber ( $\nu$ , expressed in  $\text{cm}^{-1}$ ) for each of the four detectors are also given. The last column lists the mean dispersion,  $\delta\nu$  in  $10^{-3} \text{ cm}^{-1}/\text{pixel}$ , for detector 3. A <sup>c</sup> indicates that the order number must also be specified as a parameter. Illumination outside of the unvignetted spectral range is affected by lack of reproducibility at more than 1% level, for a 0.4 arcsec slit: wavenumber values given in *italic* fall outside the uncontaminated range. The accuracy on the positioning of the reference wavelength is  $\approx 30$  pixels. Overheads due to wavelength setting changes are minimized by ordering the templates by decreasing grating encoder values. See *Table 4a-4k* for *spectral ranges in wavelength*.

$\lambda_{\text{ref}}$	$\mathcal{O}$	Grating encoder	Unvign. range		Det. 1		Det. 2		Det. 3		Det. 4		$\delta\nu$
			$\nu_{\text{min}}$	$\nu_{\text{max}}$									
971.0	58	206561	10397.2	10260.6	<i>10463.5</i>	<i>10406.9</i>	10391.8	10338.1	10324.2	10273.3	10260.6	<i>10213.5</i>	-49.3
974.0	58	194930	10364.8	10229.1	<i>10428.6</i>	<i>10373.4</i>	10358.4	10305.0	10291.2	10241.7	10229.1	<i>10183.3</i>	-48.4
983.3	58	157901	10263.8	10131.7	<i>10322.0</i>	<i>10270.1</i>	10255.4	10206.2	10193.7	10146.1	10134.8	<i>10090.8</i>	-45.6
986.3	58	145622	10232.3	10100.0	<i>10289.1</i>	<i>10237.5</i>	10222.9	10175.0	10161.6	10116.3	10104.1	<i>10061.4</i>	-44.7
988.0	57	206690	10218.7	10083.7	<i>10282.8</i>	<i>10228.1</i>	10212.4	10160.5	10146.1	10096.9	10083.7	<i>10037.1</i>	-48.4
991.0	57	195256	10187.4	10052.3	<i>10249.1</i>	<i>10194.7</i>	10180.2	10128.6	10115.3	10066.4	10054.3	<i>10008.0</i>	-47.6
1000.6	57	157688	10088.8	9954.2	<i>10144.0</i>	<i>10092.9</i>	10078.6	10030.1	10017.0	9971.1	9959.2	<i>9915.7</i>	-44.8
1003.6	57	145618	10058.3	9923.6	<i>10111.2</i>	<i>10060.4</i>	10047.2	9999.0	9987.0	9941.3	9930.5	<i>9888.3</i>	-44.0
1005.6	56	206844	10042.2	9904.9	<i>10103.1</i>	<i>10049.2</i>	10034.1	9982.0	9969.1	9919.7	9907.9	<i>9861.9</i>	-47.6
1008.7	56	195245	10011.0	9874.6	<i>10069.5</i>	<i>10016.0</i>	10002.0	9951.2	9937.4	9890.2	9877.5	<i>9832.8</i>	-46.7
1018.6	56	157183	9910.8	9778.0	<i>9964.1</i>	<i>9913.8</i>	9900.0	9852.2	9839.6	9795.3	9783.8	<i>9740.9</i>	-44.0
1021.6	56	145320	9881.4	9749.4	<i>9933.4</i>	<i>9883.4</i>	9869.7	9823.2	9810.7	9766.6	9755.1	<i>9713.5</i>	-43.2
1023.8	55	207155	9863.9	9728.6	<i>9923.6</i>	<i>9869.7</i>	9855.1	9804.9	9791.4	9743.7	9731.4	<i>9686.2</i>	-46.7
1026.9	55	195760	9833.8	9698.4	<i>9891.2</i>	<i>9838.6</i>	9824.1	9774.2	9761.8	9714.4	9702.1	<i>9658.1</i>	-45.9
1037.1	55	157245	9736.2	9601.5	<i>9786.7</i>	<i>9737.1</i>	9723.8	9676.8	9664.6	9620.0	9608.9	<i>9567.5</i>	-43.2
1040.2	55	145205	9706.9	9572.1	<i>9755.1</i>	<i>9706.9</i>	9693.7	9646.9	9634.8	9591.4	9580.4	<i>9540.2</i>	-42.4
1042.7	54	207356	9687.1	9550.2	<i>9743.7</i>	<i>9690.9</i>	9676.8	9627.4	9614.5	9566.6	9554.7	<i>9511.1</i>	-45.9
1045.9	54	195811	9657.2	9520.2	<i>9711.6</i>	<i>9660.0</i>	9646.0	9596.9	9584.1	9538.3	9526.5	<i>9483.2</i>	-45.1
1056.4	54	156883	9559.3	9424.2	<i>9608.0</i>	<i>9559.3</i>	9545.6	9500.3	9487.7	9444.7	9433.1	<i>9392.3</i>	-42.4
1059.6	54	144678	9530.2	9395.8	<i>9576.7</i>	<i>9529.3</i>	9515.7	9470.6	9458.9	9416.2	9405.6	<i>9365.0</i>	-41.6
1062.3	53	207626	9509.3	9372.9	<i>9563.9</i>	<i>9512.0</i>	9498.5	9449.1	9436.6	9390.6	9379.1	<i>9335.3</i>	-45.1
1065.6	53	195955	9478.7	9344.0	<i>9532.0</i>	<i>9481.4</i>	9467.9	9419.7	9407.3	9361.5	9350.2	<i>9307.5</i>	-44.2
1076.4	53	156667	9380.0	9251.5	<i>9429.5</i>	<i>9381.7</i>	9368.6	9323.1	9311.9	9268.7	9258.4	<i>9218.3</i>	-41.5
1079.6	53	144682	9351.0	9224.2	<i>9399.4</i>	<i>9351.9</i>	9339.7	9295.4	9283.3	9242.1	9231.1	<i>9192.0</i>	-40.7
1082.7	52	207764	9327.5	9198.8	<i>9383.5</i>	<i>9332.7</i>	9318.8	9271.3	9258.4	9213.2	9202.2	<i>9159.2</i>	-44.2
1086.0	52	196318	9298.0	9171.8	<i>9352.8</i>	<i>9303.2</i>	9289.4	9243.0	9230.2	9186.1	9174.3	<i>9132.4</i>	-43.3

Table 5b: Reference wavelengths,  $\lambda_{\text{ref}}$ , in nm for the standard wavelength settings, defined as the wavelength at pixel 512 of the 3rd detector; order number ( $\mathcal{O}$ ), corresponding grating encoder, spectral range uncontaminated by adjacent orders and coverage in vacuum wavenumber ( $\nu$ , expressed in  $\text{cm}^{-1}$ ) for each of the four detectors are also given. The last column lists the mean dispersion,  $\delta\nu$  in  $10^{-3} \text{ cm}^{-1}/\text{pixel}$ , for detector 3. A <sup>c</sup> indicates that the order number must also be specified as a parameter. Illumination outside of the unvignetted spectral range is affected by lack of reproducibility at more than 1% level, for a 0.4 arcsec slit: wavenumber values given in *italic* fall outside the uncontaminated range. The accuracy on the positioning of the reference wavelength is  $\approx 30$  pixels. Overheads due to wavelength setting changes are minimized by ordering the templates by decreasing grating encoder values. See [Table 4a-4k](#) for *spectral ranges in wavelength*.

$\lambda_{\text{ref}}$	$\mathcal{O}$	Grating encoder	Unvign. range		Det. 1		Det. 2		Det. 3		Det. 4		$\delta\nu$
			$\nu_{\text{min}}$	$\nu_{\text{max}}$									
1097.2	52	156340	9197.9	9080.2	<i>9249.8</i>	<i>9203.9</i>	9190.3	9146.6	9134.9	9093.4	9082.7	<i>9043.2</i>	-40.7
1100.5	52	144207	9169.3	9053.9	<i>9220.0</i>	<i>9174.3</i>	9161.7	9118.3	9107.5	9066.2	9056.3	<i>9017.1</i>	-39.9
1103.9	51	207868	9145.8	9025.3	<i>9203.0</i>	<i>9153.3</i>	9139.9	9093.4	9081.0	9036.7	<i>9025.3</i>	<i>8983.9</i>	-43.3
1107.2	51	196622	9119.1	8996.9	<i>9173.5</i>	<i>9124.9</i>	9111.6	9065.4	9053.9	9009.8	8999.3	<i>8958.2</i>	-42.5
1118.8	51	155993	9025.3	8900.0	<i>9071.9</i>	<i>9026.1</i>	9013.1	8970.2	8959.0	8917.4	8907.1	<i>8869.2</i>	-39.9
1122.1	51	144091	8999.3	8873.1	<i>9043.2</i>	<i>8997.7</i>	8985.5	8942.9	8931.8	8892.1	8881.8	<i>8844.1</i>	-39.2
1125.9	50	208111	8972.6	8843.3	<i>9023.6</i>	<i>8975.0</i>	8961.4	8915.8	8903.9	8859.8	8848.8	<i>8808.2</i>	-42.5
1129.3	50	196769	8944.5	8816.8	<i>8994.4</i>	<i>8946.9</i>	8933.4	8888.1	8876.3	8833.9	8823.0	<i>8782.7</i>	-41.7
1141.2	50	155924	8848.8	8725.2	<i>8893.6</i>	<i>8848.8</i>	8836.3	8793.5	8782.7	8742.8	8732.9	<i>8694.9</i>	-39.1
1144.6	50	143900	8821.5	8699.4	<i>8865.2</i>	<i>8820.7</i>	8809.0	8767.3	8756.6	8716.9	8707.0	<i>8670.0</i>	-38.4
1148.8	49	208370	8792.8	8667.8	<i>8843.3</i>	<i>8795.8</i>	8782.7	8738.2	8726.0	8683.6	8672.3	<i>8632.6</i>	-41.6
1152.3	49	196925	8765.8	8641.5	<i>8814.5</i>	<i>8768.1</i>	8755.0	8710.8	8699.4	8657.3	8646.8	<i>8607.3</i>	-40.9
1164.6	49	155543	8671.5	8549.2	<i>8714.6</i>	<i>8670.8</i>	8658.8	8617.0	8606.6	8566.8	8557.2	<i>8520.1</i>	-38.3
1168.1	49	143410	8644.5	8523.0	<i>8686.6</i>	<i>8643.8</i>	8631.9	8591.1	8580.0	8541.9	8531.7	<i>8495.5</i>	-37.6
1172.7	48	208475	8614.7	8490.4	<i>8663.3</i>	<i>8617.0</i>	8603.6	8560.2	8548.5	8506.3	8496.2	<i>8456.7</i>	-40.8
1176.2	48	197270	8588.9	8464.5	<i>8635.6</i>	<i>8589.6</i>	8577.1	8533.9	8522.2	8481.8	8471.0	<i>8432.4</i>	-40.0
1188.9	48	155417	8495.5	8373.1	<i>8536.8</i>	<i>8493.3</i>	8481.8	8441.0	8430.3	8392.1	8382.2	<i>8345.9</i>	-37.5
1192.5	48	143189	8468.8	8347.9	<i>8509.2</i>	<i>8466.7</i>	8455.2	8415.4	8404.8	8366.8	8357.0	<i>8322.2</i>	-36.8
1197.5	47	208949	8437.4	8313.2	<i>8483.9</i>	<i>8438.1</i>	8426.0	8382.2	8371.0	8330.6	8320.2	<i>8281.6</i>	-39.9
1201.2	47	197355	8410.4	8287.8	<i>8455.9</i>	<i>8411.1</i>	8398.4	8356.3	8345.2	8305.0	8294.6	<i>8257.0</i>	-39.2
1214.3	47	155079	8317.4	8198.1	<i>8357.7</i>	<i>8316.0</i>	8304.3	8264.5	8254.2	8216.3	8206.8	<i>8171.3</i>	-36.7
1217.9	47	143100	8292.6	8173.3	<i>8331.2</i>	<i>8289.8</i>	8278.8	8239.3	8229.1	8192.7	8183.3	<i>8148.6</i>	-36.0
1223.5	46	209047	8258.3	8136.0	<i>8303.6</i>	<i>8259.0</i>	8246.7	8204.1	8193.4	8153.3	8143.3	<i>8105.0</i>	-39.1
1227.2	46	197696	8233.2	8111.0	<i>8276.8</i>	<i>8233.2</i>	8221.0	8179.3	8168.6	8128.8	8118.9	<i>8082.1</i>	-38.4
1240.7	46	155057	8143.3	8020.5	<i>8180.0</i>	<i>8138.7</i>	8127.4	8088.7	8078.2	8041.8	8032.1	<i>7997.4</i>	-35.9
1244.4	46	143009	8118.9	7996.2	<i>8153.9</i>	<i>8113.6</i>	8102.4	8063.9	8054.1	8018.0	8009.0	<i>7975.1</i>	-35.2

Table 5c: Reference wavelengths,  $\lambda_{\text{ref}}$ , in nm for the standard wavelength settings, defined as the wavelength at pixel 512 of the 3rd detector; order number ( $\mathcal{O}$ ), corresponding grating encoder, spectral range uncontaminated by adjacent orders and coverage in vacuum wavenumber ( $\nu$ , expressed in  $\text{cm}^{-1}$ ) for each of the four detectors are also given. The last column lists the mean dispersion,  $\delta\nu$  in  $10^{-3} \text{ cm}^{-1}/\text{pixel}$ , for detector 3. A <sup>c</sup> indicates that the order number must also be specified as a parameter. Illumination outside of the unvignetted spectral range is affected by lack of reproducibility at more than 1% level, for a 0.4 arcsec slit: wavenumber values given in *italic* fall outside the uncontaminated range. The accuracy on the positioning of the reference wavelength is  $\approx 30$  pixels. Overheads due to wavelength setting changes are minimized by ordering the templates by decreasing grating encoder values. See [Table 4a-4k](#) for *spectral ranges in wavelength*.

$\lambda_{\text{ref}}$	$\mathcal{O}$	Grating encoder	Unvign. range		Det. 1		Det. 2		Det. 3		Det. 4		$\delta\nu$
			$\nu_{\text{min}}$	$\nu_{\text{max}}$									
1250.6	45	209311	8082.1	7957.3	8123.5	8080.2	8067.8	8027.0	8016.0	7976.4	7966.9	7929.6	-38.2
1254.4	45	197920	8056.7	7933.4	8097.2	8054.1	8042.5	8001.9	7991.0	7952.9	7942.8	7906.4	-37.6
1268.4	45	154666	7965.0	7846.2	8001.3	7961.1	7949.8	7912.0	7902.0	7866.0	7856.7	7822.9	-35.1
1272.2	45	142554	7940.3	7822.9	7975.8	7935.9	7925.2	7887.7	7877.7	7842.5	7833.9	7800.9	-34.4
1279.0	44	209386	7902.0	7781.5	7943.4	7900.8	7888.9	7848.7	7837.6	7799.7	7790.0	7753.7	-37.4
1282.9	44	197948	7877.1	7757.4	7917.7	7875.3	7864.1	7824.1	7813.7	7776.0	7766.4	7731.0	-36.7
1297.3	44	154442	7788.2	7670.5	7822.9	7783.9	7773.0	7735.7	7726.2	7690.5	7681.7	7648.8	-34.3
1301.2	44	142284	7764.6	7647.6	7797.9	7759.2	7748.3	7711.9	7702.4	7668.1	7659.3	7626.6	-33.6
1299.2	43	236191	7780.9	7659.9	7824.1	7780.3	7768.8	7727.4	7716.6	7677.5	7667.5	7630.7	-38.0
1303.2	43	225045	7756.7	7635.9	7797.9	7755.5	7743.5	7703.0	7692.9	7654.0	7644.7	7608.6	-37.4
1318.1	43	182361	7666.4	7550.0	7703.6	7663.4	7652.3	7614.4	7604.6	7568.9	7559.7	7526.2	-35.0
1322.1	43	170551	7642.3	7527.3	7678.7	7639.4	7628.3	7591.3	7581.5	7546.0	7536.9	7504.1	-34.4
1337.0	43	125126	7555.2	7442.7	7586.7	7550.0	7539.8	7504.7	7495.7	7463.2	7454.9	7423.9	-32.0
1340.9	43	112827	7533.0	7420.6	7562.6	7526.7	7516.5	7482.8	7473.8	7441.6	7433.3	7403.6	-31.3
1330.0	42	236563	7600.5	7482.8	7642.9	7600.5	7588.4	7548.3	7538.1	7499.6	7490.1	7454.3	-37.2
1334.1	42	225407	7576.3	7459.9	7617.3	7575.8	7564.3	7525.0	7514.3	7477.2	7467.7	7432.2	-36.5
1349.5	42	182303	7489.0	7373.0	7524.5	7485.0	7474.4	7437.2	7427.8	7392.6	7383.9	7350.8	-34.2
1353.5	42	170769	7466.6	7350.8	7500.2	7462.1	7451.6	7415.1	7405.2	7370.8	7362.1	7329.8	-33.6
1368.9	42	124914	7381.7	7266.9	7409.6	7373.5	7363.8	7329.8	7321.2	7289.2	7281.2	7251.1	-31.2
1373.0	42	112288	7358.9	7244.8	7386.1	7350.8	7341.1	7307.8	7298.7	7267.4	7259.5	7230.1	-30.6
1362.3	41	236920	7422.8	7302.5	7461.6	7420.0	7408.5	7369.7	7358.9	7321.7	7312.6	7277.5	-36.3
1366.4	41	226037	7400.3	7280.7	7437.7	7397.0	7385.5	7347.0	7336.8	7300.3	7290.8	7256.4	-35.7
1382.4	41	182351	7312.1	7196.3	7345.4	7307.3	7296.6	7260.6	7251.1	7216.6	7208.2	7175.7	-33.4
1386.5	41	170813	7290.2	7175.1	7321.7	7284.4	7274.3	7238.5	7229.1	7195.8	7187.0	7155.6	-32.8
1402.5	41	124290	7204.6	7092.7	7232.2	7196.8	7187.5	7154.6	7145.9	7114.4	7106.8	7077.1	-30.4
1406.6	41	111952	7182.9	7072.1	7209.3	7175.1	7165.4	7133.2	7124.5	7094.2	7086.2	7057.7	-29.8

Table 5d: Reference wavelengths,  $\lambda_{\text{ref}}$ , in nm for the standard wavelength settings, defined as the wavelength at pixel 512 of the 3rd detector; order number ( $\mathcal{O}$ ), corresponding grating encoder, spectral range uncontaminated by adjacent orders and coverage in vacuum wavenumber ( $\nu$ , expressed in  $\text{cm}^{-1}$ ) for each of the four detectors are also given. The last column lists the mean dispersion,  $\delta\nu$  in  $10^{-3} \text{ cm}^{-1}/\text{pixel}$ , for detector 3. A <sup>c</sup> indicates that the order number must also be specified as a parameter. Illumination outside of the unvignetted spectral range is affected by lack of reproducibility at more than 1% level, for a 0.4 arcsec slit: wavenumber values given in *italic* fall outside the uncontaminated range. The accuracy on the positioning of the reference wavelength is  $\approx 30$  pixels. Overheads due to wavelength setting changes are minimized by ordering the templates by decreasing grating encoder values. See [Table 4a-4k](#) for *spectral ranges in wavelength*.

$\lambda_{\text{ref}}$	$\mathcal{O}$	Grating encoder	Unvign. range		Det. 1		Det. 2		Det. 3		Det. 4		$\delta\nu$
			$\nu_{\text{min}}$	$\nu_{\text{max}}$									
1396.2	40	237335	7242.7	7125.0	<i>7280.1</i>	7240.1	7229.1	7190.6	7180.3	7144.4	7134.7	7100.8	-35.4
1400.5	40	226200	7219.7	7103.3	<i>7256.4</i>	7216.6	7205.6	7167.9	7158.2	7122.5	7113.4	7079.6	-34.8
1417.0	40	182244	7133.7	7020.5	<i>7165.9</i>	7128.6	7118.5	7083.2	7073.6	7040.8	7031.9	7000.8	-32.5
1421.2	40	170713	7112.4	6999.4	<i>7143.4</i>	7106.3	7096.2	7061.6	7052.7	7020.0	7011.6	6980.8	-31.9
1437.7	40	123891	7028.9	6918.5	<i>7055.2</i>	7021.0	7011.6	6979.3	6970.6	6940.6	6932.4	6904.2	-29.7
1441.9	40	111556	7007.7	6898.5	<i>7032.8</i>	6999.4	6990.1	6958.5	6950.2	6920.4	6912.8	6884.7	-29.1
1431.9	39	237586	7062.6	6946.9	<i>7098.7</i>	7059.7	7048.7	7011.1	7001.3	6966.2	6957.0	6923.8	-34.6
1436.2	39	226739	7040.8	6926.2	<i>7076.1</i>	7037.3	7026.9	6990.1	6980.3	6945.4	6936.7	6903.7	-34.0
1453.3	39	182336	6956.0	6844.6	<i>6986.7</i>	6950.7	6940.6	6906.1	6897.0	6864.8	6856.4	6825.9	-31.7
1457.7	39	170556	6934.8	6823.6	<i>6964.3</i>	6928.6	6918.5	6885.2	6876.2	6844.2	6836.2	6806.0	-31.1
1474.7	39	123510	6852.6	6744.9	<i>6878.1</i>	6844.6	6835.3	6804.1	6795.8	6766.4	6758.6	6730.8	-28.9
1479.1	39	110903	6831.5	6724.5	<i>6855.9</i>	6823.1	6814.3	6783.3	6775.5	6746.3	6739.0	6711.9	-28.3
1469.4	38	238033	6882.8	6769.1	<i>6917.5</i>	6879.5	6868.6	6832.5	6822.7	6788.4	6779.7	6746.7	-33.7
1473.9	38	226975	6861.1	6748.5	<i>6895.1</i>	6857.3	6847.0	6811.1	6801.8	6767.7	6759.0	6727.2	-33.1
1491.5	38	182457	6778.3	6668.9	<i>6807.8</i>	6772.3	6762.7	6729.5	6720.4	6689.0	6680.9	6651.1	-30.9
1496.0	38	170721	6757.2	6648.9	<i>6786.1</i>	6751.3	6741.7	6708.7	6700.2	6668.9	6660.9	6631.7	-30.3
1513.6	38	123256	6676.5	6571.2	<i>6701.1</i>	6668.9	6660.0	6629.1	6621.2	6592.4	6585.0	6557.8	-28.1
1518.1	38	110688	6656.5	6551.4	<i>6679.6</i>	6648.1	6639.2	6609.4	6601.1	6572.9	6566.0	6539.4	-27.6
1509.0	37	238310	6702.4	6591.5	<i>6736.3</i>	6698.8	6688.5	6652.9	6643.6	6610.3	6601.5	6569.9	-32.8
1513.6	37	227306	6681.4	6571.2	<i>6714.1</i>	6677.4	6667.6	6632.6	6623.4	6590.2	6582.0	6550.5	-32.3
1531.9	37	182232	6599.8	6492.2	<i>6628.2</i>	6593.7	6584.6	6551.8	6543.2	6512.5	6504.5	6475.4	-30.1
1536.4	37	170804	6580.2	6473.3	<i>6607.6</i>	6573.8	6564.3	6532.1	6524.0	6493.5	6485.9	6457.4	-29.5
1554.7	37	122741	6500.7	6396.3	<i>6524.0</i>	6492.2	6483.8	6454.1	6446.2	6418.1	6411.1	6384.5	-27.4
1559.3	37	110229	6480.9	6378.0	<i>6503.2</i>	6472.1	6463.7	6434.6	6426.7	6399.6	6392.2	6366.6	-26.8
1550.8	36	238580	6522.7	6412.7	<i>6554.8</i>	6518.1	6508.3	6473.7	6464.5	6432.1	6423.4	6392.6	-31.9
1555.5	36	227647	6502.4	6393.5	<i>6533.4</i>	6497.7	6487.6	6453.7	6445.0	6412.7	6404.5	6374.3	-31.4

Table 5e: Reference wavelengths,  $\lambda_{\text{ref}}$ , in nm for the standard wavelength settings, defined as the wavelength at pixel 512 of the 3rd detector; order number ( $\mathcal{O}$ ), corresponding grating encoder, spectral range uncontaminated by adjacent orders and coverage in vacuum wavenumber ( $\nu$ , expressed in  $\text{cm}^{-1}$ ) for each of the four detectors are also given. The last column lists the mean dispersion,  $\delta\nu$  in  $10^{-3} \text{ cm}^{-1}/\text{pixel}$ , for detector 3. A <sup>c</sup> indicates that the order number must also be specified as a parameter. Illumination outside of the unvignetted spectral range is affected by lack of reproducibility at more than 1% level, for a 0.4 arcsec slit: wavenumber values given in *italic* fall outside the uncontaminated range. The accuracy on the positioning of the reference wavelength is  $\approx 30$  pixels. Overheads due to wavelength setting changes are minimized by ordering the templates by decreasing grating encoder values. See [Table 4a-4k](#) for *spectral ranges in wavelength*.

$\lambda_{\text{ref}}$	$\mathcal{O}$	Grating encoder	Unvign. range		Det. 1		Det. 2		Det. 3		Det. 4		$\delta\nu$
			$\nu_{\text{min}}$	$\nu_{\text{max}}$									
1574.4	36	182375	6421.4	6317.5	<i>6449.5</i>	6416.0	6406.6	6375.1	6366.6	6336.7	6329.1	6300.8	-29.2
1579.1	36	170763	6401.2	6298.8	<i>6428.8</i>	6395.9	6386.9	6355.7	6347.6	6317.9	6310.3	6283.0	-28.7
1598.0	36	122454	6322.3	6225.5	<i>6346.8</i>	6316.3	6308.0	6279.0	6271.6	6244.1	6237.1	6211.6	-26.6
1602.7	36	110003	6304.0	6206.6	<i>6327.1</i>	6296.8	6288.5	6260.2	6252.7	6226.3	6219.3	6194.3	-26.1
1595.0	35	238838	6339.9	6237.1	<i>6373.1</i>	6337.5	6327.9	6294.5	6285.4	6253.9	6245.7	6215.4	-31.0
1599.9	35	227752	6319.9	6217.7	<i>6352.0</i>	6317.1	6307.6	6274.7	6266.1	6234.8	6226.6	6197.3	-30.5
1619.4	35	182324	6243.8	6141.0	<i>6270.0</i>	6237.5	6228.6	6197.7	6189.7	6160.7	6153.1	6125.6	-28.4
1624.2	35	170792	6225.1	6122.2	<i>6250.4</i>	6218.1	6209.3	6179.3	6171.3	6142.5	6135.3	6108.4	-27.9
1643.7	35	122331	6150.8	6047.8	<i>6170.6</i>	6140.6	6132.7	6104.6	6097.2	6070.5	6063.9	6039.0	-25.9
1648.6	35	109712	6132.3	6029.5	<i>6150.8</i>	6121.4	6113.6	6086.1	6078.7	6052.9	6046.3	6021.9	-25.4
1641.8	34	239069	6163.3	6055.1	<i>6191.2</i>	6156.9	6147.4	6115.1	6106.5	6075.3	6067.6	6038.3	-30.2
1646.8	34	228087	6144.4	6036.5	<i>6171.3</i>	6137.6	6128.2	6096.1	6087.5	6057.3	6049.6	6020.8	-29.7
1667.0	34	182385	6068.7	5962.0	<i>6091.2</i>	6059.5	6050.7	6020.8	6012.9	5984.8	5977.3	5951.0	-27.6
1672.0	34	170718	6050.3	5943.9	<i>6071.6</i>	6040.5	6032.1	6002.4	5994.8	5966.9	5959.8	5933.7	-27.1
1692.2	34	121939	5977.3	5872.0	<i>5993.8</i>	5964.8	5956.6	5929.4	5922.4	5896.6	5890.0	5865.8	-25.1
1697.2	34	109429	5958.8	5854.8	<i>5974.4</i>	5946.4	5938.6	5911.6	5904.6	5879.6	5873.0	5849.3	-24.6
1691.5	33	239170	5984.8	5874.1	<i>6009.6</i>	5976.2	5966.9	5935.4	5927.0	5896.9	5889.3	5861.0	-29.3
1696.6	33	228306	5966.2	5856.9	<i>5990.2</i>	5957.3	5948.1	5917.2	5908.8	5879.6	5872.0	5844.2	-28.8
1717.5	33	182433	5890.7	5786.7	<i>5911.9</i>	5881.3	5873.0	5843.9	5836.0	5808.6	5801.8	5775.7	-26.8
1722.7	33	170657	5872.0	5769.3	<i>5892.8</i>	5862.7	5854.5	5825.8	5818.4	5791.4	5784.4	5759.0	-26.3
1743.6	33	121662	5798.1	5701.3	<i>5817.0</i>	5788.7	5781.0	5754.7	5747.8	5722.8	5716.6	5693.1	-24.4
1748.7	33	109270	5781.0	5684.7	<i>5798.4</i>	5771.0	5763.7	5737.6	5730.7	5706.5	5700.0	5677.3	-23.9
1744.3	32	239310	5801.1	5699.0	<i>5827.5</i>	5795.1	5786.4	5755.7	5747.5	5718.5	5711.0	5683.4	-28.4
1749.6	32	228358	5783.0	5681.5	<i>5808.6</i>	5776.7	5768.0	5737.9	5730.0	5701.3	5694.1	5667.0	-27.9
1771.2	32	182375	5711.0	5612.0	<i>5732.6</i>	5702.9	5694.8	5666.7	5659.3	5632.5	5625.9	5600.7	-26.0
1776.5	32	170734	5693.5	5595.0	<i>5714.3</i>	5685.0	5677.0	5649.4	5642.1	5616.1	5609.5	5584.7	-25.5

Table 5f: Reference wavelengths,  $\lambda_{\text{ref}}$ , in nm for the standard wavelength settings, defined as the wavelength at pixel 512 of the 3rd detector; order number ( $\mathcal{O}$ ), corresponding grating encoder, spectral range uncontaminated by adjacent orders and coverage in vacuum wavenumber ( $\nu$ , expressed in  $\text{cm}^{-1}$ ) for each of the four detectors are also given. The last column lists the mean dispersion,  $\delta\nu$  in  $10^{-3} \text{ cm}^{-1}/\text{pixel}$ , for detector 3. A <sup>c</sup> indicates that the order number must also be specified as a parameter. Illumination outside of the unvignetted spectral range is affected by lack of reproducibility at more than 1% level, for a 0.4 arcsec slit: wavenumber values given in *italic* fall outside the uncontaminated range. The accuracy on the positioning of the reference wavelength is  $\approx 30$  pixels. Overheads due to wavelength setting changes are minimized by ordering the templates by decreasing grating encoder values. See *Table 4a-4k* for *spectral ranges in wavelength*.

$\lambda_{\text{ref}}$	$\mathcal{O}$	Grating encoder	Unvign. range $\nu_{\text{min}}$ $\nu_{\text{max}}$	Det. 1 $\nu_{\text{min}}$ $\nu_{\text{max}}$	Det. 2 $\nu_{\text{min}}$ $\nu_{\text{max}}$	Det. 3 $\nu_{\text{min}}$ $\nu_{\text{max}}$	Det. 4 $\nu_{\text{min}}$ $\nu_{\text{max}}$	$\delta\nu$
1798.1	32	121633	5623.3 5527.6	<i>5640.5</i> 5613.2	5606.0 5580.4	5573.5 5549.4	5543.2 5520.6	-23.6
1803.4	32	109145	5606.3 5511.5	<i>5622.7</i> 5596.0	5588.8 5563.6	5556.8 5533.1	5527.3 5505.1	-23.1
1800.5	31	239445	5621.1 5520.0	<i>5645.6</i> 5614.2	5605.7 5576.0	5568.2 5539.9	5532.8 5506.3	-27.5
1806.0	31	228438	5603.5 5503.3	<i>5627.1</i> 5596.3	5587.8 5558.6	5550.9 5523.3	5516.3 5490.0	-27.0
1828.4	31	182247	5532.2 5436.3	<i>5553.4</i> 5524.6	5516.6 5489.4	5482.2 5456.4	5449.9 5425.6	-25.2
1833.8	31	170755	5515.1 5420.6	<i>5535.9</i> 5507.5	5499.6 5472.9	5466.0 5440.4	5434.2 5410.1	-24.7
1856.2	31	121424	5446.0 5355.9	<i>5463.9</i> 5437.7	5430.4 5405.7	5399.0 5375.8	5369.7 5347.6	-22.9
1861.6	31	109094	5429.8 5340.2	<i>5446.9</i> 5420.9	5413.9 5389.7	5383.3 5360.2	5354.5 5332.8	-22.4
1860.5	30	239487	5438.6 5343.0	<i>5463.6</i> 5433.3	5424.8 5396.1	5388.5 5361.4	5354.5 5328.5	-26.6
1866.1	30	228640	5421.8 5326.8	<i>5446.0</i> 5416.2	5408.0 5379.5	5372.3 5345.3	5338.5 5313.2	-26.2
1889.3	30	182344	5353.6 5261.5	<i>5374.3</i> 5346.4	5338.7 5312.4	5305.3 5280.4	5274.3 5250.7	-24.4
1894.9	30	170813	5337.3 5245.8	<i>5357.3</i> 5329.9	5322.3 5296.3	5289.6 5265.1	5258.7 5235.9	-23.9
1918.1	30	121366	5270.9 5182.2	<i>5287.6</i> 5262.0	5255.1 5231.2	5224.9 5202.1	5196.4 5175.2	-22.1
1923.7	30	108989	5255.1 5166.9	<i>5270.9</i> 5246.0	5239.2 5215.7	5209.4 5187.3	5181.6 5160.8	-21.7
1924.6	29	239591	5258.2 5164.2	<i>5281.5</i> 5252.4	5244.1 5216.5	5209.1 5182.7	5176.0 5151.2	-25.7
1930.4	29	228734	5241.9 5148.5	<i>5264.5</i> 5235.9	5227.9 5200.5	5193.2 5167.4	5160.8 5136.4	-25.3
1954.5	29	182245	5175.4 5085.2	<i>5195.1</i> 5168.0	5160.8 5135.1	5128.5 5104.4	5098.1 5075.6	-23.5
1960.3	29	170697	5159.7 5070.2	<i>5178.4</i> 5152.0	5144.8 5119.8	5113.0 5089.3	5083.4 5061.0	-23.1
1984.3	29	121245	5095.3 5009.0	<i>5111.2</i> 5086.5	5079.8 5056.6	5050.5 5028.7	5023.1 5002.5	-21.4
1990.1	29	108853	5080.0 4994.3	<i>5095.0</i> 5071.0	5064.3 5041.6	5035.5 5014.0	5008.8 4988.5	-21.0
1993.3	28	239659	5077.2 4985.8	<i>5099.4</i> 5071.3	5063.5 5036.5	5029.4 5004.0	4997.8 4973.6	-24.8
1999.4	28	228631	5061.0 4970.7	<i>5082.9</i> 5055.1	5047.4 5021.1	5014.0 4989.0	4982.6 4959.1	-24.4
2024.3	28	182256	4996.8 4909.9	<i>5015.8</i> 4989.8	4982.8 4958.1	4951.7 4928.3	4922.5 4900.5	-22.7
2030.3	28	170725	4981.3 4895.5	<i>5000.0</i> 4974.4	4967.5 4943.2	4936.8 4914.0	4908.2 4886.6	-22.3
2055.2	28	121185	4918.6 4836.5	<i>4934.9</i> 4911.1	4904.6 4882.1	4876.4 4855.1	4849.7 4830.0	-20.6
2061.2	28	108806	4903.9 4822.5	<i>4919.3</i> 4896.0	4889.7 4867.6	4861.9 4841.2	4835.8 4816.5	-20.2

Table 5g: Reference wavelengths,  $\lambda_{\text{ref}}$ , in nm for the standard wavelength settings, defined as the wavelength at pixel 512 of the 3rd detector; order number ( $\mathcal{O}$ ), corresponding grating encoder, spectral range uncontaminated by adjacent orders and coverage in vacuum wavenumber ( $\nu$ , expressed in  $\text{cm}^{-1}$ ) for each of the four detectors are also given. The last column lists the mean dispersion,  $\delta\nu$  in  $10^{-3} \text{ cm}^{-1}/\text{pixel}$ , for detector 3. A <sup>c</sup> indicates that the order number must also be specified as a parameter. Illumination outside of the unvignetted spectral range is affected by lack of reproducibility at more than 1% level, for a 0.4 arcsec slit: wavenumber values given in *italic* fall outside the uncontaminated range. The accuracy on the positioning of the reference wavelength is  $\approx 30$  pixels. Overheads due to wavelength setting changes are minimized by ordering the templates by decreasing grating encoder values. See [Table 4a-4k](#) for *spectral ranges in wavelength*.

$\lambda_{\text{ref}}$	$\mathcal{O}$	Grating encoder	Unvign. range		Det. 1		Det. 2		Det. 3		Det. 4		$\delta\nu$
			$\nu_{\text{min}}$	$\nu_{\text{max}}$									
2067.1	27	239709	4895.2	4808.2	<i>4917.4</i>	4890.2	4882.6	4856.7	4849.9	4825.6	4819.3	4796.2	-23.9
2073.4	27	228727	4880.0	4793.4	<i>4901.5</i>	4874.7	4867.1	4841.7	4835.1	4810.9	4804.9	4781.9	-23.5
2099.3	27	182210	4818.1	4734.4	<i>4836.8</i>	4811.6	4804.7	4781.0	4774.6	4752.4	4746.5	4725.5	-21.9
2105.5	27	170718	4803.5	4720.3	<i>4821.4</i>	4796.6	4790.0	4766.7	4760.5	4738.4	4732.8	4712.1	-21.5
2131.3	27	121222	4743.6	4663.3	<i>4758.7</i>	4735.7	4729.5	4707.9	4702.1	4681.9	4676.6	4657.4	-19.9
2137.6	27	108687	4729.3	4649.4	<i>4743.6</i>	4721.0	4715.0	4693.7	4688.2	4668.1	4663.1	4644.3	-19.5
2146.6	26	239717	4714.5	4629.2	<i>4735.3</i>	4709.0	4701.9	4676.8	4670.3	4646.8	4640.8	4618.5	-23.0
2153.1	26	228807	4699.9	4615.3	<i>4720.1</i>	4694.2	4687.1	4662.4	4656.1	4632.8	4627.1	4605.1	-22.7
2180.0	26	182289	4639.9	4558.7	<i>4657.7</i>	4633.5	4626.8	4604.1	4597.9	4576.4	4570.8	4550.4	-21.1
2186.5	26	170686	4625.8	4545.2	<i>4642.7</i>	4618.9	4612.5	4590.1	4584.2	4562.9	4557.5	4537.6	-20.7
2213.3	26	121171	4567.7	4490.5	<i>4582.3</i>	4560.4	4554.1	4533.5	4528.0	4508.4	4503.3	4484.9	-19.2
2219.8	26	108720	4553.7	4477.5	<i>4567.9</i>	4546.3	4540.3	4520.0	4514.5	4495.4	4490.3	4472.3	-18.8
2232.4	25	239822	4533.3	4451.2	<i>4553.3</i>	4528.2	4521.2	4497.2	4491.0	4468.1	4462.3	4440.9	-22.2
2239.1	25	229012	4519.2	4437.9	<i>4538.9</i>	4513.9	4507.1	4483.5	4477.3	4454.9	4449.2	4428.1	-21.8
2267.2	25	182293	4461.3	4383.3	<i>4478.5</i>	4455.3	4448.8	4426.9	4421.1	4400.4	4395.0	4375.4	-20.3
2273.9	25	170794	4447.6	4370.4	<i>4464.3</i>	4441.5	4435.2	4413.6	4408.0	4387.5	4382.3	4363.2	-19.9
2302.0	25	120870	4391.4	4317.4	<i>4405.7</i>	4384.6	4378.7	4358.8	4353.5	4334.6	4329.8	4312.2	-18.4
2308.7	25	108524	4378.1	4305.0	<i>4391.9</i>	4371.2	4365.5	4345.7	4340.7	4322.3	4317.4	4300.2	-18.0
2325.2	24	240159	4352.2	4273.5	<i>4371.6</i>	4347.4	4340.7	4317.6	4311.6	4289.8	4284.3	4263.7	-21.3
2332.2	24	229321	4338.6	4260.8	<i>4357.7</i>	4333.7	4327.1	4304.4	4298.5	4277.2	4271.7	4251.3	-20.9
2361.7	24	182240	4282.5	4208.0	<i>4299.2</i>	4277.0	4270.9	4249.7	4244.3	4224.2	4219.2	4200.4	-19.5
2368.7	24	170706	4269.3	4195.7	<i>4285.6</i>	4263.7	4257.7	4236.9	4231.6	4211.9	4207.0	4188.5	-19.1
2398.1	24	120552	4215.0	4144.6	<i>4229.2</i>	4208.8	4203.3	4184.1	4179.0	4160.9	4156.3	4139.4	-17.7
2405.1	24	108163	4202.0	4132.7	<i>4215.9</i>	4195.9	4190.4	4171.7	4166.7	4149.0	4144.4	4127.8	-17.3
2425.9	23	240745	4171.4	4096.0	<i>4190.2</i>	4167.0	4160.6	4138.4	4132.6	4111.7	4106.4	4086.6	-20.4
2433.2	23	229919	4158.5	4083.6	<i>4176.8</i>	4153.9	4147.5	4125.8	4120.1	4099.5	4094.3	4074.8	-20.1

Table 5h: Reference wavelengths,  $\lambda_{\text{ref}}$ , in nm for the standard wavelength settings, defined as the wavelength at pixel 512 of the 3rd detector; order number ( $\mathcal{O}$ ), corresponding grating encoder, spectral range uncontaminated by adjacent orders and coverage in vacuum wavenumber ( $\nu$ , expressed in  $\text{cm}^{-1}$ ) for each of the four detectors are also given. The last column lists the mean dispersion,  $\delta\nu$  in  $10^{-3} \text{ cm}^{-1}/\text{pixel}$ , for detector 3. A <sup>c</sup> indicates that the order number must also be specified as a parameter. Illumination outside of the unvignetted spectral range is affected by lack of reproducibility at more than 1% level, for a 0.4 arcsec slit: wavenumber values given in *italic* fall outside the uncontaminated range. The accuracy on the positioning of the reference wavelength is  $\approx 30$  pixels. Overheads due to wavelength setting changes are minimized by ordering the templates by decreasing grating encoder values. See [Table 4a-4k](#) for *spectral ranges in wavelength*.

$\lambda_{\text{ref}}$	$\mathcal{O}$	Grating encoder	Unvign. range		Det. 1		Det. 2		Det. 3		Det. 4		$\delta\nu$
			$\nu_{\text{min}}$	$\nu_{\text{max}}$									
2464.4	23	182212	4104.4	4031.9	<i>4120.1</i>	4098.7	4092.8	4072.7	4067.4	4048.3	4043.3	4025.4	-18.7
2471.6	23	170845	4092.2	4020.1	<i>4107.3</i>	4086.1	4080.5	4060.6	4055.3	4036.7	4031.8	4014.1	-18.3
2502.8	23	119818	4039.6	3970.0	<i>4052.2</i>	4032.7	4027.4	4009.0	4004.2	3986.9	3982.5	3966.2	-16.9
2510.0	23	107598	4027.7	3958.5	<i>4039.6</i>	4020.6	4015.3	3997.3	3992.5	3975.5	3971.2	3955.4	-16.6
2515.0	22	270172	4025.9	3949.0	<i>4044.2</i>	4020.9	4014.5	3992.5	3986.6	3965.7	3960.4	3940.6	-20.4
2522.6	22	259705	4013.3	3937.3	<i>4031.1</i>	4008.2	4001.9	3980.3	3974.4	3954.0	3948.7	3929.1	-20.1
2555.9	22	212504	3959.1	3886.5	<i>3974.9</i>	3953.5	3947.7	3927.4	3922.2	3902.9	3898.0	3880.0	-18.7
2563.5	22	201401	3947.0	3875.1	<i>3962.3</i>	3941.2	3935.5	3915.6	3910.4	3891.5	3886.7	3868.9	-18.4
2596.8	22	151096	3894.2	3825.8	<i>3907.8</i>	3888.2	3882.9	3864.4	3859.7	3842.2	3837.7	3821.5	-17.0
2604.4	22	139204	3882.4	3814.9	<i>3895.4</i>	3876.3	3871.0	3853.0	3848.2	3831.1	3826.7	3810.7	-16.7
2637.6	22	85198	3831.6	3767.2	<i>3842.6</i>	3825.0	3820.1	3803.6	3799.1	3783.4	3779.6	3764.9	-15.3
2645.2	22	72315	3820.3	3756.4	<i>3830.7</i>	3813.4	3808.7	3792.3	3788.2	3772.7	3768.9	3754.5	-15.0
2633.1	21	272346	3845.1	3771.9	<i>3862.8</i>	3840.7	3834.5	3813.4	3807.8	3787.9	3782.7	3763.8	-19.5
2641.0	21	261983	3833.0	3760.8	<i>3850.4</i>	3828.6	3822.6	3801.8	3796.4	3776.6	3771.6	3752.9	-19.2
2677.1	21	213212	3779.9	3710.3	<i>3794.9</i>	3774.6	3769.0	3749.7	3744.6	3726.2	3721.6	3704.4	-17.9
2685.0	21	202203	3768.3	3699.3	<i>3783.0</i>	3762.9	3757.4	3738.5	3733.4	3715.4	3710.9	3693.9	-17.6
2721.0	21	150290	3716.9	3650.6	<i>3729.3</i>	3710.7	3705.6	3688.0	3683.4	3666.9	3662.6	3647.0	-16.2
2729.0	21	138329	3705.6	3639.8	<i>3717.6</i>	3699.3	3694.3	3677.0	3672.6	3656.2	3652.0	3636.8	-15.9
2764.9	21	82465	3656.0	3592.6	<i>3665.6</i>	3648.8	3644.2	3628.3	3624.2	3609.3	3605.6	3591.6	-14.5
2772.8	21	69634	3645.4	3582.2	<i>3654.3</i>	3637.8	3633.3	3617.8	3613.8	3599.2	3595.4	3581.8	-14.2
2761.9	20	275889	3667.0	3594.5	<i>3683.0</i>	3661.7	3655.8	3635.6	3630.3	3611.2	3606.2	3588.1	-18.7
2770.2	20	265556	3655.6	3583.8	<i>3671.2</i>	3650.2	3644.4	3624.5	3619.3	3600.5	3595.6	3577.8	-18.4
2810.0	20	214467	3603.3	3532.2	<i>3615.6</i>	3596.1	3590.8	3572.3	3567.5	3550.0	3545.6	3529.1	-17.0
2818.3	20	203465	3592.6	3521.6	<i>3604.1</i>	3585.0	3579.7	3561.6	3566.8	3539.7	3535.3	3519.1	-16.8
2858.0	20	148939	3542.0	3472.0	<i>3550.5</i>	3532.8	3528.0	3511.2	3506.8	3491.1	3487.1	3472.2	-15.4
2866.3	20	137104	3531.6	3461.6	<i>3539.4</i>	3522.0	3517.3	3500.9	3496.5	3481.0	3477.2	3462.6	-15.1

Table 5i: Reference wavelengths,  $\lambda_{\text{ref}}$ , in nm for the standard wavelength settings, defined as the wavelength at pixel 512 of the 3rd detector; order number ( $\mathcal{O}$ ), corresponding grating encoder, spectral range uncontaminated by adjacent orders and coverage in vacuum wavenumber ( $\nu$ , expressed in  $\text{cm}^{-1}$ ) for each of the four detectors are also given. The last column lists the mean dispersion,  $\delta\nu$  in  $10^{-3} \text{ cm}^{-1}/\text{pixel}$ , for detector 3. A <sup>c</sup> indicates that the order number must also be specified as a parameter. Illumination outside of the unvignetted spectral range is affected by lack of reproducibility at more than 1% level, for a 0.4 arcsec slit: wavenumber values given in *italic* fall outside the uncontaminated range. The accuracy on the positioning of the reference wavelength is  $\approx 30$  pixels. Overheads due to wavelength setting changes are minimized by ordering the templates by decreasing grating encoder values. See [Table 4a-4k](#) for *spectral ranges in wavelength*.

$\lambda_{\text{ref}}$	$\mathcal{O}$	Grating encoder	Unvign. range $\nu_{\text{min}}$ $\nu_{\text{max}}$	Det. 1 $\nu_{\text{min}}$ $\nu_{\text{max}}$	Det. 2 $\nu_{\text{min}}$ $\nu_{\text{max}}$	Det. 3 $\nu_{\text{min}}$ $\nu_{\text{max}}$	Det. 4 $\nu_{\text{min}}$ $\nu_{\text{max}}$	$\delta\nu$
2906.0	20	78065	3482.7 3413.6	<i>3487.2</i> 3471.4	3467.0 3452.1	3448.2 3434.2	3430.5 3417.4	-13.7
2914.3	20	65158	3472.5 3403.8	<i>3476.6</i> 3461.0	3456.7 3442.1	3438.2 3424.4	3421.0 3408.1	-13.4
2902.8	19	281120	3493.7 3415.2	<i>3504.6</i> 3484.2	3478.6 3459.2	3454.1 3435.8	3431.1 <i>3413.8</i>	-17.9
2911.5	19	270883	3482.9 3405.1	<i>3493.3</i> 3473.3	3467.8 3448.8	3443.8 3425.6	3421.0 <i>3403.9</i>	-17.6
2956.4	19	216337	3428.1 3353.8	<i>3436.7</i> 3418.1	3413.0 3395.5	3390.9 3374.2	3370.0 3354.2	-16.2
2965.1	19	205403	3417.6 3344.1	<i>3425.8</i> 3407.6	3402.6 3385.4	3380.8 3364.4	3360.2 3344.8	-16.0
3009.9	19	146949	3364.7 3294.8	<i>3371.1</i> 3354.5	3349.9 3334.0	3329.9 3314.9	3311.1 3297.1	-14.6
3018.6	19	135138	3354.6 3285.4	<i>3360.7</i> 3344.3	3339.8 3324.2	3320.2 3305.5	3301.7 3288.0	-14.3
3063.4	19	71522	3307.8 3242.0	<i>3307.8</i> 3292.8	3288.7 3274.6	3271.0 3257.8	3254.4 <i>3242.0</i>	-12.9
3072.1	19	58559	3297.6 3233.2	<i>3297.6</i> 3283.0	3278.9 3265.2	3261.6 3248.7	3245.4 <i>3233.2</i>	-12.6
3057.2	18	288711	3318.0 3241.7	<i>3328.1</i> 3308.5	3303.2 3284.6	3279.8 3262.2	3257.8 <i>3241.1</i>	-17.2
3066.3	18	278642	3307.8 3232.3	<i>3317.5</i> 3298.3	3293.0 3274.7	3269.9 3252.7	3248.2 <i>3231.9</i>	-16.9
3118.3	18	219101	3252.0 3177.4	<i>3258.4</i> 3240.8	3235.9 3219.2	3214.8 3199.0	3195.0 3180.1	-15.5
3127.5	18	208179	3242.3 3167.9	<i>3248.1</i> 3230.8	3226.0 3209.6	3205.2 3189.7	3185.7 3171.1	-15.2
3179.4	18	144027	3191.2 3121.4	<i>3191.2</i> 3175.5	3171.2 3156.2	3152.3 3138.2	3134.6 3121.4	-13.7
3188.6	18	132155	3181.4 3112.7	<i>3181.4</i> 3165.9	3161.6 3146.9	3143.1 3129.3	3125.8 <i>3112.7</i>	-13.5
3240.4	18	61924	3126.5 3065.2	<i>3126.5</i> 3112.5	3108.8 3095.6	3092.2 3079.9	3076.7 <i>3065.2</i>	-12.0
3249.6	18	48775	3116.9 3057.0	<i>3116.9</i> 3103.3	3099.5 3086.7	3083.4 3071.3	3068.2 <i>3057.0</i>	-11.8
3226.5	17	299609	3154.2 3070.6	<i>3154.2</i> 3135.4	3130.3 3112.5	3107.8 3090.9	3086.6 <i>3070.6</i>	-16.5
3236.2	17	289576	3144.1 3061.8	<i>3144.1</i> 3125.6	3120.5 3103.0	3098.4 3081.8	3077.5 <i>3061.8</i>	-16.2
3298.3	17	222918	3080.8 3006.3	<i>3080.8</i> 3064.1	3059.4 3043.6	3039.4 3024.3	3020.5 <i>3006.3</i>	-14.7
3307.9	17	212200	3071.3 2998.0	<i>3071.3</i> 3054.7	3050.2 3034.5	3030.5 3015.7	3012.0 <i>2998.0</i>	-14.4
3369.9	17	139809	3010.6 2945.1	<i>3010.6</i> 2995.8	2991.8 2977.7	2974.1 2960.9	2957.5 <i>2945.1</i>	-12.9
3379.6	17	127929	3001.3 2936.9	<i>3001.3</i> 2986.8	2982.8 2969.0	2965.4 2952.5	2949.2 <i>2936.9</i>	-12.7
3441.5	17	47758	2943.1 2886.5	<i>2943.1</i> 2930.2	2926.7 2914.6	2911.4 2900.1	2897.1 <i>2886.5</i>	-11.1
3451.1	17	34549	2934.2 2878.9	<i>2934.2</i> 2921.6	2918.2 2906.3	2903.2 2892.1	2889.3 <i>2878.9</i>	-10.9

Table 5j: Reference wavelengths,  $\lambda_{\text{ref}}$ , in nm for the standard wavelength settings, defined as the wavelength at pixel 512 of the 3rd detector; order number ( $\mathcal{O}$ ), corresponding grating encoder, spectral range uncontaminated by adjacent orders and coverage in vacuum wavenumber ( $\nu$ , expressed in  $\text{cm}^{-1}$ ) for each of the four detectors are also given. The last column lists the mean dispersion,  $\delta\nu$  in  $10^{-3} \text{ cm}^{-1}/\text{pixel}$ , for detector 3. A <sup>c</sup> indicates that the order number must also be specified as a parameter. Illumination outside of the unvignetted spectral range is affected by lack of reproducibility at more than 1% level, for a 0.4 arcsec slit: wavenumber values given in *italic* fall outside the uncontaminated range. The accuracy on the positioning of the reference wavelength is  $\approx 30$  pixels. Overheads due to wavelength setting changes are minimized by ordering the templates by decreasing grating encoder values. See [Table 4a-4k](#) for *spectral ranges in wavelength*.

$\lambda_{\text{ref}}$	$\mathcal{O}$	Grating encoder	Unvign. range		Det. 1		Det. 2		Det. 3		Det. 4		$\delta\nu$
			$\nu_{\text{min}}$	$\nu_{\text{max}}$									
3426.3	16	301407	2970.4	2891.5	<i>2970.4</i>	2952.6	2947.8	2931.0	2926.6	2910.7	2906.6	2891.5	-15.6
3436.6	16	291399	2960.9	2883.2	<i>2960.9</i>	2943.4	2938.6	2922.1	2917.7	2902.0	2898.0	2883.2	-15.3
3503.8	16	223591	2900.1	2830.0	<i>2900.1</i>	2884.3	2880.0	2865.1	2861.1	2847.0	2843.3	2830.0	-13.8
3514.0	16	212882	2891.1	2822.1	<i>2891.1</i>	2875.6	2871.3	2856.6	2852.7	2838.8	2835.3	2822.1	-13.6
3581.2	16	139032	2832.9	2771.3	<i>2832.9</i>	2819.0	2815.2	2802.1	2798.6	2786.1	2783.0	2771.3	-12.1
3591.4	16	127261	2824.3	2763.8	<i>2824.3</i>	2810.6	2806.9	2793.9	2790.5	2778.3	2775.2	2763.8	-11.9
3658.4	16	45436	2768.5	2715.5	<i>2768.5</i>	2756.4	2753.1	2741.8	2738.8	2728.1	2725.4	2715.5	-10.4
3668.6	16	32187	2760.1	2708.3	<i>2760.1</i>	2748.3	2745.1	2734.0	2731.0	2720.6	2718.0	2708.3	-10.2
3696.7	15	262637	2750.9	2681.2	<i>2750.9</i>	2735.2	2731.0	2716.1	2712.2	2698.1	2694.5	2681.2	-13.8
3707.5	15	252422	2742.4	2673.7	<i>2742.4</i>	2727.0	2722.6	2708.0	2704.2	2690.3	2686.8	2673.7	-13.5
3778.7	15	182258	2687.0	2625.3	<i>2687.0</i>	2673.2	2669.3	2656.1	2652.7	2640.2	2637.0	2625.3	-12.2
3789.5	15	171139	2678.8	2618.1	<i>2678.8</i>	2665.1	2661.3	2648.4	2645.0	2632.8	2629.6	2618.1	-12.0
3860.5	15	94294	2625.8	2572.0	<i>2625.8</i>	2613.6	2610.3	2598.8	2595.8	2584.9	2582.2	2572.0	-10.6
3871.3	15	81960	2617.9	2565.2	<i>2617.9</i>	2605.9	2602.7	2591.3	2588.4	2577.8	2575.1	2565.2	-10.4
3874.4	14	335861	2628.6	2556.0	<i>2628.6</i>	2612.4	2607.9	2592.5	2588.4	2573.7	2570.0	2556.0	-14.3
3885.9	14	326392	2620.3	2548.8	<i>2620.3</i>	2604.3	2599.9	2584.6	2580.6	2566.2	2562.5	2548.8	-14.1
3961.5	14	261977	2567.0	2501.9	<i>2567.0</i>	2552.4	2548.4	2534.5	2530.9	2517.8	2514.4	2501.9	-12.8
3973.0	14	251819	2559.1	2495.0	<i>2559.1</i>	2544.7	2540.7	2527.0	2523.5	2510.5	2507.2	2495.0	-12.6
4048.6	14	182263	2507.9	2450.3	<i>2507.9</i>	2494.9	2491.3	2479.1	2475.8	2464.2	2461.2	2450.3	-11.4
4060.1	14	171213	2500.3	2443.6	<i>2500.3</i>	2487.5	2484.0	2471.9	2468.7	2457.3	2454.3	2443.6	-11.2
4135.5	14	95089	2451.3	2401.0	<i>2451.3</i>	2439.9	2436.7	2425.9	2423.1	2413.0	2410.5	2401.0	-9.9
4147.0	14	82842	2443.9	2394.6	<i>2443.9</i>	2432.7	2429.7	2419.1	2416.3	2406.4	2403.9	2394.6	-9.7
4174.6	13	334207	2439.5	2372.3	<i>2439.5</i>	2424.5	2420.3	2406.0	2402.2	2388.7	2385.2	2372.3	-13.3
4186.9	13	324789	2431.9	2365.6	<i>2431.9</i>	2417.0	2413.0	2398.8	2395.2	2381.7	2378.3	2365.6	-13.1
4267.4	13	261022	2382.9	2322.7	<i>2382.9</i>	2369.4	2365.7	2352.8	2349.5	2337.3	2334.2	2322.7	-11.9
4279.6	13	251006	2375.7	2316.3	<i>2375.7</i>	2362.3	2358.7	2346.0	2342.7	2330.7	2327.6	2316.3	-11.7

Table 5k: Reference wavelengths,  $\lambda_{\text{ref}}$ , in nm for the standard wavelength settings, defined as the wavelength at pixel 512 of the 3rd detector; order number ( $\mathcal{O}$ ), corresponding grating encoder, spectral range uncontaminated by adjacent orders and coverage in vacuum wavenumber ( $\nu$ , expressed in  $\text{cm}^{-1}$ ) for each of the four detectors are also given. The last column lists the mean dispersion,  $\delta\nu$  in  $10^{-3} \text{ cm}^{-1}/\text{pixel}$ , for detector 3. A <sup>c</sup> indicates that the order number must also be specified as a parameter. Illumination outside of the unvignetted spectral range is affected by lack of reproducibility at more than 1% level, for a 0.4 arcsec slit: wavenumber values given in *italic* fall outside the uncontaminated range. The accuracy on the positioning of the reference wavelength is  $\approx 30$  pixels. Overheads due to wavelength setting changes are minimized by ordering the templates by decreasing grating encoder values. See [Table 4a-4k](#) for *spectral ranges in wavelength*.

$\lambda_{\text{ref}}$	$\mathcal{O}$	Grating encoder	Unvign. range		Det. 1		Det. 2		Det. 3		Det. 4		$\delta\nu$
			$\nu_{\text{min}}$	$\nu_{\text{max}}$									
4360.0	13	182289	2328.8	2275.3	<i>2328.8</i>	2316.7	2313.4	2302.0	2299.0	2288.2	2285.5	<i>2275.3</i>	-10.5
4372.2	13	171407	2321.8	2269.2	<i>2321.8</i>	2309.9	2306.7	2295.4	2292.5	2281.9	2279.2	<i>2269.2</i>	-10.4
4452.5	13	96182	2276.8	2230.0	<i>2276.8</i>	2266.2	2263.3	2253.3	2250.6	2241.2	2238.8	<i>2230.0</i>	-9.2
4464.7	13	84134	2270.0	2224.2	<i>2270.0</i>	2259.6	2256.8	2247.0	2244.4	2235.2	2232.8	<i>2224.2</i>	-9.0
4544.8	13	-53	2226.7	2186.8	<i>2226.7</i>	2217.6	2215.1	2206.6	2204.3	2196.3	2194.3	<i>2186.8</i>	-7.8
4525.8	12	331867	2250.1	2188.3	<i>2250.1</i>	2236.3	2232.4	2219.3	2215.8	2203.3	2200.1	<i>2188.3</i>	-12.2
4538.8	12	322660	2243.3	2182.2	<i>2243.3</i>	2229.6	2225.8	2212.8	2209.4	2197.1	2193.9	<i>2182.2</i>	-12.0
4624.6	12	259824	2198.9	2143.3	<i>2198.9</i>	2186.4	2182.9	2171.1	2168.0	2156.8	2153.9	<i>2143.3</i>	-11.0
4637.6	12	249961	2192.3	2137.5	<i>2192.3</i>	2180.0	2176.6	2164.9	2161.8	2150.8	2148.0	<i>2137.5</i>	-10.8
4723.3	12	182313	2149.7	2100.3	<i>2149.7</i>	2138.5	2135.5	2124.9	2122.2	2112.2	2109.7	<i>2100.3</i>	-9.7
4736.3	12	171611	2143.3	2094.7	<i>2143.3</i>	2132.4	2129.4	2119.0	2116.3	2106.5	2104.0	<i>2094.7</i>	-9.6
4821.9	12	97662	2102.4	2059.1	<i>2102.4</i>	2092.6	2089.9	2080.6	2078.2	2069.5	2067.3	<i>2059.1</i>	-8.5
4834.9	12	85837	2096.3	2053.9	<i>2096.3</i>	2086.7	2084.0	2074.9	2072.6	2064.0	2061.9	<i>2053.9</i>	-8.3
4920.3	12	3261	2056.9	2019.9	<i>2056.9</i>	2048.5	2046.2	2038.2	2036.1	2028.7	2026.8	<i>2019.9</i>	-7.3
4889.5	11	362306	2084.1	2024.8	<i>2084.1</i>	2070.8	2067.1	2054.5	2051.2	2039.2	2036.2	<i>2024.8</i>	-11.7
4903.4	11	353526	2077.8	2019.3	<i>2077.8</i>	2064.7	2061.1	2048.6	2045.3	2033.5	2030.5	<i>2019.3</i>	-11.6
4994.8	11	293999	2037.3	1983.7	<i>2037.3</i>	2025.2	2021.9	2010.5	2007.5	1996.7	1993.9	<i>1983.7</i>	-10.6
5008.7	11	284651	2031.2	1978.4	<i>2031.2</i>	2019.4	2016.1	2004.9	2001.9	1991.2	1988.5	<i>1978.4</i>	-10.4
5100.1	11	220949	1992.3	1944.3	<i>1992.3</i>	1981.5	1978.6	1968.3	1965.6	1955.9	1953.4	<i>1944.3</i>	-9.5
5114.0	11	210890	1986.5	1939.2	<i>1986.5</i>	1975.9	1972.9	1962.9	1960.2	1950.6	1948.2	<i>1939.2</i>	-9.3
5205.3	11	141944	1949.2	1906.6	<i>1949.2</i>	1939.5	1936.9	1927.8	1925.4	1916.8	1914.6	<i>1906.6</i>	-8.4
5219.1	11	131041	1943.6	1901.8	<i>1943.6</i>	1934.1	1931.5	1922.6	1920.3	1911.8	1909.7	<i>1901.8</i>	-8.2

## 16 Free wavelength settings

Table 6a: Available ranges of the reference wavelength  $\lambda_{\text{ref}}$  for the free settings. Values should be rounded to the closest 0.1 nm. A <sup>c</sup> besides an order number indicates that some reference wavelengths in that order are common to an adjacent order (see Table 7), in which case the order number must also be specified as a template parameter.

$\mathcal{O}$	$\lambda_{\text{ref}}^{\text{min}}$	$\lambda_{\text{ref}}^{\text{max}}$
58	971.000	986.300
57	988.000	1003.60
56	1005.60	1021.60
55	1023.80	1040.20
54	1042.70	1059.60
53	1062.30	1079.60
52	1082.70	1100.50
51	1103.90	1122.10
50	1125.90	1144.60
49	1148.80	1168.10
48	1172.70	1192.50
47	1197.50	1217.90
46	1223.50	1244.40
45	1250.60	1272.20
44 <sup>c</sup>	1279.00	1301.20
43 <sup>c</sup>	1299.20	1340.90
42 <sup>c</sup>	1330.00	1373.00
41 <sup>c</sup>	1362.30	1406.60
40 <sup>c</sup>	1396.20	1441.90
39 <sup>c</sup>	1431.90	1479.10
38 <sup>c</sup>	1469.40	1518.10
37 <sup>c</sup>	1509.00	1559.30
36 <sup>c</sup>	1550.80	1602.70
35 <sup>c</sup>	1595.00	1648.60

Table 6b: Available ranges of the reference wavelength  $\lambda_{\text{ref}}$  for the free settings. Values should be rounded to the closest 0.1 nm. A <sup>c</sup> besides an order number indicates that some reference wavelengths in that order are common to an adjacent order (see Table 7), in which case the order number must also be specified as template parameter.

$\mathcal{O}$	$\lambda_{\text{ref}}^{\text{min}}$	$\lambda_{\text{ref}}^{\text{max}}$
34 <sup>c</sup>	1641.80	1697.20
33 <sup>c</sup>	1691.50	1748.70
32 <sup>c</sup>	1744.30	1803.40
31 <sup>c</sup>	1800.50	1861.60
30 <sup>c</sup>	1860.50	1923.70
29	1924.60	1990.10
28	1993.30	2061.20
27	2067.10	2137.60
26	2146.60	2219.80
25	2232.40	2308.70
24	2325.20	2405.10
23	2425.90	2510.00
22 <sup>c</sup>	2515.00	2645.20
21 <sup>c</sup>	2633.10	2772.80
20 <sup>c</sup>	2761.90	2914.30
19 <sup>c</sup>	2902.80	3072.10
18 <sup>c</sup>	3057.20	3249.60
17 <sup>c</sup>	3226.50	3451.10
16 <sup>c</sup>	3426.30	3668.60
15	3696.70	3871.30
14	3874.40	4147.00
13 <sup>c</sup>	4174.60	4544.80
12 <sup>c</sup>	4525.80	4920.30
11 <sup>c</sup>	4889.50	5219.10

## 17 Reference wavelengths common to different orders

Table 7: Ranges of reference wavelengths that are common to 2 successive orders: for wavelengths in these ranges (inclusive), it is mandatory to specify the grating order as a template parameter. This is valid for both standard and free wavelength settings.

Common ranges		Orders
$\lambda_{\min}$	$\lambda_{\max}$	
1299.2	1301.2	44 43
1330.0	1340.9	43 42
1362.3	1373.0	42 41
1396.2	1406.6	41 40
1431.9	1441.9	40 39
1469.4	1479.1	39 38
1509.0	1518.1	38 37
1550.8	1559.3	37 36
1595.0	1602.7	36 35
1641.8	1648.6	35 34
1691.5	1697.2	34 33
1744.3	1748.7	33 32
1800.5	1803.4	32 31
1860.5	1861.6	31 30
2633.1	2645.2	22 21
2761.9	2772.8	21 20
2902.8	2914.3	20 19
3057.2	3072.1	19 18
3226.5	3249.6	18 17
3426.3	3451.1	17 16
4525.8	4544.8	13 12
4889.5	4920.3	12 11

## 18 Calibration source for wavelength calibration

The table given below lists the recommended calibration source required by the wavelength calibration template attached immediately before or after a science template. Such a template is required if a wavelength calibration more accurate than  $\approx 3$  pixels is needed; otherwise, the internal model of the instrument is sufficient.

If the entry is *sky emission lines* or *sky absorption lines*, then neither the ThAr lamp nor the Halogen + N<sub>2</sub>O or Halogen + CO gas cells provides enough lines for any useful wavelength calibration: the wavelength calibration must therefore be made using the science data themselves. Obviously, the *sky emission lines* cover the whole slit length, while the *sky absorption lines* are only useful in front of objects showing a continuum. The Halogen + CO gas cell is a good option for settings in order 24.

Note that sky emission lines can also be used red-ward of  $\approx 2500$  nm, instead of the Halogen+N<sub>2</sub>O gas cell. The [exposure time calculator \(ETC\)](#) also allows one to determine the density of sky emission lines, sky absorption lines or of lines from the Halogen lamp + N<sub>2</sub>O gas cell. A ThAr line list for the wavelength range covered by CRIRES is part of the static tables available at [http://www.eso.org/observing/dfo/quality/CRIRES/pipeline/pipe\\_calib.html](http://www.eso.org/observing/dfo/quality/CRIRES/pipeline/pipe_calib.html). However, a new table providing twice as many identified lines should be available shortly (see §7.2.1).

The CRIRES team is considering various solutions to provide accurate wavelength calibration in the spectral regions not yet covered by the current scheme. Updates will be posted in the instrument web page: <http://www.eso.org/instruments/crides/>. Potential users should email their respective contacts (§1.4).

Table 8a: Recommended wavelength calibration source.

Order	Source	Comment
59	ThAr	full range
58	ThAr	full range
57	ThAr	full range
56	ThAr	full range
55	ThAr	full range
54	ThAr	full range
53	ThAr	full range
52	ThAr	full range
51	ThAr	full range
50	ThAr	full range
49	ThAr	full range
48	ThAr	full range
47	ThAr	full range
46	ThAr	full range
45	ThAr	full range
44	ThAr	full range
43	ThAr	full range
42	ThAr	full range
41	ThAr	full range
40	ThAr	full range
39	ThAr	full range
38	ThAr	no lines in range [1514, 1520]
37	ThAr	no lines in range [1514, 1523]
36	ThAr	no lines in range [1583, 1594]
35	ThAr	no lines in range [1583, 1594]
34	ThAr	no lines in range [1659, 1672]
33	ThAr	no lines in ranges [1659, 1672], [1698, 1701]
32	ThAr	no lines in ranges [1730, 1739], [1738, 1747], [1764, 1784], [1803, 1811]
31	ThAr	no lines in ranges [1764, 1784], [1803, 1811], [1816, 1825]
30	ThAr	no lines in range [1880, 1890]

Table 8b: Recommended wavelength calibration source.

Order	Source	Comment
29	ThAr	few lines
28	ThAr	few lines
27	ThAr	few lines
26	ThAr	few lines
25	sky absorption lines	full range
24	HALOGEN+CO	full range
23	sky absorption lines	full range
22	HALOGEN+N <sub>2</sub> O	useful ranges [2581.0, 2640.6], [2645.4, 2652.7]
21	HALOGEN+N <sub>2</sub> O	useful range [2651.2, 2698.3]
20	HALOGEN+N <sub>2</sub> O	useful ranges [2742.3, 2781.3], [2847.8, 2917.7]
19	HALOGEN+N <sub>2</sub> O	useful range [2860.6, 3016.7]
18	sky emission lines	full range
17	sky emission lines	full range
16	HALOGEN+N <sub>2</sub> O	useful range [3533.8, 3629.9]
15	HALOGEN+N <sub>2</sub> O	useful ranges [3581.6, 3629.5], [3831.8, 3927.0]
14	HALOGEN+N <sub>2</sub> O	useful ranges [3831.8, 4145.9], [4161.9, 4177.9]
13	HALOGEN+N <sub>2</sub> O	useful ranges [4136.7, 4145.9], [4161.9, 4177.9], [4234.3, 4368.8] [4411.7, 4528.6]
12	HALOGEN+N <sub>2</sub> O	useful range [4484.0, 4702.4]
11	HALOGEN+N <sub>2</sub> O	useful range [5250.0, 5395.6]

## 19 Differential tracking

### 19.1 Introduction

Differential tracking allows to close the loop and/or to guide on an object that is moving relative to the target to be observed.

Typical examples of the use of such a mode are:

1. using a satellite of a planet as an AO guide star to observe a feature on the parent planet;
2. using a (angularly small) planet, asteroid or comet to observe a feature moving relative to its optical photo-center;
3. using a star as an AO guide star or SVGS to observe a planet, asteroid, comet passing in its vicinity.

In P85, differential tracking is offered both in service and visitor mode.

### 19.2 Tracking tables

Differential tracking is triggered by the use of one of the two specific acquisition templates: `CRIRES_spec_acq_NGS_difftrack` or `CRIRES_spec_acq_NoAO_difftrack`.

These templates have a reduced set of parameters compared to their similar, non-differential-tracking templates. However, they contain 2 additional, unique parameters:

- `SEQ.TRACK.REF` (P2PP: *Reference star tracking table file*),
- `SEQ.TRACK.TARG` (P2PP: *Target tracking table file*).

These parameters expect the names of PAF files, in other words, files with a specific format. The main content of these files are the ephemerides for the right ascension and declination for the object used as a reference star (AO star or slit viewer guiding star) and the target, respectively.

In order to produce these files, the following steps must be executed:

1. create the ephemerides for the reference star and for the target. The required format can be easily fulfilled using the JPL Horizons tool.
  - Use the <http://ssd.jpl.nasa.gov/horizons.cgi>
  - for each of the following settings (left column), set the value given in the right column

Ephemeris type	OBSERVER
Target Body	<i>favorite target or reference object</i>
Observer location	Cerro Paranal [309]
Time Span	<i>start and end of the ephemerides, time step</i>
Table Settings observer quantities	1 Astrometric RA & DEC <i>other quantities are optional</i>
Table settings, observer-table settings	date/time format: Julian day angle format: hours/degrees minutes seconds refraction model: airless model (no refraction) airmass limit : 2.6 ( <i>or smaller</i> ) elevation cutoff: 20 ( <i>or larger</i> ) skip daylight : checked extra precision : checked reference system: ICRF/J2000.0 CSV format : checked

Display/Output download/save

- the file for the target created this way can be edited by a spreadsheet to calculate the RA and DEC of a specific feature on its surface; it is crucial however to output any processed information back into a comma-separated variable (csv) format;
- once the file created, it must be converted into a PAF using the `crossEphem2paf.tcl` tool, available in the CRIRES tools page <http://www.eso.org/sci/facilities/paranal/instruments/crires/tools/>; this tool requires to have `tcl` installed. Assuming this file is in the current directory, the usage is

```
tclsh crossEphem2paf.tcl -i sourceFileName -o fileName.paf
```

where the *sourceFileName* is the name of the file produced by Horizons (or modified by a spreadsheet), and *fileName.paf* is the name of the output PAF file (extension .paf). Note that useful lines are identified as being located between the character strings `$$SOE` and `$$EOE`; all other lines will be treated as comments. Note that the PAF file contains the time in the usual ISO format (YYYY-MM-DDTHH:MM:ss.sss), calculated from the Julian day.

If the reference star is in fact really a star, then the tool should be used with the following syntax:

```
tclsh crossEphem2paf.tcl -ra HHMMSS.SSS -dec sddmmss.sss -o fileName.paf
```

where `HHMMSS.SSS` and `sddmmss.sss` are the coordinates of the star at the epoch and equinox given in the acquisition template parameter.

The number of entries *per night* of observations is limited to 300, which corresponds to a minimum time step of 5 min if the target can be observed the whole night. However, the file can include data for a whole period.

Examples of ephemerides and their corresponding PAF files are given in the CRIRES tools page: <http://www.eso.org/sci/facilities/paranal/instruments/crises/tools/>.

### 19.3 Acquisition and observation

In differential tracking in AO mode, (using `CRIRES_spec_acq_NGS_difftrack`) the slit viewer guide star and the AO guide star are identical.

In case of AO, the following steps are executed during acquisition:

1. at the start of the execution of the OB, the observation software (OS) calculates the current RA and DEC of the reference star and sends a preset to this coordinates to the telescope; it also calculates the current additional velocity of the target and sends that information to the telescope;
2. the reference star is acquired by the MACAO and the AO loop is closed;
3. slit viewer guiding is started;
4. the OS calculates the current difference of RA and DEC between the reference star and the target and offsets to the target;
5. adjustment is made to take into account possible differential chromatic effects, such as differential refraction between the observing wavelength and the slit viewer filter effective wavelength;
6. a slit viewer image is taken.
7. the observation can start using the observing template `CRIRES_spec_obs_AutoNodOnSlit`, `CRIRES_spec_obs_SpectroAstrometry`, `CRIRES_spec_obs_GenericOffset`; during the observation, the field selector and/or the slit viewer guiding window location is continuously adjusted to keep track of the difference of coordinates between the field selector and the target; the additional velocity sent to the telescope are also continuously modified.

In case of NoAO (`CRIRES_spec_acq_NoAO_difftrack`), the first 2 steps are skipped.

*Version 85.1 of the manual reported that the `CRIRES_spec_obs_GenericOffset` behaved differently in differential tracking mode compared to the usual tracking mode. In fact, futher tests showed that this is in fact not the case: this template behaves as expected.*

## Part V

# Tips for successful observations

## 20 Checklist

In this section, we provide a number of recommendations in order to increase the chances that a program is executed successfully.

### 20.1 Phase 1

Before submitting an ESO proposal involving CRIRES, the following points should be taken into account:

1. Tables [4a-4k](#) and [5a-5k](#) provide the current best estimate of the uncontaminated spectral ranges for each standard setting, i.e, the one for which illumination should be reproducible to the 1% level. If the interesting spectral features are affected by detector glow or vignetting in a standard setting, a free wavelength setting may be chosen to optimize their location on the detectors. See also § [7.1](#).
2. The expected S/N for each object should be given in the time justification; it must be stated if it corresponds to the S/N per pixel or per resolution element. For extended objects, it is important to state if it corresponds to the S/N per pixel in the spatial direction or over the whole expected extension along the spatial direction.
3. Overheads can only be reasonably estimated if the DIT has been appropriately chosen. Although long DITs allow to reduce overheads, it is important to note that (a) the total object plus sky spectrum should not have more than about 10,000 ADUs ( $\approx 70,000e^{-1}$ ); this is particularly relevant for observations in the L or M bands; (b) for observations of relatively faint targets in the J, H or K bands, the choice of long DITs ( $\geq 60s$ ) should be balanced with the increased noise brought by the detector glow and the advantage that multiple exposures allow a better flat-field correction, in particular if some jitter is introduced.
4. *Service mode* programmes are executed using Observing Blocks (OBs) that should last less than 1 hour. Except for an associated telluric OB, a science OB is the typical unit of observation that should be completely independent of other OBs of the same programme. Indeed, different OBs of a given programme are usually observed in different nights. As a consequence:
  - (a) The amount of time to request has to take into account all overheads, in particular, the ones associated with preset and acquisition for each OB.
  - (b) Typically, each science OB should have one associated telluric OB. Some exceptions occur: for example, when targetting a specific line located away from any telluric absorption features. The amount of time to request has to take into account the time to execute all associated telluric OBs. In particular, one should *not* assume that one telluric OB will be useful for several science OBs.

## 20.2 Phase 2

1. If the slit orientation on the sky is not important for the science objective, the ELEV mode is recommended. This avoids slit losses due to atmospheric refraction.
2. In the choice of wavelength settings, the interesting science features should avoid the vignetted and detector glow areas: the latter point is particularly critical for DITs longer than 60s. The wavelength coverage of the chosen wavelength settings can be compared with the output spectra of the CRIRES [ETC](#). The position of the science features can be compared with [Fig. 13](#) and the unvignetted range in [Tables 4a-4k](#) or [5a-5k](#). If the interesting spectral features are affected by detector glow or vignetting in a standard setting, a free wavelength setting may be chosen to optimize their location on the detectors. See also [§ 7.1](#)
3. The selection of the DIT value does not only depend on the brightness of the target but also on the brightness of the infrared sky. The longer the wavelength, the brighter the sky, the shorter the DIT (to avoid saturation of the sky). This should be carefully checked with the help of the [ETC](#).
4. In case the target is not the SV guide star (or the pointing position is located between two or more targets in the slit ), special care has to be taken to correctly define the offsets. See [§14.1.1](#) for definitions and conventions.
5. It is worth noting that the default telescope pointing is not centered on the 40'' slit (see [Fig. 18](#)). The distance to the North and South edge are 22'' and 18'', respectively (in the slit viewer detector). Therefore the nodding throw and jitter width should be chosen carefully, such that the targets stay in the slit area at all nodding/jittering positions. This is especially important when an extended object or multiple targets are in the slit.
6. Telluric standards should be chosen close in right ascension and airmass to the target. To avoid any confusion in the assignment of a telluric to a science target, it is recommended to name the telluric OB according to the science OB, i.e. 'CAL\_<science OB name>'.
7. Finding charts should be created from infrared images (e.g. 2MASS) and should clearly indicate the location of the target, AO star and SVGS. The necessary information on the target, AO and SV stars should be given in the Instrument Comments field of each OB.
8. More detailed information on Phase 2 requirements can be found in [§11](#) and at <http://www.eso.org/sci/observing/phase2/P2PP/P2PPTool.html>.